WADD-TR-61-123
Part II

Results inconclusive

PROPERTIES OF YTTRIUM AND THE RARE EARTH METALS, EFFECT OF MINOR ADDITIONS TO NIOBIUM-BASE ALLOY ON ELEVATED TEMPERATURE OXIDATION RESISTANCE, Part II.

TECHNICAL DOCUMENTARY REPORT NO. WADD-TR-61-123, PART II

June 1962

Directorate of Materials and Processes
Aeronautical Systems Division
Air Force Systems Command
Wright-Patterson Air Force Base, Ohio

Project No. 7351, Task No. 735103

(Prepared under Contract No. AF 33(616)-6829
by Research Chemicals, Phoenix, Ariz.;
Craig G. Kirkpatrick, author)

NOTICES

When Government drawings, specifications, or other data are used for any purpose other than in connection with a definitely related Government procurement operation, the United States Government thereby incurs no responsibility nor any obligation whatsoever; and the fact that the Government may have formulated, furnished, or in any way supplied the said drawings, specifications, or other data, is not to be regarded by implication or otherwise as in any manner licensing the holder or any other person or corporation, or conveying any rights or permission to manufacture, use, or sell any patented invention that may in any way be related thereto.

Qualified requesters may obtain copies of this report from the Armed Services Technical Information Agency, (ASTIA), Arlington Hall Station, Arlington 12, Virginia.

This report has been released to the Office of Technical Services, U.S. Department of Commerce, Washington 25, D.C., for sale to the general public.

Copies of this report should not be returned to the Aeronautical Systems Division unless return is required by security considerations, contractual obligations, or notice on a specific document.

C

FOREWORD

This report was prepared by Research Chemicals, Phoenix, Arizona under USAF Contract No. AF 33(616)-6829. The contract was initiated under Project No. 7351, "Metallic Materials," Task No. 735103, "Unique Metallic Materials and Techniques." The work was administered under the direction of the Directorate of Materials and Processes, Deputy Commander/ Technology, Aeronautical Systems Division, Wright-Patterson Air Force Base, Ohio. Mr. K. L. Kojola and Lt. S. A. Worcester, Jr. were the project engineers.

This report covers work done from November 1, 1960 through October 30, 1961.

2-21C, 700, 8-31-62

ABSTRACT

Approximately 180 compositions in 19 niobium based alloy types were prepared for study. Atmospheric corrosion tests were completed for 9 series of alloys. Improved corrosion resistance is indicated for a niobium alloy containing 7% titanium, 20% tungsten, and 3% molybdenum when rare earth metals are added. Possible improvement, on the addition of rare earths, is also suggested for a niobium alloy containing 11.3% titanium and 7.9% molybdenum. Metallurgical investigations of two alloy series failed to indicate correlation between metal interface movement or microhardness values with corrosion resistance as established by weight gain measurements.

This report has been reviewed and is approved.

I. PERLMUTTER
Chief, Physical Metallurgy Branch
Metals and Ceramics Laboratory
Directorate of Materials and Processes

TABLE OF CONTENTS

TABLE OF CONTENTS (continued)

LIST OF TABLES

LIST OF ILLUSTRATIONS

LIST OF ILLUSTRATIONS (Continued)

LIST OF ILLUSTRATIONS (Continued)

LIST OF ILLUSTRATIONS (Continued)

LIST OF ILLUSTRATIONS (Continued)

LIST OF ILLUSTRATIONS (Continued)

LIST OF ILLUSTRATIONS (Continued)

LIST OF ILLUSTRATIONS (Continued)

LIST OF ILLUSTRATIONS (Continued)

LIST OF ILLUSTRATIONS (Continued)

LIST OF ILLUSTRATIONS (Continued)

LIST OF ILLUSTRATIONS (Continued)

LIST OF ILLUSTRATIONS (Continued)

LIST OF ILLUSTRATIONS (Continued)

INTRODUCTION

The work reported is an extension of studies of the properties of yttrium and the rare earth metals. Previous work under this contract comprises a literature survey, WADD TR 60-864, and WADD TR 61-123. The additional work under this contract is concerned with atmospheric oxidation resistance studies of a number of niobium based alloys.

Manuscript released by author as a WADD Technical Report.

CORROSION RESISTANT NIOBIUM ALLOYS

Background. Niobium is a transition element with a relatively high melting point (2475°C.) and a not excessively high specific gravity (8.57 g/cc). Recent developments in production technology have made this material available for service as a high-strength metal at elevated temperatures. The usefulness of niobium, unfortunately, is limited in air at elevated temperatures due to its very high rate of atmospheric corrosion.

The equilibrium diagram for the niobium-oxygen system was recently determined by Elliott (5). Three compounds were found, corresponding to the formulas; NbO, NbO_2, and Nb_2O_5. The nature of the oxides of niobium has been studied by Brauer (2, 3), Shafer and Roy (16), Goldschmidt (6), and Holtzberg and co-workers (7). Both NbO and NbO_2 have fairly simple cubic structures, but Nb_2O_5, has been recognized in six different forms; amorphous, delta (a partially crystallized form of gamma) gamma, beta (a partially crystallized form of alpha),

alpha, and an unidentified high temperature form which is found above 1280°C (16).

The reaction of niobium with oxygen can be divided into five stages, according to Hurlen (8), each stage following a different rate law. The initial weight increase corresponds to a linear rate law, and is due to oxygen dissolution, phase boundary controlled. A second stage follows a parabolic rate law, and is due to oxygen dissolution with traces of nucleation, diffusion controlled. The third stage follows a linear rate law, and is due to oxide growth with phase boundary control. The fourth and fifth stages follow parabolic laws with oxide growth controlled by diffusion. Oxide flakes may form and fall away from the metal between stages four and five.

The effect of alloying additions on the rate of oxidation of niobium has been studied by a number of investigators over the past few years. Recent studies include those of Paprocki and Stacy (14) Simms, Klopp,

and Jaffee (17), Barrett and Clauss (1, 4), Michael (13), and Love (11). Comprehensive summaries of research investigations have been reported by Klopp (9), and Tietz and co-workers (18).

Theoretical aspects of the effects of alloying additions on oxidation behavior have been studied by Pranatis and Seigle (15), Clauss and Barrett (4), Wainer (19), and Kubaschewski and Hopkins (10). Oxidation behavior has been found dependent upon a number of factors. Thus Clauss and Barrett report that elements which can form trivalent positive ions of a size comparable with the pentavalent niobium ions promote formation of adherent protective scales which improve oxidation resistance. Wainer (19) reports that oxidation stabilizers are characterized by a smaller atomic radius and greater heat of oxide formation than niobium. Diffusion barrier elements (which include the rare earth elements) reduce oxidation rates by impeding the diffusion of niobium ions through an adherent scale. When alloying additions exceed the solubility limit in the base

metal, oxides other than niobium oxide are formed. These may be the oxides of the alloy addition element, mixed oxides, or spinels.

RARE EARTH ALLOY THEORY

Background. The development of rare earth alloys has, to date, been based largely upon empirical or quasi-theoretical considerations, which, in turn, were based upon the examination of ordinary metals (s and sp orbitals) and some examination of the transition metals (spd orbitals). The role of the f electrons (4f in the lanthanide, 5f in the actinide, series), has been less thoroughly examined. Generally, it has been presumed that the effect of these orbitals can be safely ignored since the experimental evidence to date does not show their ability to be involved in any bonding.

Exclusive of europium and ytterbium, which have stable divalent states, the rare earth metals have hexagonal structures. The cerium group metals have a lanthanum hexagonal structure (ABAC stacking), the yttrium group rare

earths have a magnesium hexagonal structure (ABAB stacking). Samarium, which is the intermediate element between the two groups, has an intermediate rhombohedral structure. This structure has also been found as an intermediate phase in the gadolinium-lanthanum system and in the yttrium-neodymium system, and there is some evidence of its existance in systems of yttrium with other cerium group element. There is currently no explanation for this structure based on existing theory.

SCOPE OF THE PROGRAM

The field of investigation in this contract has been based upon the state of technology of the materials under consideration as briefly discussed above. Studies of the atmospheric corrosion behavior of niobium-based alloys were of a screening nature designed to investigate a large number of compositions to determine the effect of the addition of rare earth metals upon corrosion rates. Niobium alloys were prepared containing one or more of the elements; chromium, aluminum, titanium, molybdenum, nickel,

tungsten, iron, and zirconium. Each of several different rare earths were added to these alloys at different composition levels. The rate of corrosion resistance was determined at 1000°C. An attempt was made to correlate the effect of alloy additions on oxidation resistance with the microstructure of the base metal, the type of oxide formed and the depth of contamination. Approximately 150 compositions were prepared and examined.

ALLOY PREPARATION

Nineteen basic niobium alloys have been prepared for study during the reported period. Each was prepared as a base alloy and in up to nine modifications containing added rare earths. A total of approximately 180 compositions were prepared. The base alloy compositions and the identification system used for the various rare earth additions are indicated in Table I.

Alloys number 1, 2, and 3 were excessively brittle; with low potential for structural applications thus indicated, they were not tested further. Alloys number 6,

7, 8, and 10 showed segregation when machined, and were consequently subjected to additional arc-melts to attempt homogenization.

DISCUSSION

Materials and Equipment

The systems investigated were all multi-component (three to five elements), and interpretation of physical and metallurgical data was complex. In order to minimize possible effects of varying impurity contents, sufficient quantities of all metals required for the program were reserved so that all alloys were made from the same lots of starting materials. Chemical and spectrographic analysis were made of all materials to check, and to supplement data furnished by the vendors. The primary matrix niobium was obtained as high purity niobium chips from the Wah Chang Corporation, and chemical and spectrographic analysis in our laboratories confirmed the vendor's specification.

Alloys were prepared in a non-consumable arc-melting furnace of local design and construction which has been previously described (12). Machined corrosion samples were tested in a 15 Kw Globar furnace. Examination of

corrosion products and corroded specimens was made by conventional metallographic and X-ray diffraction techniques. Polishing of specimens was conducted in rotating laps and using electrolytic techniques. Micro structures were examined with a Leitz micro-hardness tester and a Reichert polarizing microscope "Zetopan". X-ray diffraction was conducted on a General Electric XRD5 diffractometer using both copper and chromium radiation.

The analytical equipment included a three meter Baird spectrograph, a comparator densitometer, a Beckman spectrophotometer, and apparatus for oxygen determination by vacuum fusion.

Corrosion Tests

Specimen Preparation. The first alloys subjected to metallurgical studies as described below were niobium-tungsten-titanium and niobium-tungsten-molybdenum-platinum alloys, each with various small percentages of yttrium or erbium added. The alloys were prepared by non-consumable arc-melting, and specimens were cut for corrosion

testing in the form of flat rectangular plates. These were polished by the techniques used for metallographic examination. The final polishing was by hand with 600 grit silicon carbide abrasive. Excess kerosene was removed by rinsing with acetone and wiping dry. Samples were stored under argon until tested. The above alloys were prepared for corrosion testing in the first quarter.

The following standard procedure has been used for all other alloys prepared on this program. A sub-alloy is prepared by non-consumably arc-melting all minor constituents. The niobium is then added, and the alloy is prepared as a circular button, arc-melted 3 times and turned between each melt. This button is then arc-melted into a rectangular bar 1/2"x1/2"x1-1/2". The bar is subjected to 4 arc-melts, being turned each time. The alloy at this stage, therefore, has had 7 arc-melting steps from the time of addition of all constituents. The bar is machined into a maximum diameter cylinder and, while still on the lathe, is smoothed with a fine file, rough

polished with 300 grit emery cloth, and sanded smooth with 400 grit sandpaper. Discs approximately 1/4" thick are cut from the cylinder using an abrasive cut-off wheel. The cut faces are polished with 600 grit silicon carbide abrasive. The various stages of specimen preparation are illustrated in Figure 53, reduced approximately 30% for reproduction.

Test Procedure. Corrosion tests were run in a large tube type furnace. A slow stream of air, pre-dried by passage through a "drierite" column, was maintained throughout all runs. The test specimens were placed at an angle in small crucibles to permit maximum air circulation. The crucibles were centered in the furnace in a pre-heated massive holder to help minimize temperature variations. Tests made in the previous year (12) on the niobium-tungsten-titanium and niobium-tungsten-molybdenum-platinum alloys were made at 600°C. All other tests were at 1000°C. The furnace temperature was found to be constant within ± 2°C. at both temperatures. All samples were exposed for a total

of 8 hours unless early results indicated that corrosion would be excessive (above approximately 8-10 gms/dm^2) and except for alloy system number 16 which was extended to 16 hours for additional information.

After exposure, the crucibles were immediately covered and transferred to a desiccater to cool. Weight increases were calculated as grams per square decimeter, and plotted against time.

600°C. Atmospheric Corrosion Tests.

Results. The rate of corrosion of the niobium-15% tungsten-5% molybdenum-2% platinum alloy containing small additions of erbium and of yttrium, as tested at 600°C., are shown in Figures 70 and 71 respectively. The addition of erbium to the alloy did not markedly effect the corrosion rate. 1% erbium increased the rate slightly, 1/2% and 2% decreased the rate. Yttrium appeared to be somewhat more effective. The 1/2% and 2% alloys had slightly decreased corrosion rates. The rate of the 1% yttrium alloy was only about 1/3 the rate for the base alloy.

The corrosion rates for a niobium-20% tungsten-2% titanium alloy, and the alloy plus additions of erbium and of yttrium, are shown in Figures 72 and 73. Two arc-melted heats of this alloy were prepared. It is observed that the 2 heats of this base alloy corroded at considerably different rates. From x-ray and metallographic examination it appeared that the alloys were homogeneous and single phase. No explanation for the variance can presently be offered. All of the erbium and yttrium containing alloys corroded much more slowly. There was very little difference between the rates for the various rare earth containing compositions (relative for the base alloy), the average rate being 20% of that for the better of the 2 base alloys, and less than 10% of that for the poorer base alloy.

1000°C. Atmospheric Corrosion Tests.

Results. Alloy number 4; 42% titanium, 4% aluminum, balance niobium (Figures 74, 28-30). All compositions containing rare earths corroded more rapidly than the

homogeneous base alloy.

Alloy number 5; 6.0% chromium, 8.7% titanium, balance niobium. Corrosion data are presented in Figures 1, 2, and 3. The only composition showing lower corrosion rate than the base alloy contains 1/4% added yttrium. The rate difference was small and is considered to be probably within the limits of experimental error.

Alloy number 9; 11.7% titanium, 3.1% vanadium, balance niobium (Figures 4, 5, 6). Again, the composition containing 1/4% added yttrium showed a slightly lower corrosion rate than the base alloy, as did the composition containing 1/4% added cerium. These differences too, are probably within the limits of experimental error.

Alloy number 10; 11.3% titanium, 7.9% molybdenum, balance niobium (Figures 7-9). Corrosion rates of compositions containing additions of 1/4% cerium, 1/4% yttrium, and 4% dysprosium were somewhat lower than that of the base alloy, particularly in the time interval between 1 and 8 hours exposure. The reduction in rate approached

20% and may indicate slightly improved corrosion resistance.

Alloy number 12; 45.7% zirconium, 2.5% titanium, balance niobium (Figures 10-12). All compositions containing rare earths corroded more rapidly than the base alloy.

Alloy number 13; 3% aluminum, 3% vanadium, balance niobium (Figures 13-15). All compositions containing rare earths corroded more rapidly than the base alloy.

Alloy number 14; 7.0% titanium, 0.8% zirconium, balance niobium (Figures 16-18). All compositions containing rare earths corroded as rapidly or more rapidly than the base alloy.

Alloy number 15; 7% titanium, 28% tungsten, balance niobium (Figures 19-21). The composition with 1% added yttrium appeared to show some improvement over the base alloy. Compositions containing 1/4% yttrium, and 1% cerium, has very nearly the same rate as the base alloy. No positive improvement is indicated.

Alloy number 16; 7% titanium, 20% tungsten, 3% molybdenum, balance niobium (Figures 22-24). The base alloy had an indicated uniform corrosion rate of 0.44 gms/dm^2/hr for the first four hours. This increased to an average rate of 0.93 gms/dm^2/hr for the next four hours. Compositions containing 1/4% and 1% of cerium or yttrium corroded at very nearly the same rate or slightly faster than the base alloy for the first two hours, but then slowed to an average rate of only 0.21 gms/dm^2/hr. The dysprosium containing alloys were similar, except that the rate for the first two hours was significantly greater than for the base alloy, then slowing to 0.43 gms/dm^2/hr. The consistency of behavior of all the rare earth containing alloys, and the fact that the rates of corrosion after two hours of the cerium and yttrium containing alloys were only about one-half of the early corrosion rate of the base alloy, suggested that the additions of rare earths had a significant effect in reducing the atmospheric corrosion rates of this alloy. The tests were therefore continued for

an additional eight hours, and it is observed that the rare earth containing compositions continued to increase in weight at a slower rate than the base alloy (Figures 22-24).

Alloy number 18; 8% hafnium, 20% tungsten, balance niobium (Figures 25-27). The corrosion rate of this base alloy was considerably greater than the rates of the other alloys herein reported. It appeared, indeed, to approach that of niobium metal. All compositions containing added rare earths corroded more rapidly, except for the 1% yttrium alloy which showed a slightly reduced rate.

Alloys numbered 6, 7, 8, 11, 17, and 19 resisted all attempts to produce a homogeneous sample and were therefore not subjected to further examination.

METALLURGICAL STUDIES

Two series of niobium alloys were examined in detail by metallurgical techniques at the conclusion of their corrosion tests; alloy number 4 containing 4.0% aluminum and 42.0% titanium, and alloy number 5 containing 6.0% chromium and 8.7% titanium. Corrosion curves for alloy number 4 are shown in Figures 28-30. The corrosion curves for alloy number 5 are shown in Figures 1-3. Examination was made of the base alloy and of all compositions containing added rare earth on a comparative basis. Studies included microscopic examination using both Bright-field and polarized light, and metal interface movement and microhardness determinations.

MICROSCOPIC INVESTIGATIONS

Preliminary microscopic examination was made on the niobium-tungsten-titanium, and niobium-tungsten-molybdenum-platinum alloys subjected to corrosion tests as discussed above. Examination indicated that some of the alloys had a thin, but hard and adherent, surface layer (which was adjacent to the metal and under the original

loose oxide scale). Table V summarizes the alloys examined and the observed adherent films.

Comparison of these corrosion and microscopic results indicates that there is an almost exact correlation between the presence of the adherent film and the corrosion resistance of the alloy. The more evident this layer is under microscopic examination, the more corrosion resistant is the alloy.

Bright-field microscopic examination served primarily to establish homogeneity, and, if it occurred, to detect the presence of the thin, hard surface layer reported above. Specimens were initially prepared for examination by mechanical polishing followed by chemical polish with a solution of hydrofluoric, nitric, and lactic acids (10:10:30). Corrosion test speciments, also polished well at 6 amps/cm^2 in a sulfuric-hydrofluoric (90:10) acid electrolyte.

Slight segragation was detected in several of the compositions, but appeared to be minor in importance

except for the base alloy (number 4A) which was found to be badly segregated. In consideration of its use as a comparision reference for the effect of rare earth additions, a new alloy specimen was prepared, checked for homogeneity, and its corrosion rate determined. The corrosion rate of this new specimen was found to be significantly lower than for the segregated alloy. (Figures 28-30).

The only other specimen showing massive segregation was composition 5D (alloy 5 with 4% added cerium). The corrosion rate for this specimen was somewhat faster than the rates for the other compositions in this series (Figure 1), but since the rates for compositions containing 1/4% and 1% cerium additions, and most other rare earth additions (Figures 2 and 3) were about the same or faster than that of the base alloy, it was not considered likely that retesting this composition would result in materially improved corrosion resistance.

The thin and adherent surface layer (adjacent to the metal but under the loose oxide scale) previously found present on the niobium - 20% tungsten - 2% titanium alloy was found present on alloy number 5 compositions but not on alloy number 4 compositions. The microhardness values reported below again substantiate the presence of this layer.

Dissolved oxygen has been shown to introduce tetragonality in the body centered cubic lattice structure of niobium. Examination under plain polarized light has revealed only scattered areas of activity at the immediate surface of a few of the test specimens. No photographic evidence could be obtained. We will conclude, therefore, that for the alloys examined, oxygen is present primarily as a precipitate and not interstitially.

METAL INTERFACE MOVEMENT

Metal interface movement was established by direct measurement. The diameter of the right circular cylin-

der test specimen was determined, two values at right angles being averaged. The metal interface movement is defined as one-half of the difference in diameter before and after test. Data are shown in Tables II and III.

Comparison of these data with the weight increase data (Figures 28-30 - 1-3) emphasizes the need for both types of measurement. In alloys 5E, 5F, and 5G there is a direct correlation between weight gain and metal interface measurements. In general this correlation does not hold.

MICROHARDNESS DETERMINATION

A typical microhardness traverse is seen in Figure 54 which illustrates sample number 1285, after corrosion testing (77.5 Nb, 20 W, 2Ti, 0.5Er). The relatively large and uniform indents of the interior portion of the metal quite suddenly become small as the surface is approached. Although hardly detectable in the photographic reproduction, the hard layer is visually detected to a depth of approximately 0.035 millimeters.

Graphs of hardness vs distance from the edge of the specimen are illustrated in Figures 55-69 for the alloys described in Table V. The shape of the initial portion of the curve is not yet certain and has been indicated by a dashed line. Figures 55-60 for specimens 1282-1287 indicate the presence of a hard surface layer as predicated from visual examination. Figures 61-66 for specimens 1288-1293 indicate that the surface of these alloys is only very slightly harder than the interior and substantiate the absence of visible layers. Figures 67-69 are for specimens 1294-1296 which showed apparent hard layers on some parts of the specimens, but not on most of the surface. In each case the hardness measured was greater where the layer was visible.

An attempt was made to correlate the inner boundary of the layer with the hardness curves. The position of this inner boundary is indicated in each of the figures shown. No correlation could be established, the layer terminating near the top, center, or bottom of the

curve in the several figures.

Microhardness determinations were also made on the number 4 and 5 alloy series compositions and on two specimens of niobium metal after the corrosion tests. For most specimens, measurements were made in three areas. Where corrosion was severe, only one or two areas could be tested. Measurements were taken using a Vickers diamond and a 100 gram load (25 gram load for samples 4H and 4I and 200 gram load for sample 5F).

The hardness curves for the niobium metal specimens are essentially flat and show very little increase in hardness from the base metal to the surface (Figures 31-32).

The hardness curve for the base alloy number 4 (Figure 33) shows higher values immediately near the surface, which then drop rapidly to that of the base metal. The hardness of the base metal is quite close to that of the unalloyed niobium. Alloy number 4 compositions with added rare earths all showed very similar type curves (Figures 34-42) except for composition 4E (containing 1/4%

yttrium) which was similar in two areas but which showed a maximum hardness value 0.1 mm from the surface in the third area, and which had a generally higher hardness level in the area (Figure 37).

The hardness curve for base alloy number 5 (Figure 43) shows a high value near the surface and an abrupt transition, at approximately 0.3 mm from the surface, to the hardness of the base alloy; which, again, is approximately the same as niobium. The curves for most of the compositions containing added rare earths (Figures 44-52) are generally similar except for composition 5F (containing 1% yttrium) (Figure 42). This alloy had a badly cracked surface and only one set of hardness values could be obtained. These values were somewhat higher than those of the other compositions and were also higher to a considerable depth. It is possible that this alloy was physically defective and that the interior of the specimen was subject to direct atmospheric exposure. As noted above, microscopic examination of these alloys also reveal-

ed the presence of a hard adherent layer whose depth corresponded well with the measured hardness values.

X-RAY DIFFRACTION ANALYSIS

The atmospheric corrosion products from the first two alloys in the series and from alloys numbered four and five have been examined by x-ray diffraction. The patterns produced were quite complex and it has not been possible to identify the structure or structures present.

Unalloyed Niobium. A sample of niobium hydroxide was examined after heat treatment at various temperatures up to 880°C. Heating at 440°C. yielded a simple diffraction pattern indicating a hexagonal unit cell of detection a_o=6.25A°: C_o= 3.93A° (Table IV). The diffraction pattern obtained from the sample annealed 480°C. was the same as for the sample annealed at 400°C. Annealing at 810°C. produced a diffraction pattern resembling the one produced at the lower temperature except that several of the lines were split. It would appear that the crystal structure of this sample represents a distortion of the

previous sample. The diffraction pattern from a sample annealed at 880°C. is completely different with broad diffraction maxima indicating a lack of crystallization.

The diffraction data for all niobium hydroxide samples up to 880°C. do not correspond to any published data. It is possible that in our work and in the work of others the "Oxides" are really hydrated so the annealing times and temperatures play an important role.

The diffraction pattern from the surface of a sample of niobium metal at 400°C. in the Tem-Pres furnace was that of body centered niobium only. At 600°C. no body centered niobium lines were detectable and a simple diffraction pattern was produced which was in approximate agreement with the published data for Nb_2O_5 in this temperature range. Room temperature examination of the oxide produced in the high temperature specimen holder at 800°C. yielded a very complex diffraction pattern with bad resolution and broad lines. After 12 hours annealing at 1000°C. in oxygen this material yielded the same dif-

fraction pattern as before but with much better resolution and well defined maxima. The diffraction maxima at 800°C. and 1000°C. agree with the powder data given by Brauer.

After removing the top layer of oxide there remained a tightly adherent coating on the surface of the sample. The diffraction pattern of this product differed drastically from the others described above. Some peaks were in common with the pattern observed at 600°C. but certain lines are different. No published data agree with this diffraction pattern. This would seem to indicate that a different kind of oxide product may be found adjacent to the surface of niobium metal niobium alloys. Examination of powder diffraction pattern films for alaloy systems 4, 5 and 18 have yielded nine different types of patterns. Group 1 alpha pattern was characteristic of alloys A4 (2), B4, D4, F4, G4, I4, J4, and K4. Group 1 beta alloys were E4. Group 1 gamma alloys H4. Group 1 delta alloys A4. Group 2 alpha alloys A5, B5, C5, D5, E5,

F5, H5, I5, J5, and K5. Group 2 beta G5. Group 3 alloys AA, AB, C4. Group 4 alpha alloys A18, B18, C18, E18, and H18. Group 4 beta alloys F18.

The alloys were categorized in these nine groups and sub-groups as follows:

Group 1 alpha: The diffraction pattern which this group revealed was simple, consisting of fewer lines than any other of the patterns. It seems likely that these samples contain only one crystallographic species.

Group 1 beta and 1 gamma: Diffraction maxima observed in group 1 alpha are also present in 1 gamma and 1 beta. In addition these two samples have extra lines which "appear" to be due to a "second phase" present in the sample. The material of the second phase is different in 1 beta than in 1 gamma. It is possible that 1 alpha, 1 beta and 1 gamma represent three crystallographically different species.

Group 1 delta: Although many of the powder lines in the sample coincide in position with those of group 1 alpha,

the intensity is considerably different. It seems therefore, very likely that this group represents a new crystallographic species not present in any of the other 8 groups.

Group 2 alpha and 2 beta: The diffraction pattern of group 2 alpha appears to be very closely related to that of 1 gamma. All the lines present in 1 gamma are also present in this group. Two alpha, therefore, may be a two phase sample consisting of 1 gamma plus X.

The position of diffraction maxima observed in 2 beta are the same as observed in 2 alpha except that a great many of them have split into doublets, indicating a change in crystal structure probably by a lowering of symetry. Two beta, therefore, appears to be a new phase not present in any other group.

Group 4 alpha: This group contains all the lines present in group 3 and some strong additional lines which make it seem unlikely that it is a two phase sample containing group 3. The extra lines appear to be due to a change in crystal structure rather than a second phase.

Group 4 beta: This sample is most likely a two phase sample consisting of 4 alpha plus X.

Reproduction of X-ray diffraction film strips showing the patterns typical of each of these nine groups and subgroups are contained in Figures 75-83.

Summary: The difficulties encountered in interpretation of the diffraction patterns are due to the complexity of the structures of the oxides.

There is much confusion in the literature on the crystal structure of the various oxides of niobium. It has not been possible, except in a few cases, to find agreement between our observations and the published literature. It has not even been possible to correlate various papers on the same subject with one another because of drastic differences in the observation of "the same object". In order to identify all the various phases observed it would be necessary to carry out a very pains-taking and elaborate research program extending over several years and well beyond the scope of the current program. Magneli's group at the University

of Stockholm are presently working on the problem of identification of the niobium oxides and more reliable information should be available in a few years.

SUMMARY AND CONCLUSION

The effect of the addition of rare earth metals and yttrium on the corrosion resistance of selected niobium base alloys has been determined. Among the nine base alloys examined, those with highest resistance to atmospheric corrosion were found to be brittle, being composed of intermetallic compounds and not body centered cubic niobium. A niobium alloy containing 7% titanium, 20% tungsten and 3% molybdenum showed improved corrosion resistance on the addition of rare earth metals. A similar alloy containing 11.3% titanium, 7.9% molybdenum showed some possibility for improvement. Metallurgical investigations were conducted, in an attempt to correlate metal interface movement or microhardness traverses with corrosion resistance as established by the usual weight gain measurements. No correlation has been observed in those systems examined and the reason for the lack of the correlation is not altogether clear. Inability to achieve correlation here poses a most serious problem, since weight

gain studies are economically made and are commonly used for screening in corrosion tests, while the ultimate success or failure of a material in a corrosive atmosphere is determined by the metal interface movement (assuming as we have seen here that there is no excessive embrittlement of the base metal).

The complexity of the system niobium-oxygen has caused great difficulty in the analysis of the corrosion product.

There would seem to be two areas of sufficient interest where future investigations are warranted, (1) the determination of the reason for lack of correlation between metal interface movement and weight gain studies and (2) the determination of the niobium-oxygen system as pure elements and containing selected impurities.

REFERENCES

1. Barrett, C. A. and Clauss, F. J.; Oxidation of Columbium-Chromium Alloys at Elevated Temperatures, Electrochemical Society Symposium on Columbium, May, 1957.

2. Brauer, G.; Naturwissenschaften, 28, 30 (1940).

3. Brauer, G.; Z anorg u allgem Chem, 248, 1 (1941).

4. Clauss, F. J., Barrett, C. A.; Preliminary Study of the Effect of Binary Alloy Additions on the Oxidation Resistance of Columbium, Electrochemical Society Symposium on Columbium, May, 1957. Technology of Columbium, Gonser, B. W., and Sherwood, E. M. Wiley, 1958, pp 92-97.

5. Elliott, R. B.; Niobium Phase Diagrams, ARF 2120-3, April 27, 1959.

6. Goldschmidt, H. J.; J. Inst. Metals, 87, 235 (1958).

7. Holtzberg, F., Reisman, A., Berry, M., and Berkenblit, M.; J. Am. Chem. Soc., 79, 2039, (1957).

8. Hurlen, T., Kjollesdal, J., Markali, J., Nico, N.; Oxidation of Niobium, Central Institute for Industrial Research, Norway, Tech Note #1, Contract AF 61(052)-90, (April, 1959).

9. Klopp, W. P.; Oxidation Behavior and Protective Coatings for Columbium and Columbium Base Alloys,

DMIC Report 123, (1960) DMIC BMI Columbus, Ohio.

10. Kubaschewski, O., and Hopkins, B. E.; Oxidation of Metals and Alloys, Butterworth's Sci. Pub. Lon. (1953).

11. Love, B.; The Technology of Scandium, Yttrium, and the Rare Earth Metals. A Literature Survey; WADD Technical Report 60-864, Wright Air Development Division, Wright-Patterson Air Force Base, Ohio (1960).

12. Love, B.; Properties of Yttrium and the Rare Earth Metals; Oxygen and Alloy Systems; WADD Technical Report 61-123, Wright Air Development Division, Wright-Patterson Air Force Base, Ohio, (1961).

13. Michael, A. B.; The Oxidation of Columbium Base and Tantalum Base Alloys, Paper presented at the AIME Regional Conference on Reactive Metals, Buffalo, N. Y., May, 1958.

14. Paprocki, S. J., and Stacy, J. T.; Investigation of Some Columbium Base Alloys, BMI Rep. BMI 1143 (1956).

15. Pranatis, A. L. and Seigle, L. L.; Sylvania Electric Products Progress Report SEP 235 (February, 1957), Progress Report SEP 240 (April, 1957).

16. Shafer, M. W., and Roy, R.; Z Krist 110, 241 (1958).

REFERENCES, continued

17. Simms, C. T., Klopp, W. D., Jaffee, R. I.; Studies of the Oxidation and Contamination Resistance of Binary Columbium Alloys, BMI Rep BMI 1169 (1957).

18. Tietz, T. E., Wilcox, B. A., Wilson, J. W.; Mechanical Properties and Oxidation Resistance of Certain Refractory Metals, SRI Project SU-2436.

19. Wainer, E.; Protection of Niobium from Oxidation, U. S. Pat. #2,833,282, (April 21, 1959).

TABLE I

NIOBIUM ALLOY COMPOSITIONS PREPARED FOR ATMOSPHERIC CORROSION TESTING

ALLOY NO.	COMPOSITION		ALLOY NO.	COMPOSITION	
1.	Aluminum	9.8%	8.	Chromium	13.0%
	Chromium	15.2		Nickel	11.0
	Niobium	75.0		Niobium	76.0
2.	Aluminum	9.7	9.	Titanium	11.7
	Iron	16.1		Vanadium	3.1
	Niobium	74.2		Niobium	85.2
3.	Aluminum	8.7	10.	Titanium	11.3
	Molybdenum	12.5		Molybdenum	7.9
	Niobium	78.8		Niobium	80.8
4.	Aluminum	4.0	11.	Iron	17.1
	Titanium	42.0		Cobalt	7.3
	Niobium	54.0		Niobium	75.6
5.	Chromium	6.0	12.	Zirconium	45.7
	Titanium	8.7		Titanium	2.5
	Niobium	85.3		Niobium	51.8
6.	Chromium	13.0	13.	Aluminum	3.0
	Cobalt	8.8		Vanadium	3.0
	Niobium	78.2		Niobium	94.0
7.	Chromium	7.0	14.	Titanium	7.0
	Molybdenum	9.7		Zirconium	0.8
	Niobium	83.3		Niobium	92.2

TABLE I (Continued)

NIOBIUM ALLOY COMPOSITIONS PREPARED
FOR ATMOSPHERIC CORROSION TESTING

ALLOY NO.	COMPOSITION		ALLOY NO.	COMPOSITION	
15.	Titanium	7.0%	18.	Hafnium	8.0%
	Tungsten	28.0		Tungsten	20.0
	Niobium	65.0		Niobium	72.0
16.	Titanium	7.0	19.	Tungsten	10.0
	Tungsten	20.0		Zirconium	5.0
	Molybdenum	3.0		Niobium	85.0
	Niobium	70.0			
17.	Titanium	10.0			
	Tungsten	20.0			
	Vanadium	3.0			
	Niobium	67.0			

RARE EARTH ADDITIONS

A	Base Alloy	G	4% Yttrium
B	1/4% Cerium	H	1/4% Dysprosium
C	1% Cerium	I	1% Dysprosium
D	4% Cerium	J	4% Dysprosium
E	1/5% Yttrium	K	1% Scandium
F	1% Yttrium		

TABLE II

METAL INTERFACE MOVEMENT IN NIOBIUM ALLOY SERIES NO. 4 (4% ALUMINUM, 42% TITANIUM, AND ADDED RARE EARTHS) AFTER 8 HOURS IN DRY AIR AT 1000°C

CODE	COMPOSITION	METAL INTERFACE MOVEMENT (Cm)
AA	Niobium	0.035
AB	Niobium	0.088
4A	Base Alloy	0.010
4B	Alloy with 1/4% Cerium	0.030
4C	1% Cerium	0.009
4D	4% Cerium	0.008
4E	1/4% Yttrium	0.062
4F	1% Yttrium	0.050
4G	4% Yttrium	0.023
4H	1/4% Dysprosium	0.008
4I	1% Dysprosium	0.006
4J	4% Dysprosium	0.022

TABLE III

METAL INTERFACE MOVEMENT IN NIOBIUM ALLOY SERIES NO. 5 (6.0% CHROMIUM, 8.7% TITANIUM, AND ADDED RARE EARTHS) AFTER 8 HOURS IN DRY AIR AT 1000°C

CODE	COMPOSITION	METAL INTERFACE MOVEMENT (Cm)
5A	Base Alloy	0.007
5B	Alloy with 1/4% Cerium	0.057
5C	1% Cerium	0.057
5D	4% Cerium	0.014
5E	1/4% Yttrium	0.010
5F	1% Yttrium	0.076
5G	4% Yttrium	0.082
5H	1/4% Dysprosium	0.018
5I	1% Dysprosium	0.020
5J	4% Dysprosium	0.022

TABLE IV

X-RAY DIFFRACTION AT 25°C of $Nb(OH)_5$ AFTER 72 HOURS AT 440°C

Observed 2θ	Observed Sin $^2\theta$	hkl	Calc. Sin $^2\theta$	Sin $^2\theta$ Calc.-Obs
27.6	.0384	001	.0384	.0000
28.6	.0610	110	.0609	.0001
36.8	.0996	111	.0993	.0003
46.2	.1539	002	.1536	.0003
50.7	.1833	102	.1739	.0094
55.2	.2146	112	.2145	.0001
56.1	.2211	301	.2211	.0000
59.1	.2433	220	.2436	.0003
64.2	.2824	221	.2820	.0004
71.0	.3372	302	.3363	.0009
78.2	.3978	222	.3972	.0006
79.3	.4072	113	.4065	.0007
81.5	.4261	410	.4263	.0002
86.2	.4669	411	.4647	.0022

$$\text{Sin}^2\theta = .0203\,(L^2 + hk + k^2) + .03845.1^2$$

$$A_o^2 = \frac{.79237}{.0203} = 39.033\ A^{o2};\quad A_o = 6.25\ A^o$$

$$C_o^2 = \frac{.59427}{.03845} = 15.456\ A^{o2};\quad C_o = 3.93\ A^o$$

TABLE V

METALLOGRAPHIC OBSERVATIONS OF THE ATMOSPHERIC CORROSION LAYER ON SOME NIOBIUM ALLOYS

Metallographic Sample No.	Nominal Alloy Composition Wt. % Nb	W	Ti	Mo	Pt	Y	Er	Film Observation
1295	78	20	2	-	-	-	-	Very thin layer.
1294	78	20	2	-	-	-	-	Questionable layer.
1282	77.5	20	2	-	-	0.5	-	Well defined adherent layer.
1283	77	20	2	-	-	1.	-	Well defined adherent layer.
1284	76	20	2	-	-	2.	-	Well defined adherent layer.
1285	77.5	20	2	-	-	-	0.5	Well defined adherent layer.
1286	77	20	2	-	-	-	1.	Well defined adherent layer.
1287	76	20	2	-	-	-	2.	Well defined adherent layer.
1296	78	15	-	5	2	-	-	No layer evident.
1288	77.5	15	-	5	2	0.5	-	No layer evident.
1289	77	15	-	5	2	1.	-	Very thin layer.
1290	76	15	-	5	2	2.	-	Thin layer.
1291	77.5	15	-	5	2	-	0.5	No layer evident.
1292	77	15	-	5	2	-	1.	No layer evident.
1293	76	15	-	5	2	-	2.	No layer evident.

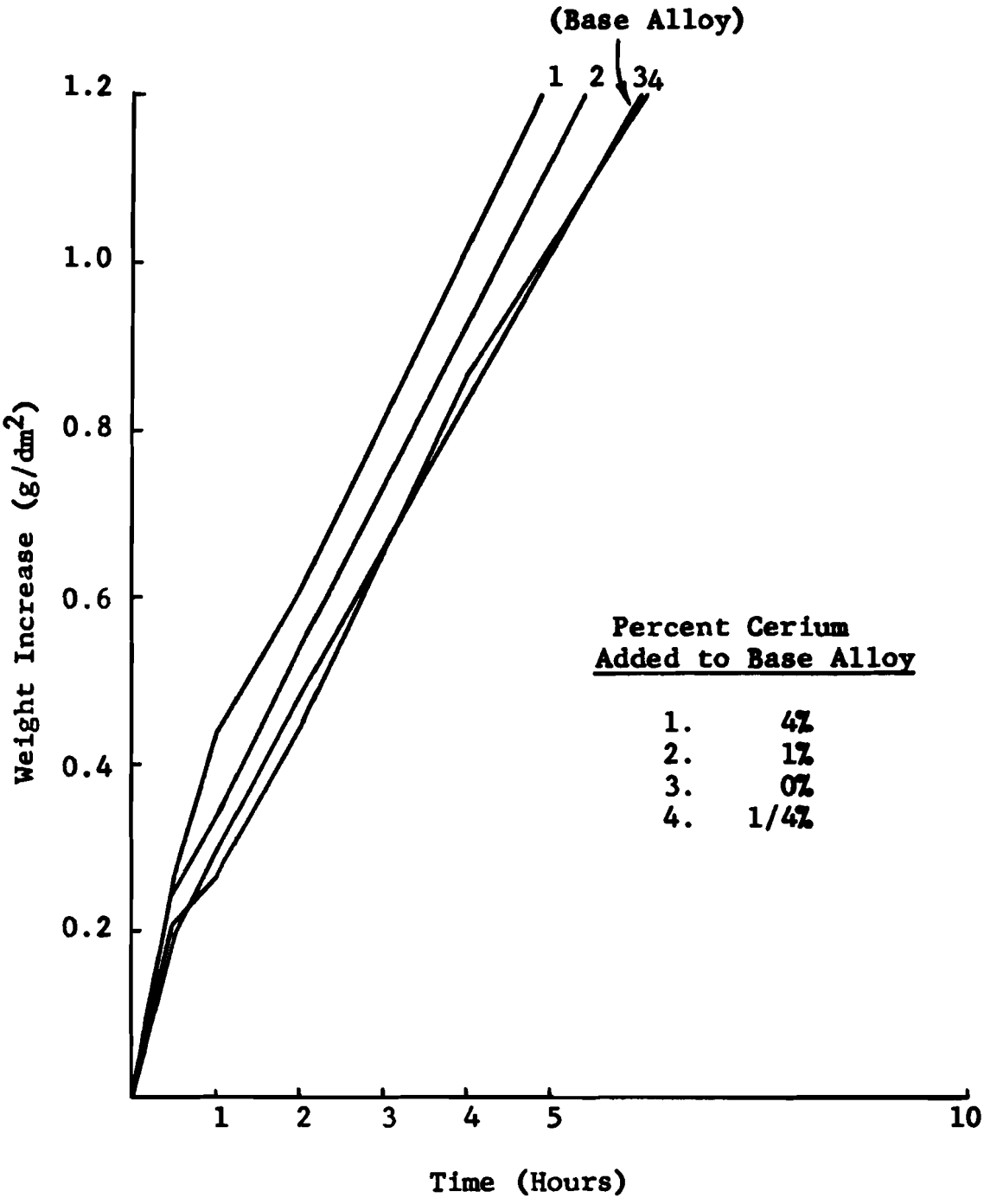

Figure 1. Atmospheric Corrosion of a Niobium Alloy Containing 6.0% Chromium and 8.7% Titanium with Cerium Additions. Dry Air at 1000°C.

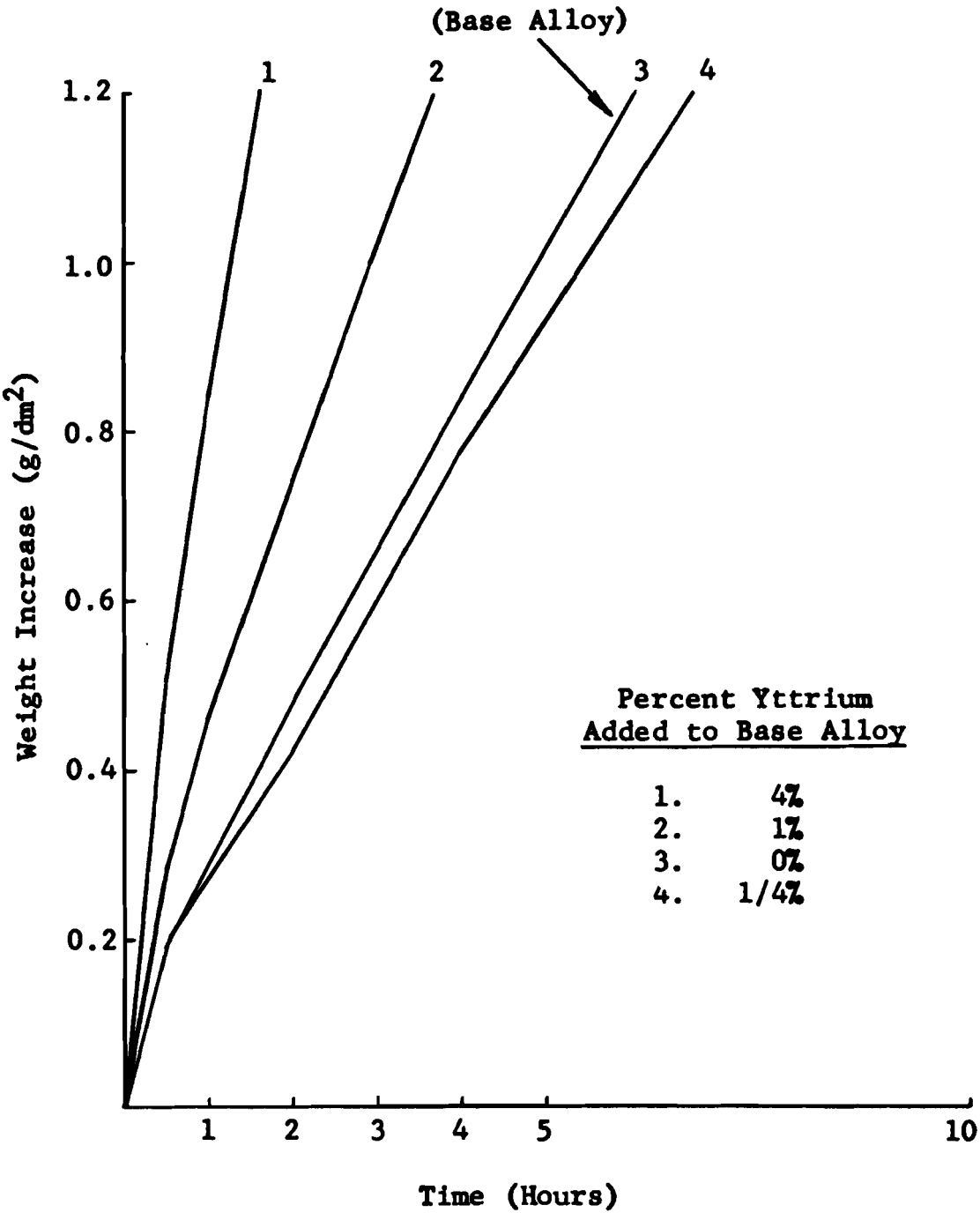

Figure 2. Atmospheric Corrosion of a Niobium Alloy Containing 6.0% Chromium and 8.7% Titanium with Yttrium Additions. Dry Air at 1000°C.

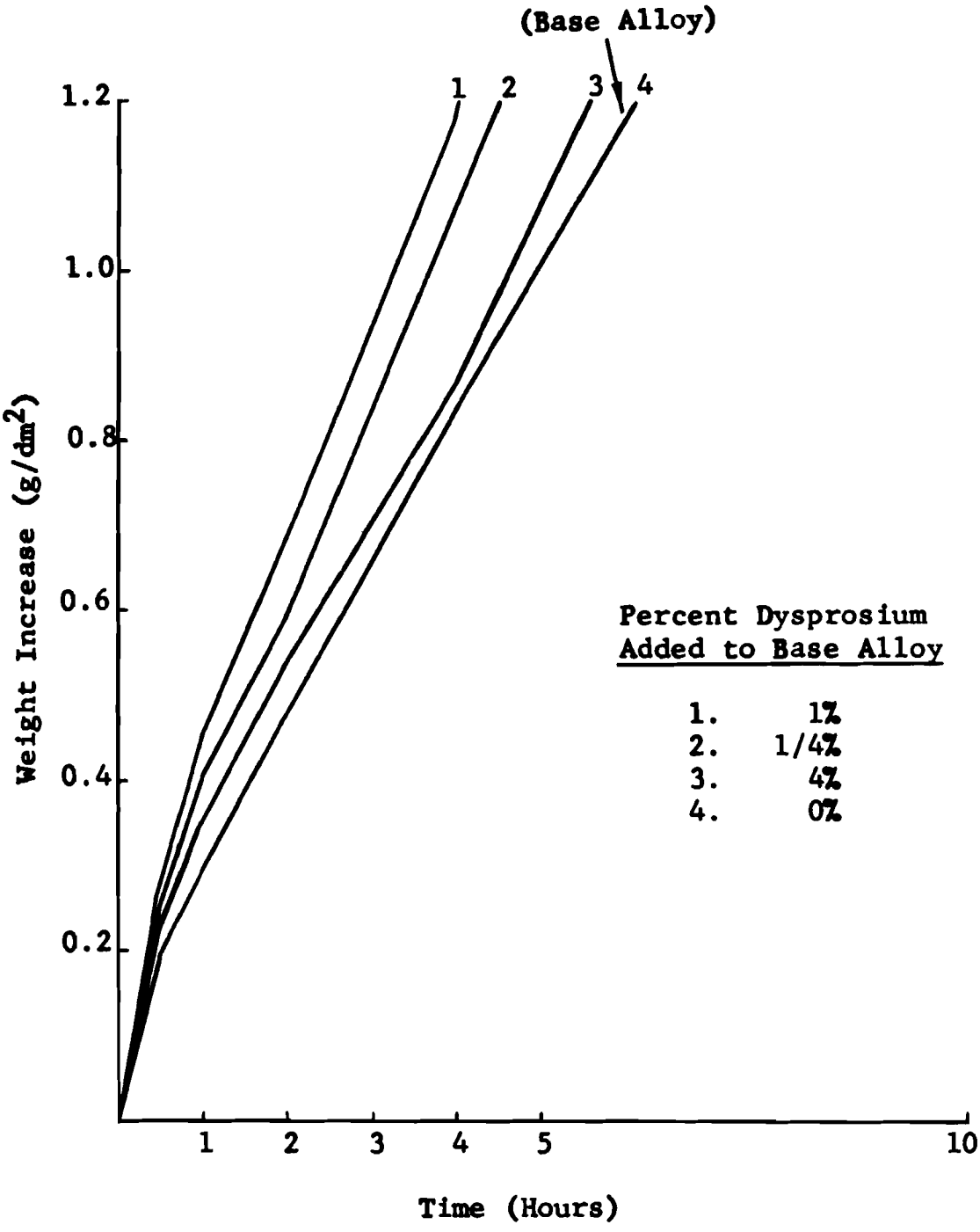

Figure 3. Atmospheric Corrosion of a Niobium Alloy Containing 6.0% Chromium and 8.7% Titanium with Dysprosium Additions. Dry Air at 1000°C.

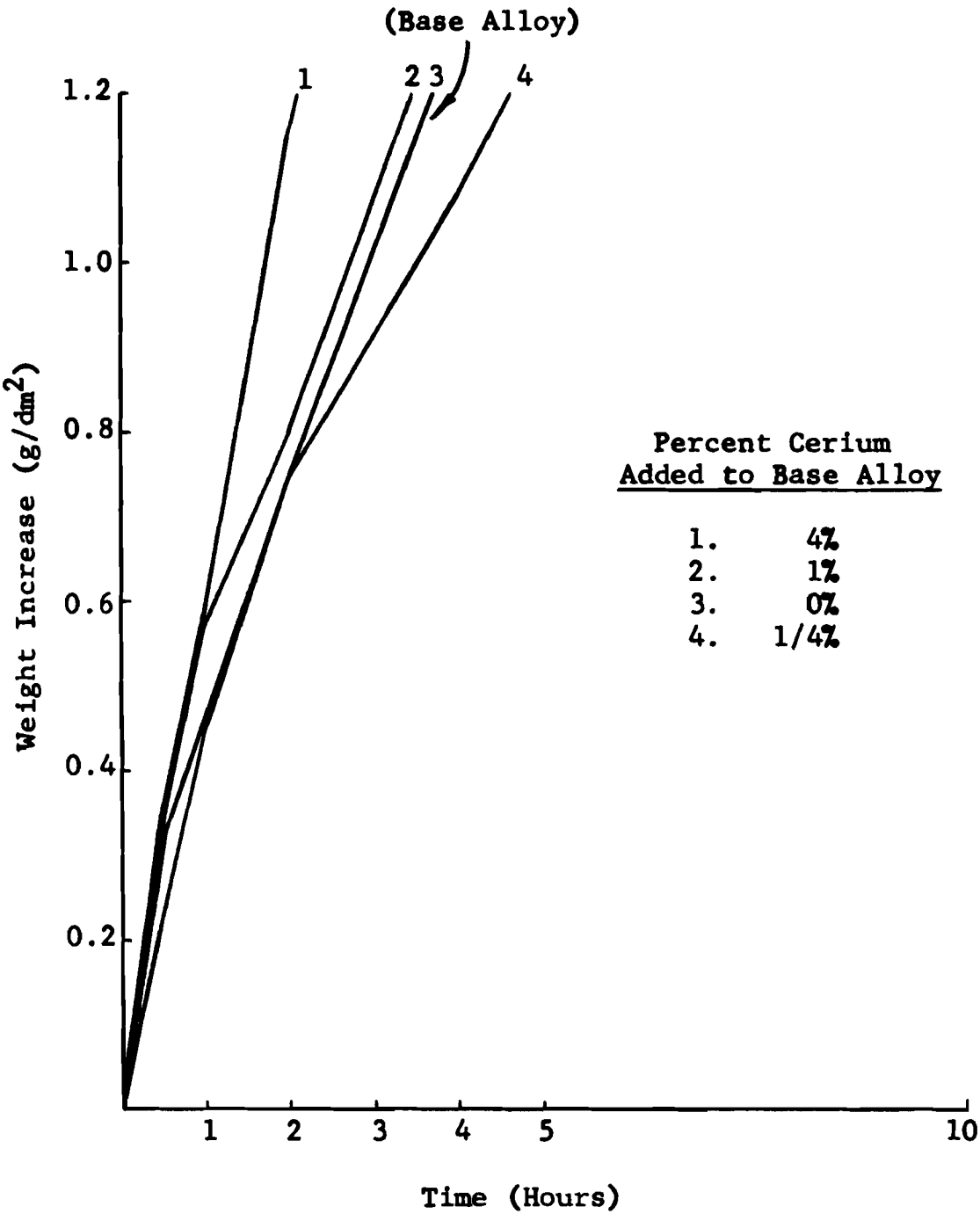

Figure 4. Atmospheric Corrosion of a Niobium Alloy Containing 11.7% Titanium and 3.1% Vanadium with Cerium Additions. Dry Air at 1000°C.

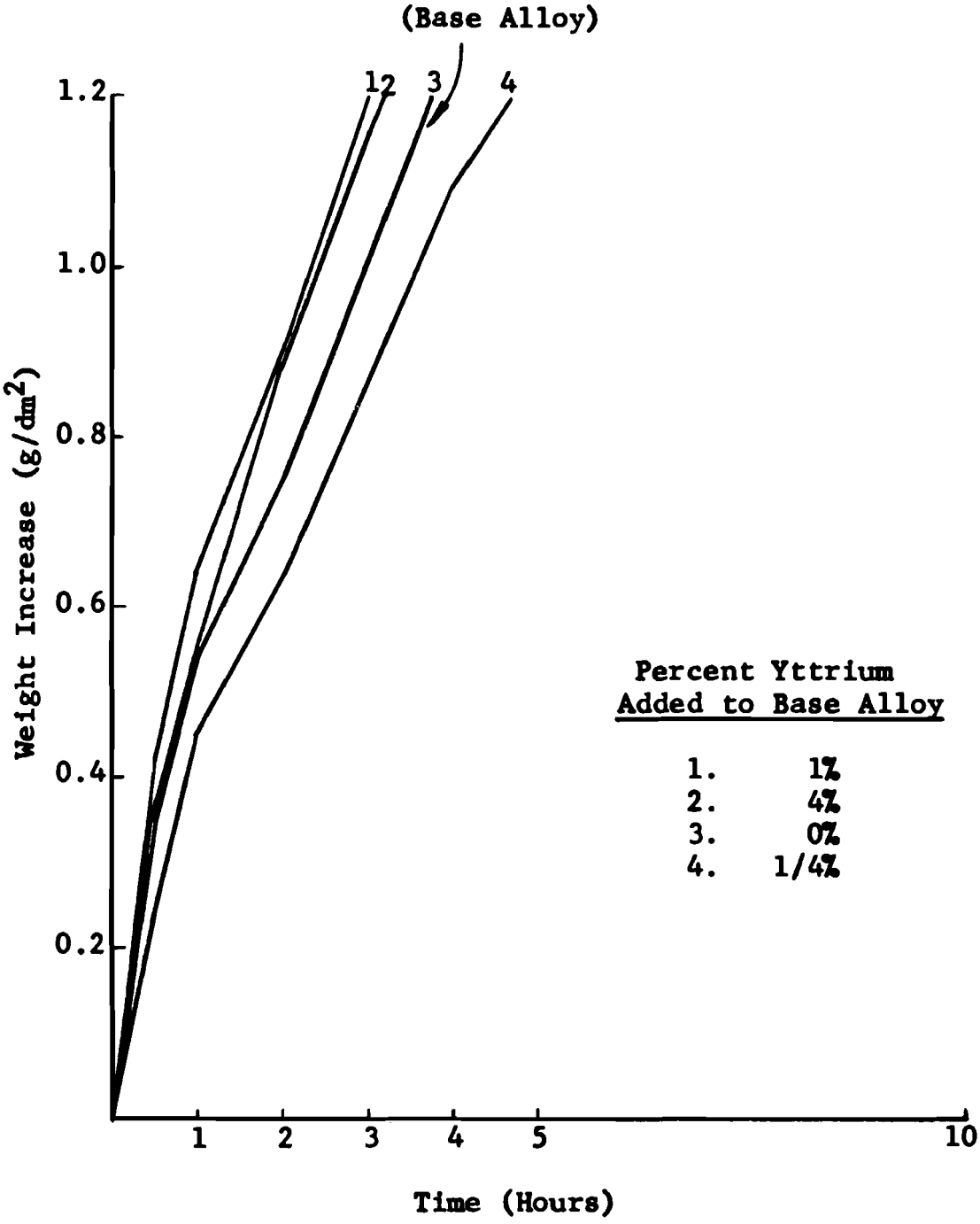

Figure 5. Atmospheric Corrosion of a Niobium Alloy Containing 11.7% Titanium and 3.1% Vanadium with Yttrium Additions. Dry Air at 1000°C.

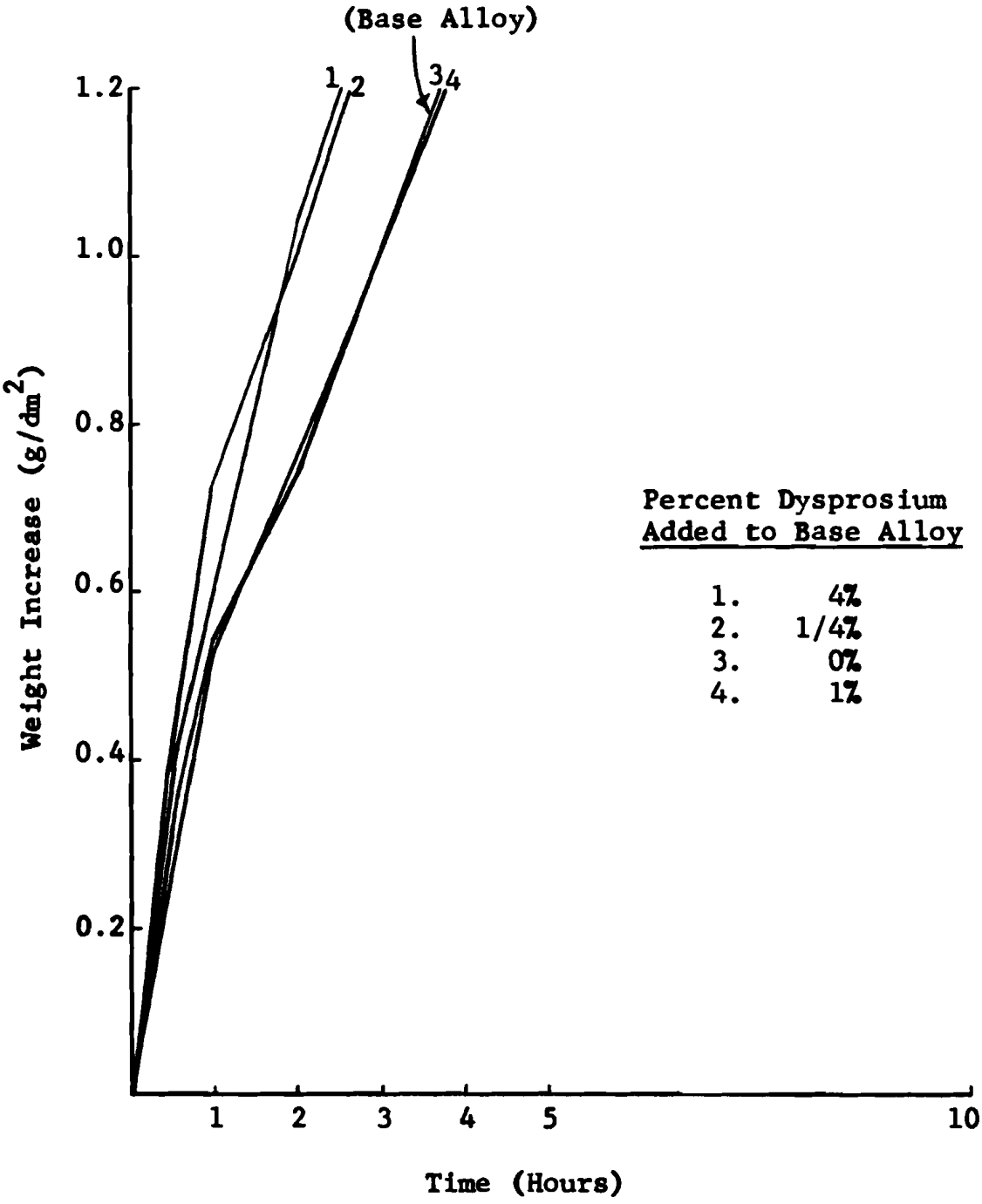

Figure 6. Atmospheric Corrosion of a Niobium Alloy Containing 11.7% Titanium and 3.1% Vanadium with Dysprosium Additions. Dry Air at 1000°C.

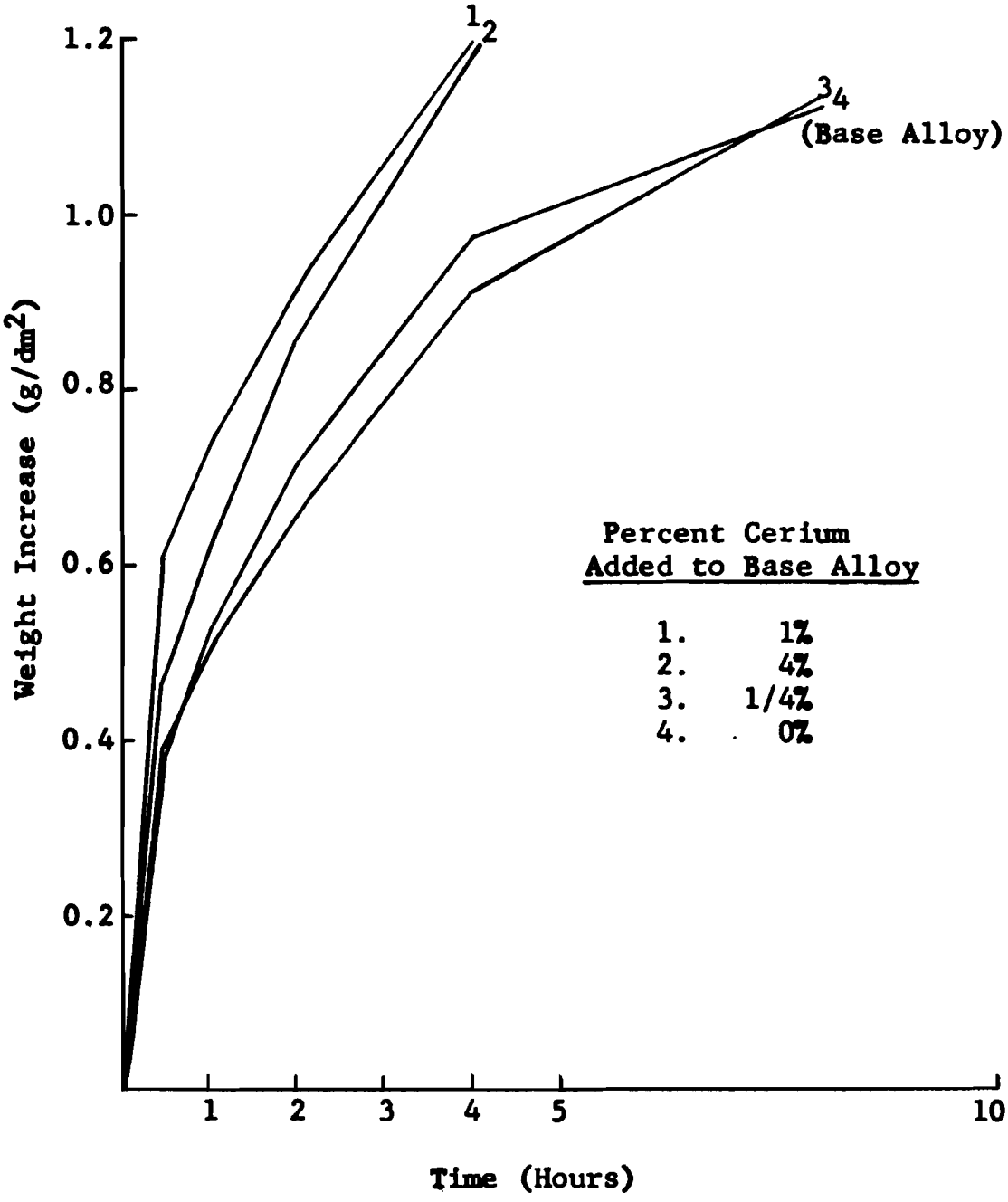

Figure 7. Atmospheric Corrosion of a Niobium Alloy Containing 11.3% Titanium and 7.9% Molybdenum with Cerium Additions. Dry Air at 1000°C.

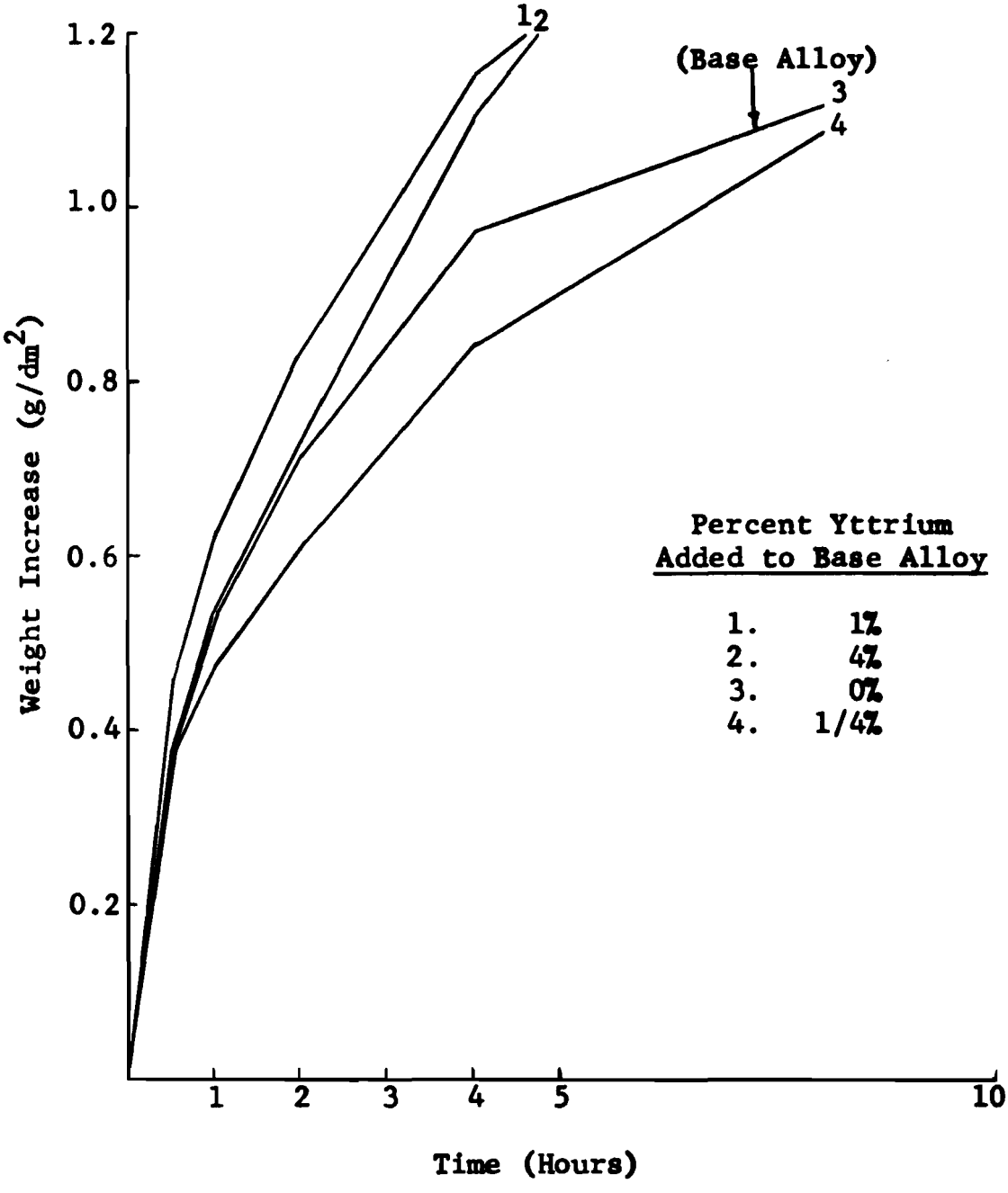

Figure 8. Atmospheric Corrosion of a Niobium Alloy Containing 11.3% Titanium and 7.9% Molybdenum with Yttrium Additions. Dry Air at 1000°C.

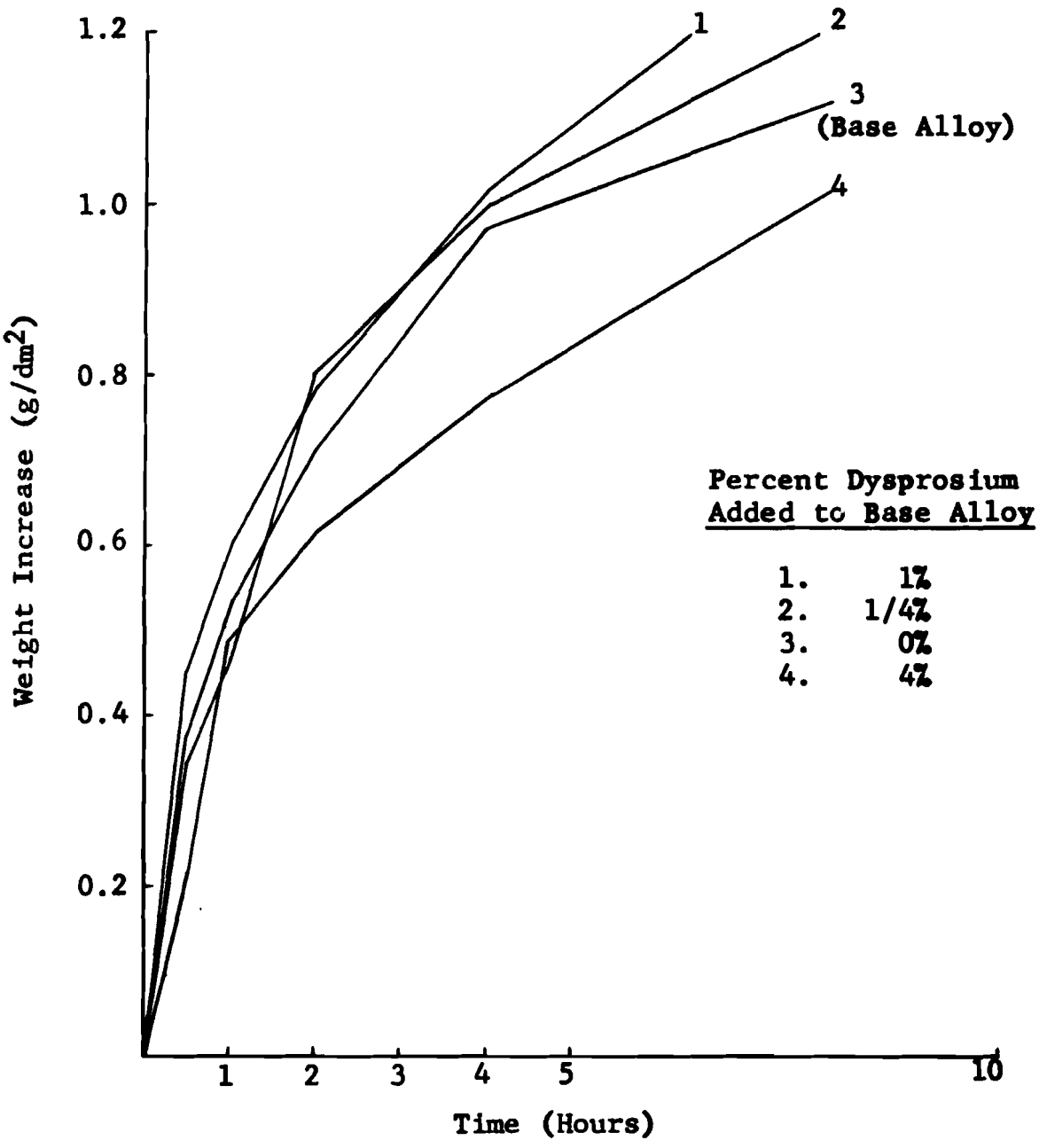

Figure 9. Atmospheric Corrosion of a Niobium Alloy Containing 11.3% Titanium and 7.9% Molybdenum with Dysprosium Additions. Dry Air at 1000°C.

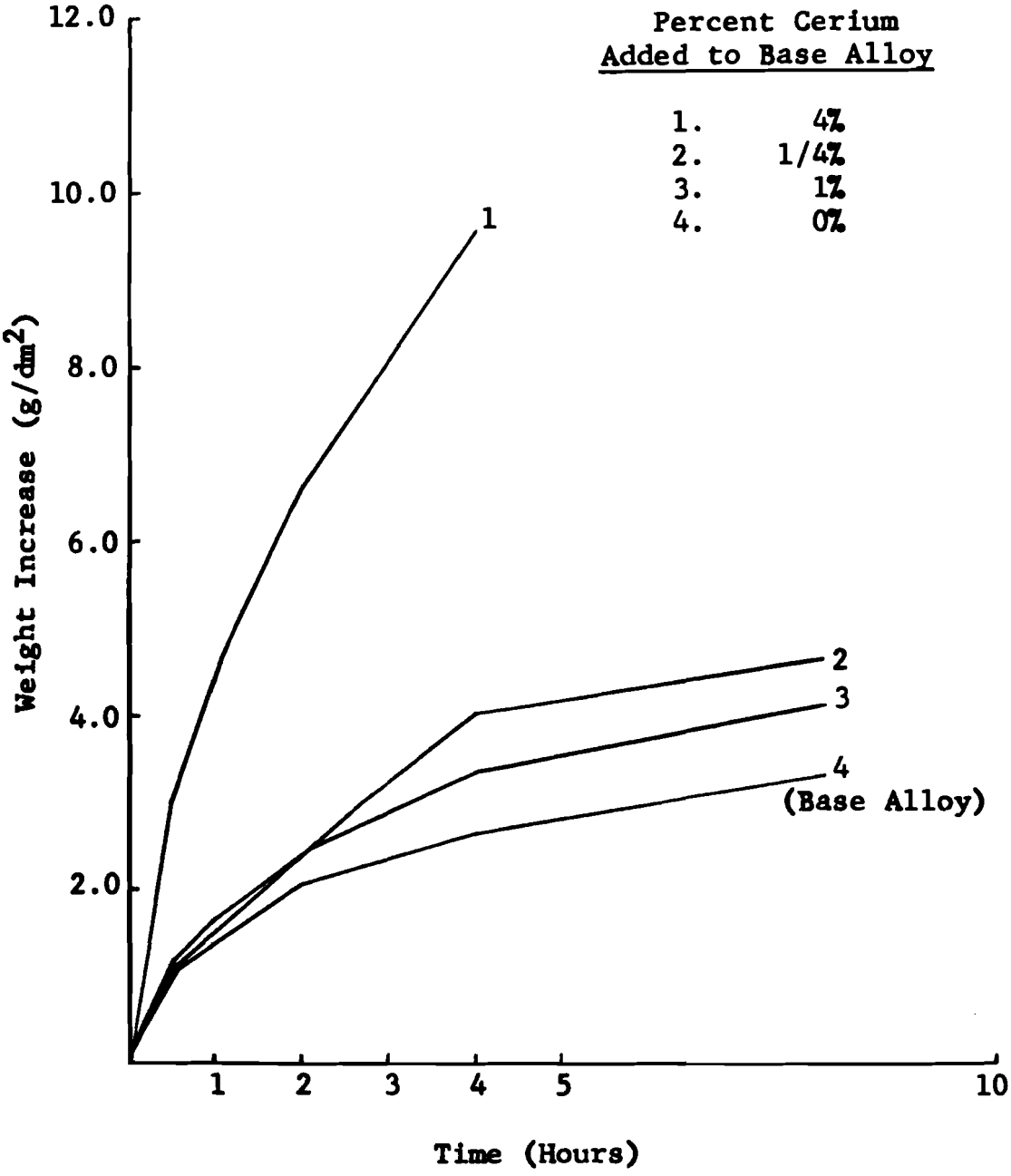

Figure 10. Atmospheric Corrosion of Niobium Alloy Containing 45.7% Zirconium and 2.5% Titanium with Cerium Additions. Dry Air at 1000°C.

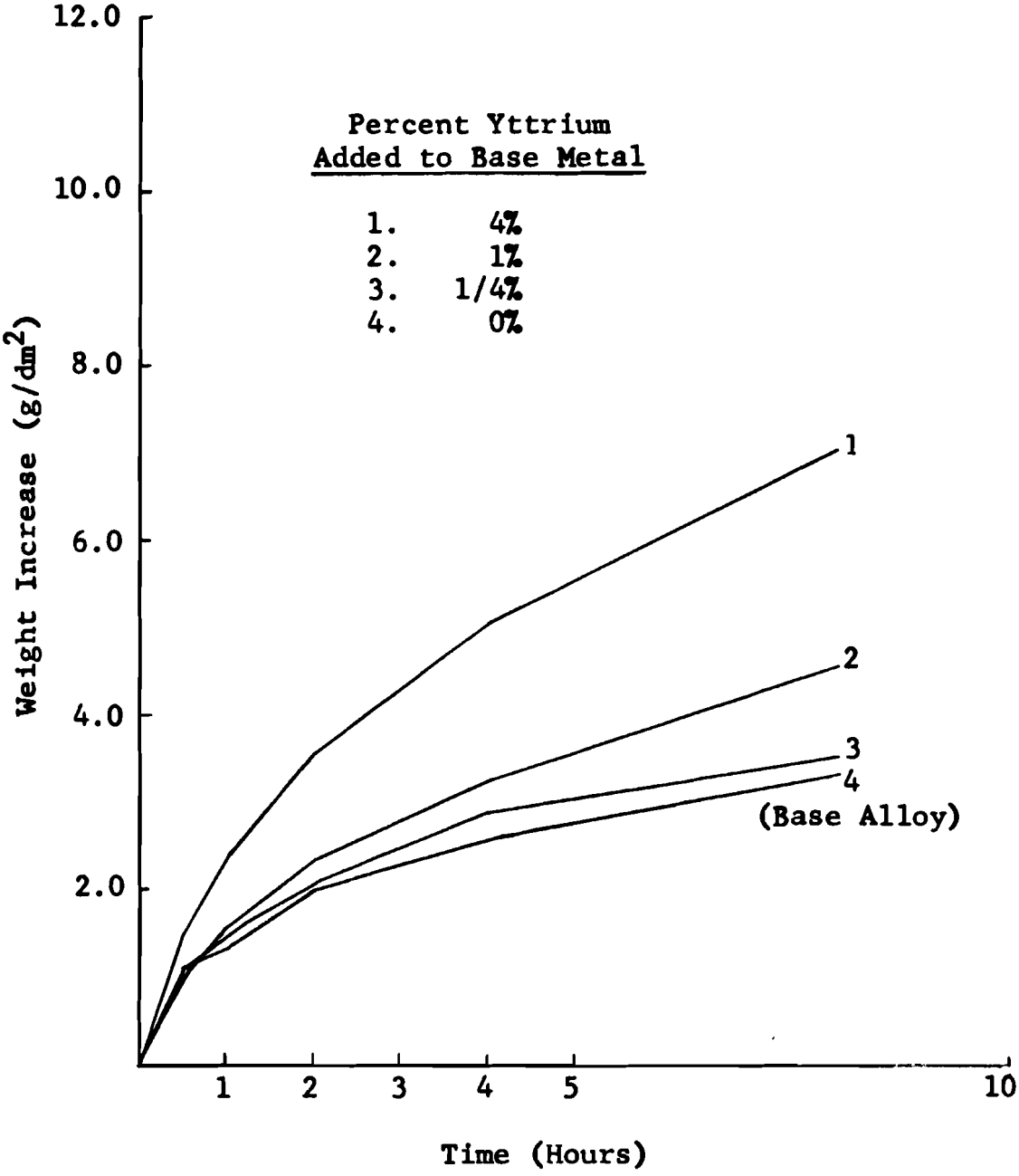

Figure 11. Atmospheric Corrosion of a Niobium Alloy Containing 45.7% Zirconium and 2.5% Titanium with Yttrium Additions. Dry Air at 1000°C.

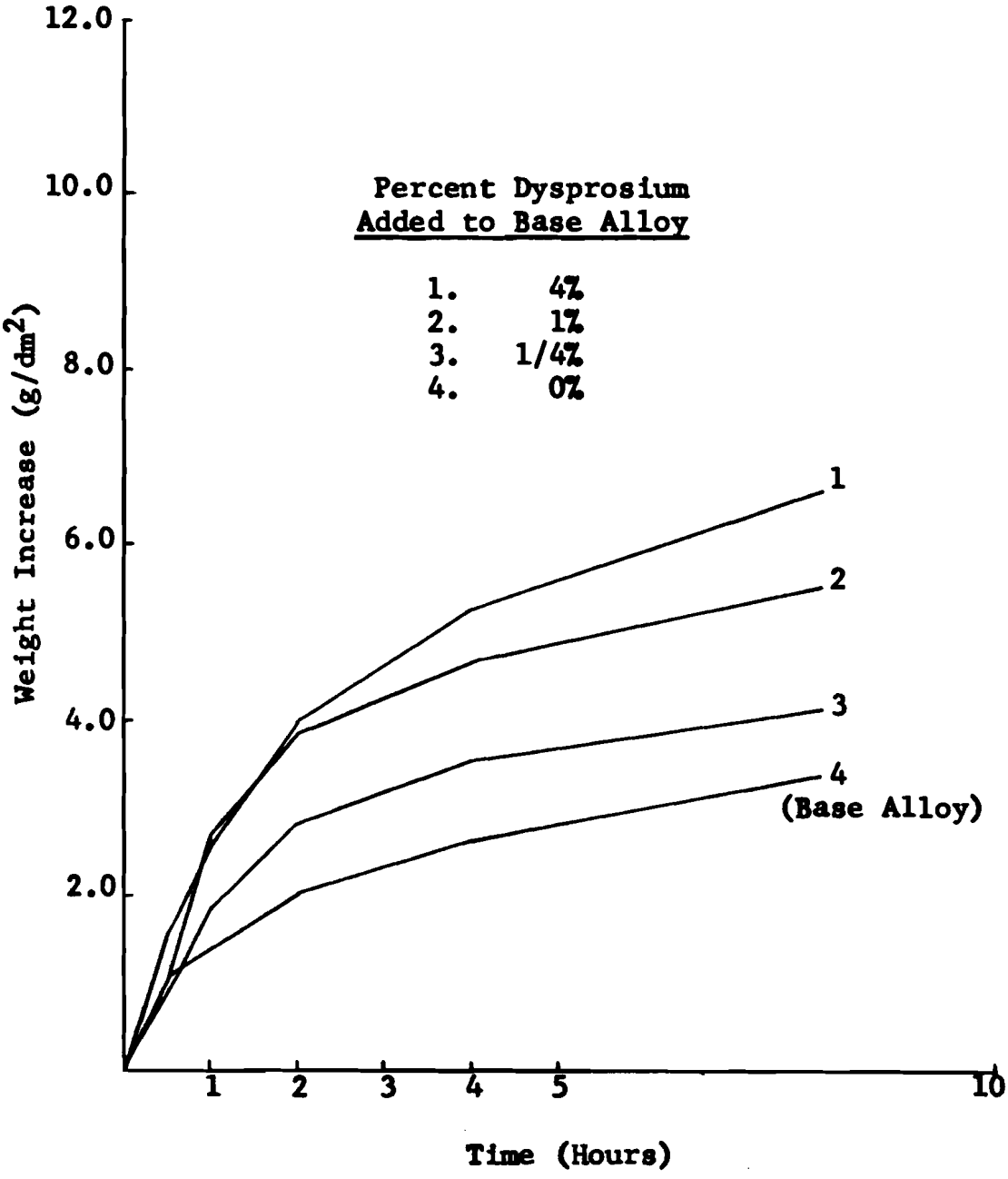

Figure 12. Atmospheric Corrosion of a Niobium Alloy Containing 45.7% Zirconium and 2.5% Titanium with Dysprosium Additions. Dry Air at 1000°C.

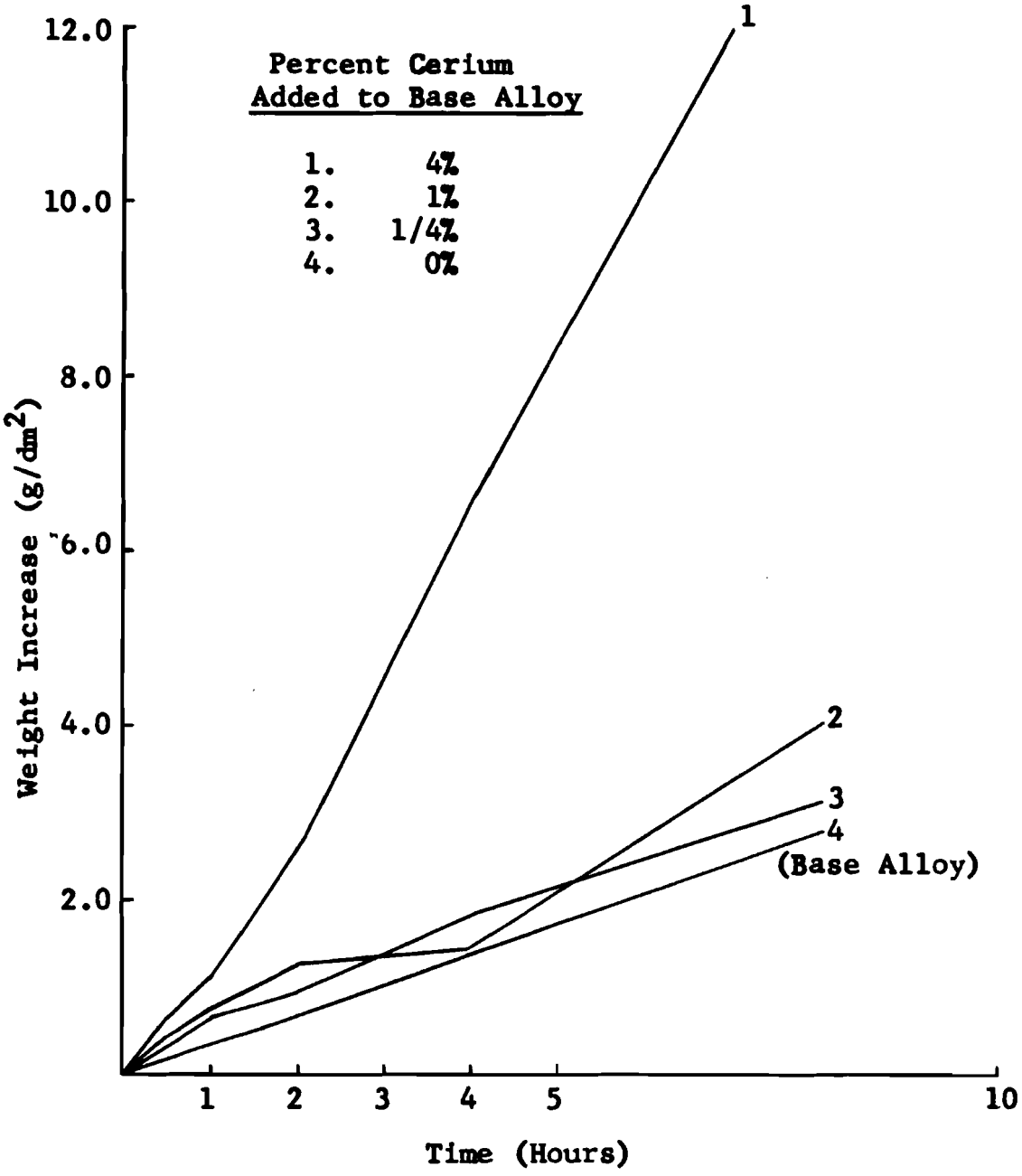

Figure 13. Atmospheric Corrosion of a Niobium Alloy Containing 3% Aluminum and 3% Vanadium with Cerium Additions. Dry Air at 1000°C.

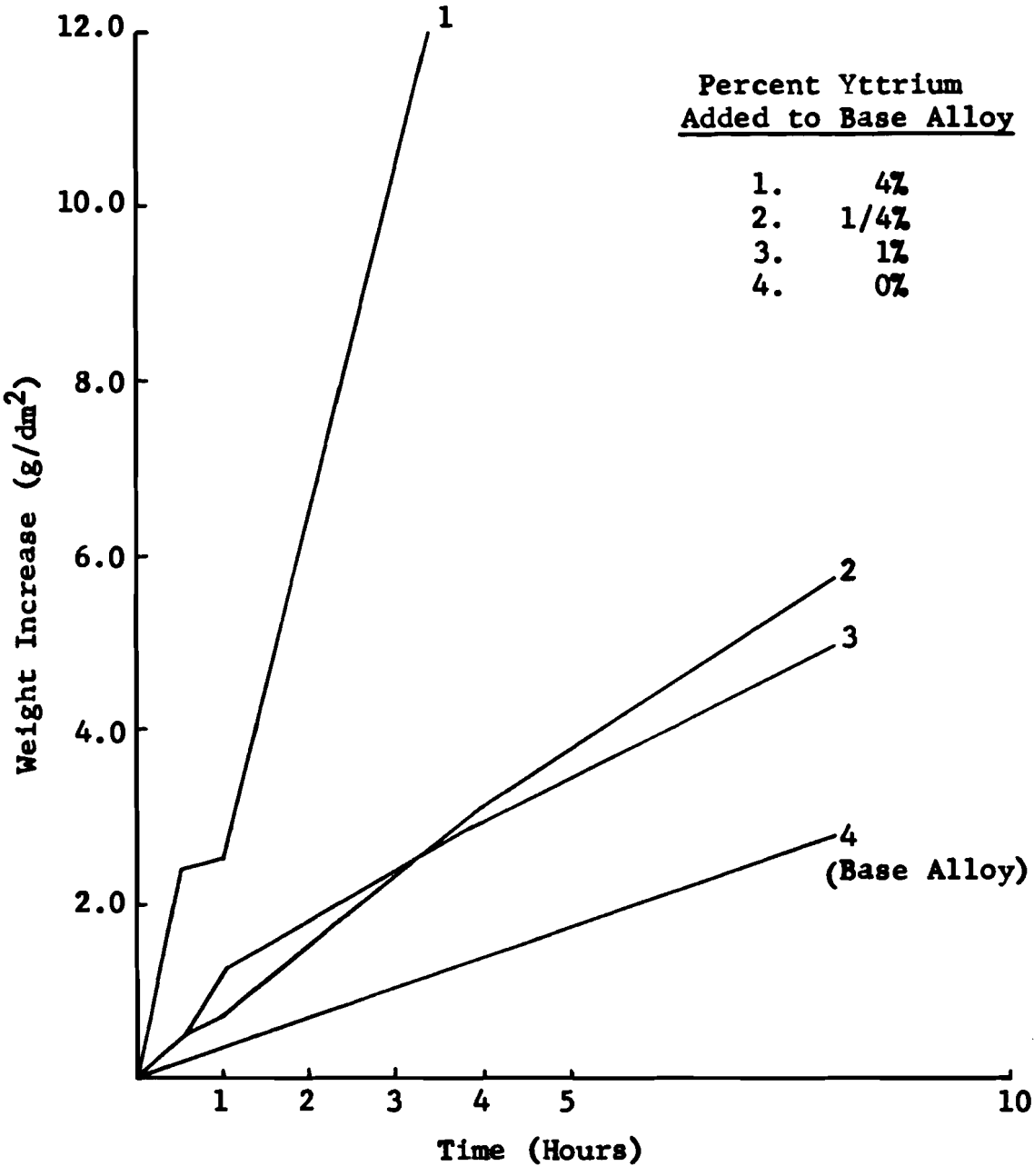

Figure 14. Atmospheric Corrosion of a Niobium Alloy Containing 3% Aluminum and 3% Vanadium with Yttrium Additions. Dry Air at 1000°C.

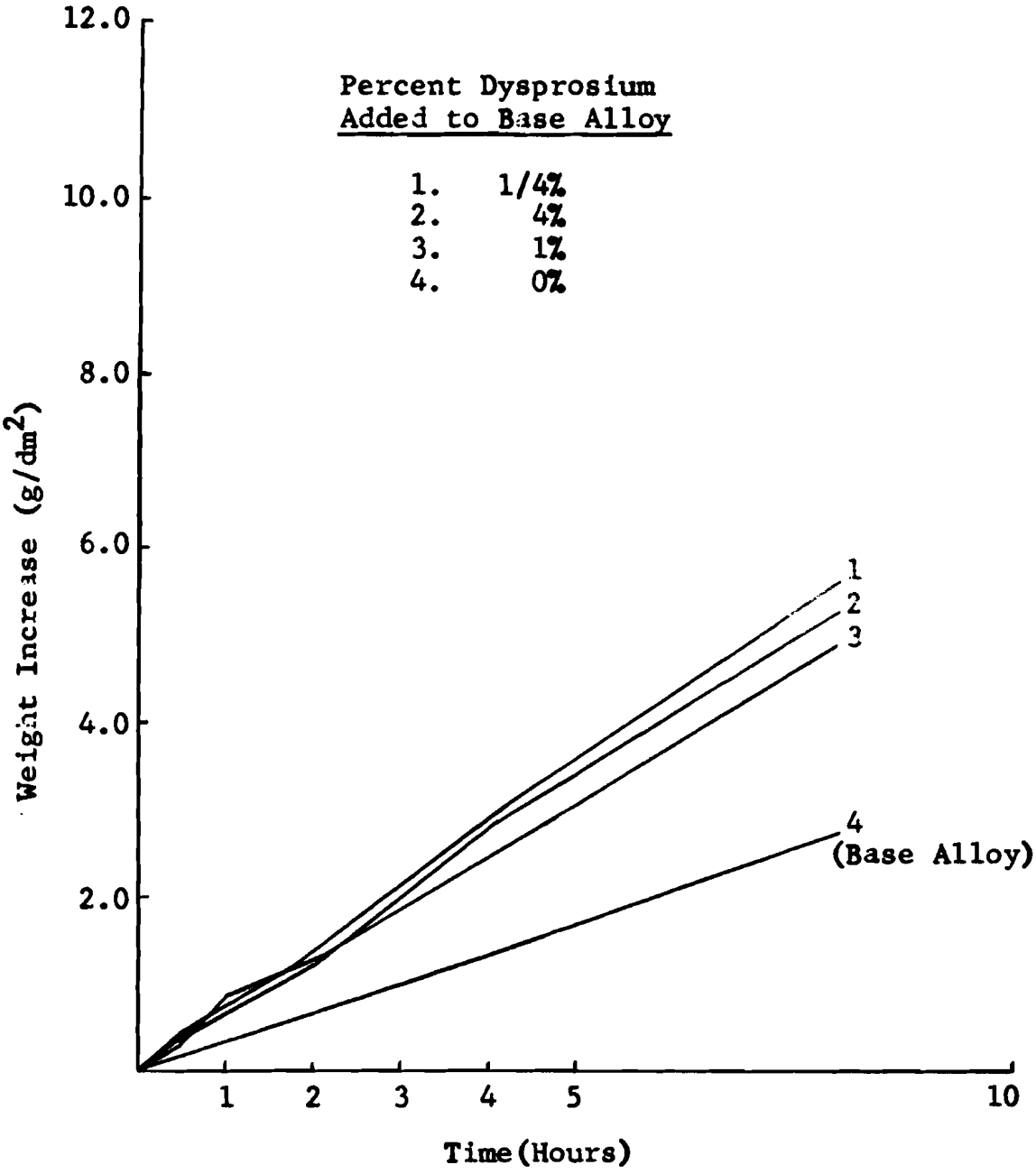

Figure 15. Atmospheric Corrosion of a Niobium Alloy Containing 3% Aluminum and 3% Vanadium with Dysprosium Additions. Dry Air at 1000°C.

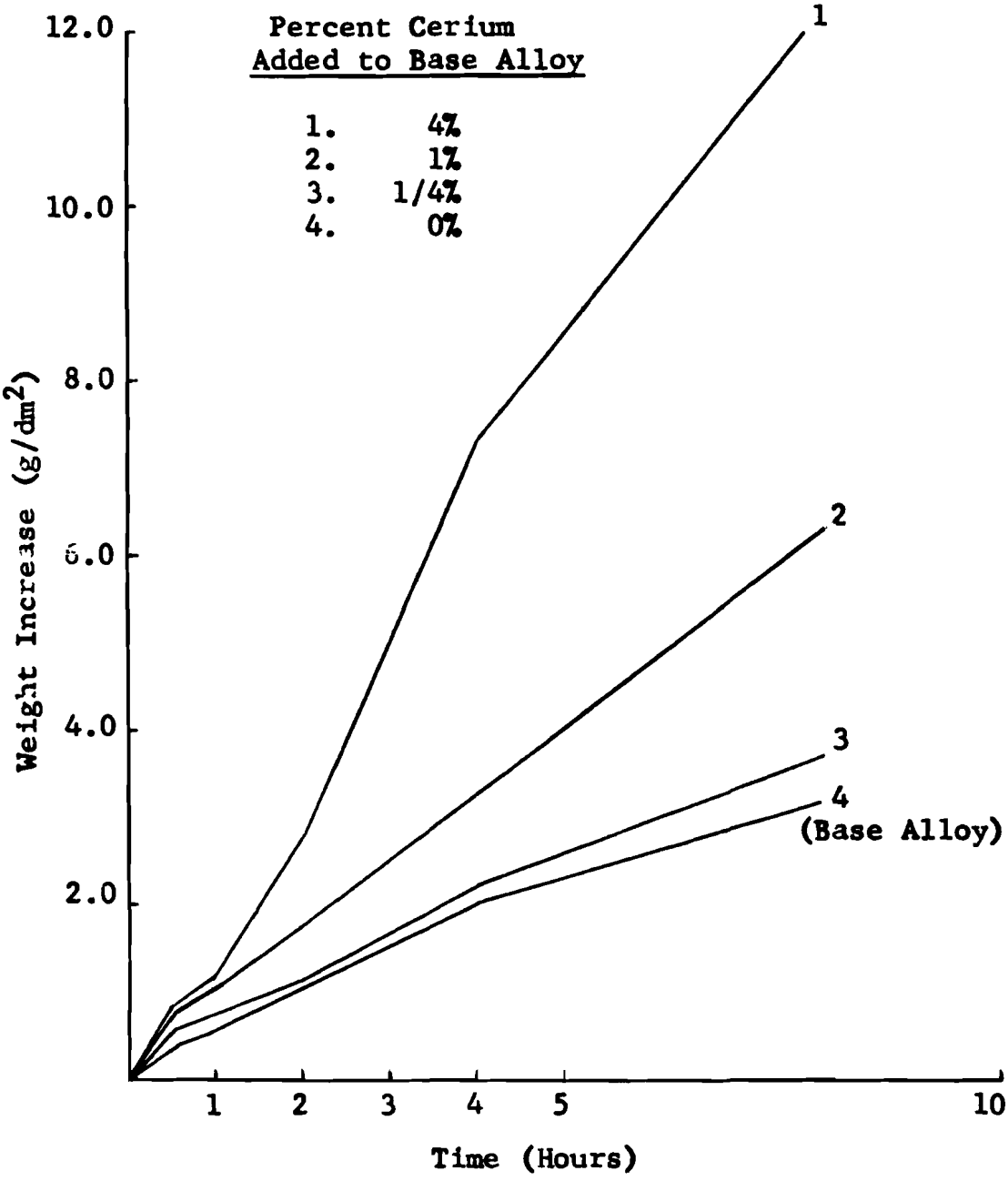

Figure 16. Atmospheric Corrosion of a Niobium Alloy Containing 7.0% Titanium and 0.8% Zirconium with Cerium Additions. Dry Air at 1000°C.

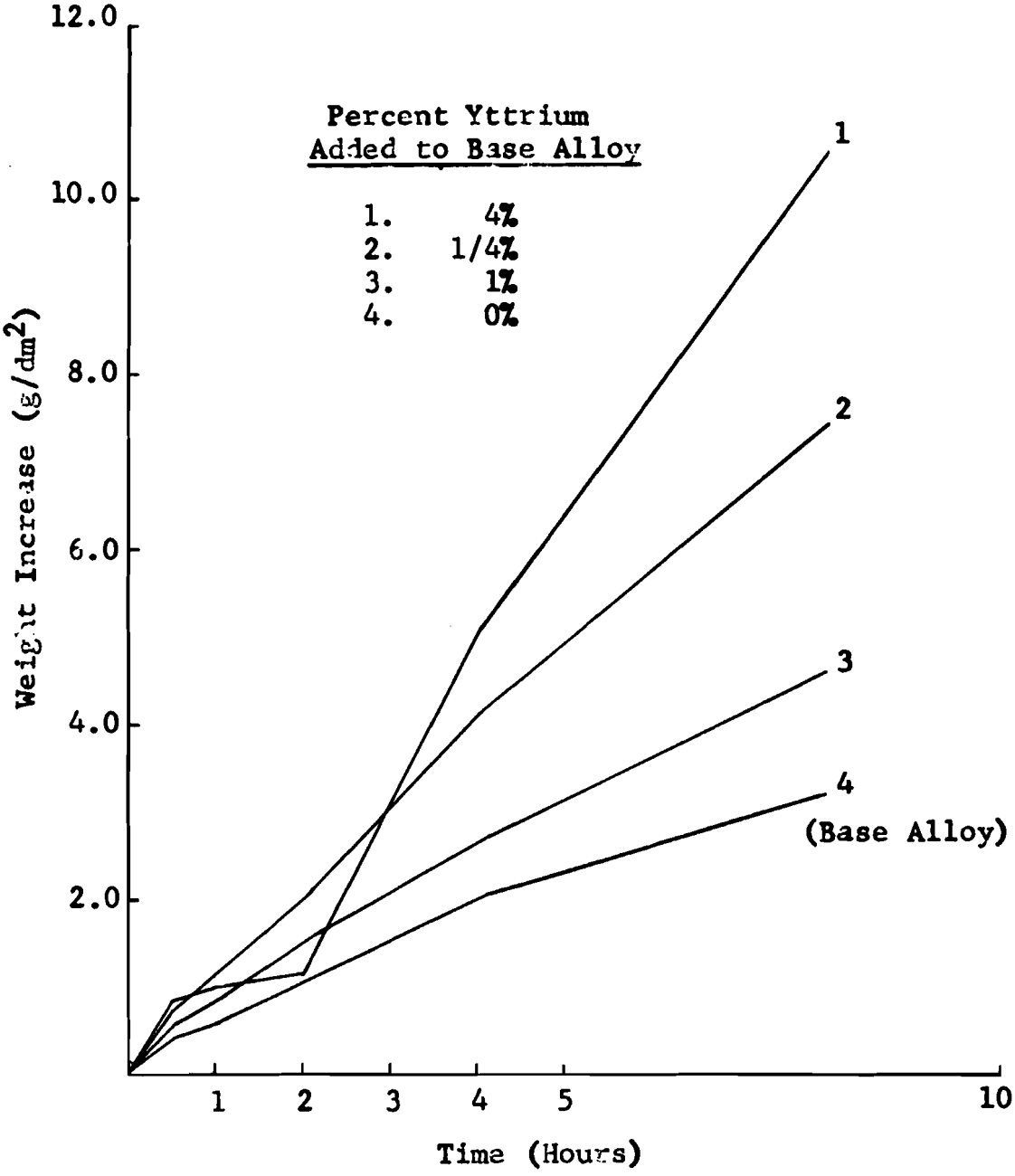

Figure 17. Atmospheric Corrosion of a Niobium Alloy Containing 7.0% Titanium and 0.8% Zirconium with Yttrium Additions. Dry Air at 1000°C.

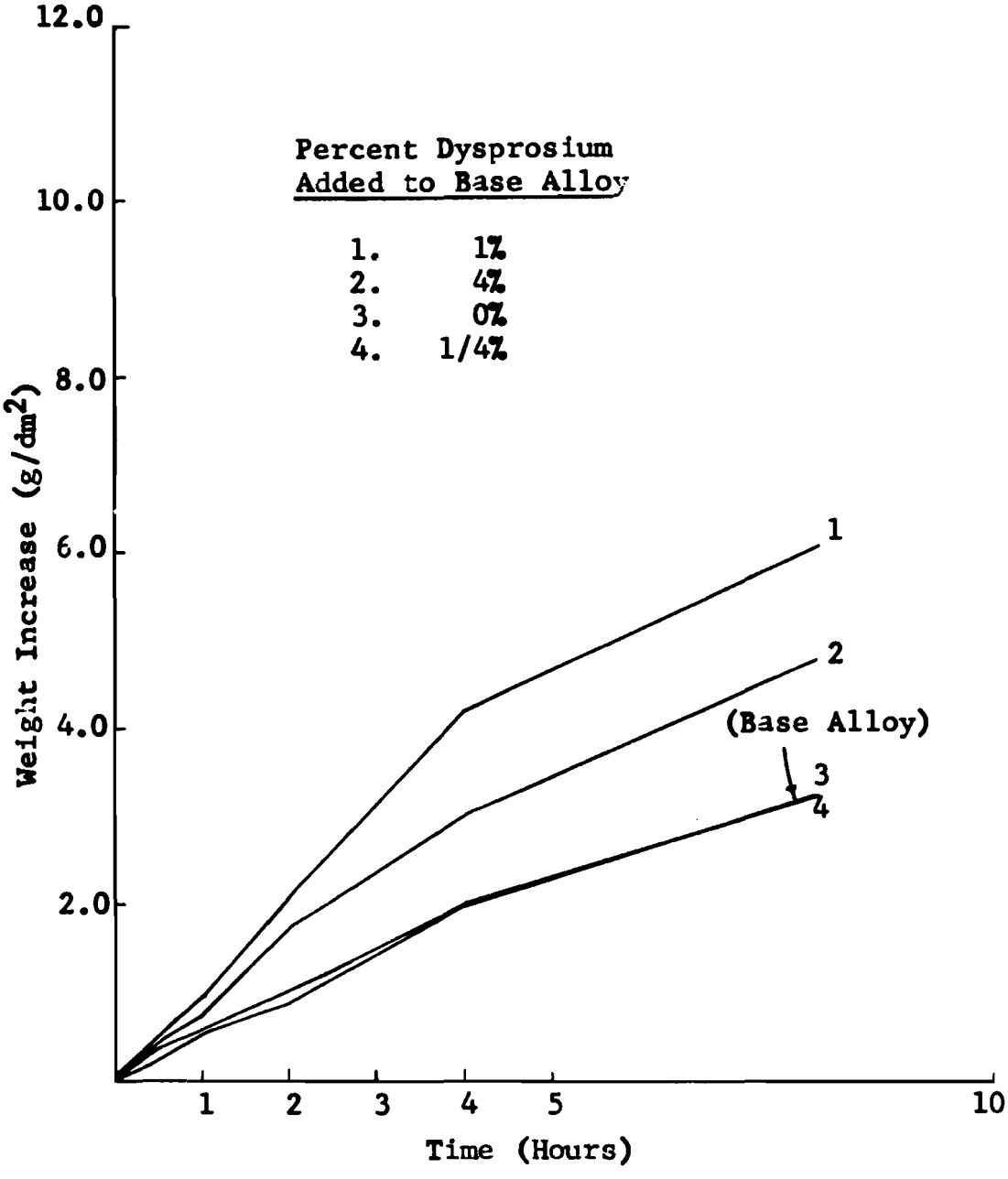

Figure 18. Atmospheric Corrosion of a Niobium Alloy Containing 7.0% Titanium and 0.8% Zirconium with Dysprosium Additions. Dry Air at 1000°C.

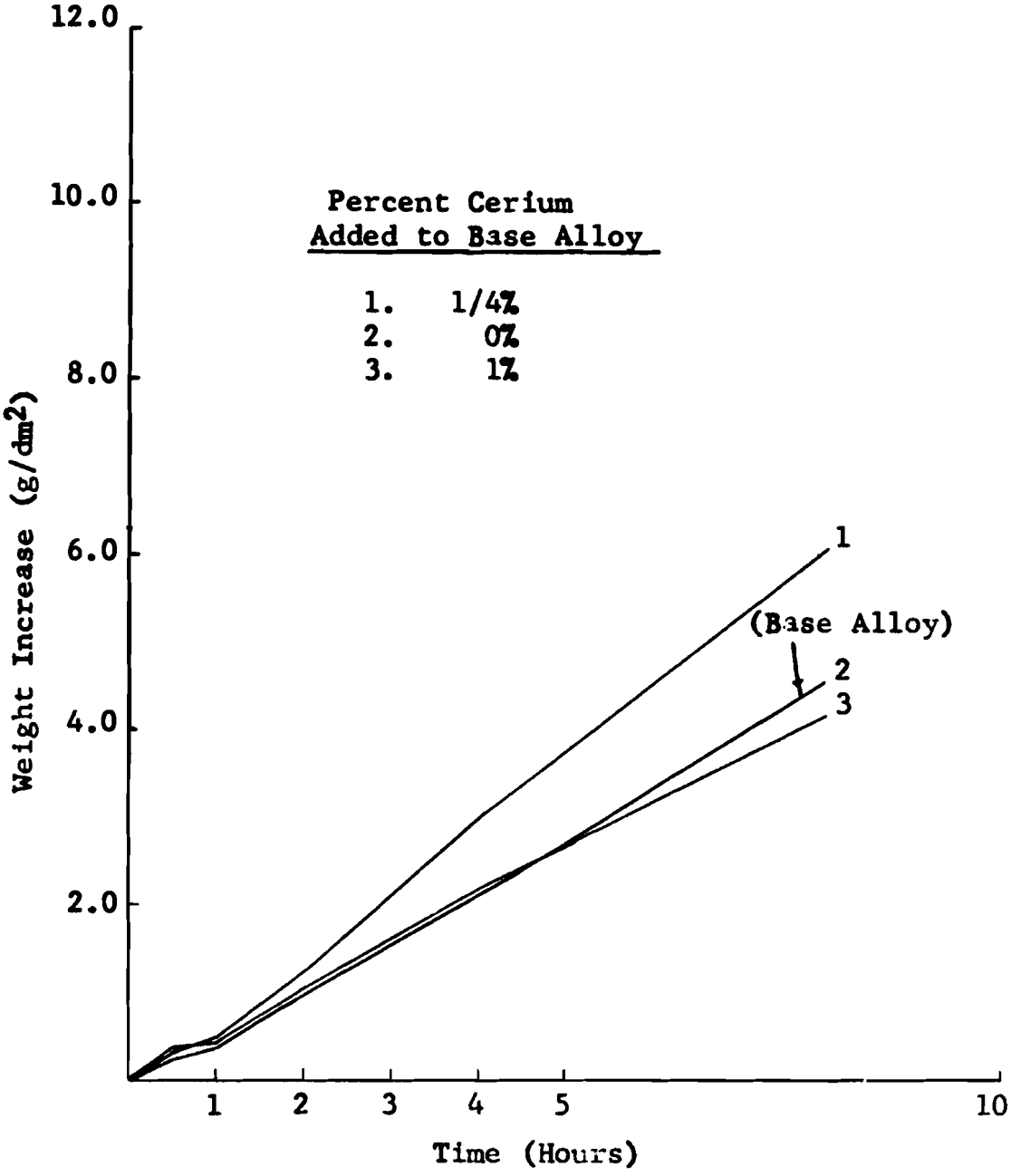

Figure 19. Atmospheric Corrosion of a Niobium Alloy Containing 7% Titanium and 28% Tungsten with Cerium Additions. Dry Air at 1000°C.

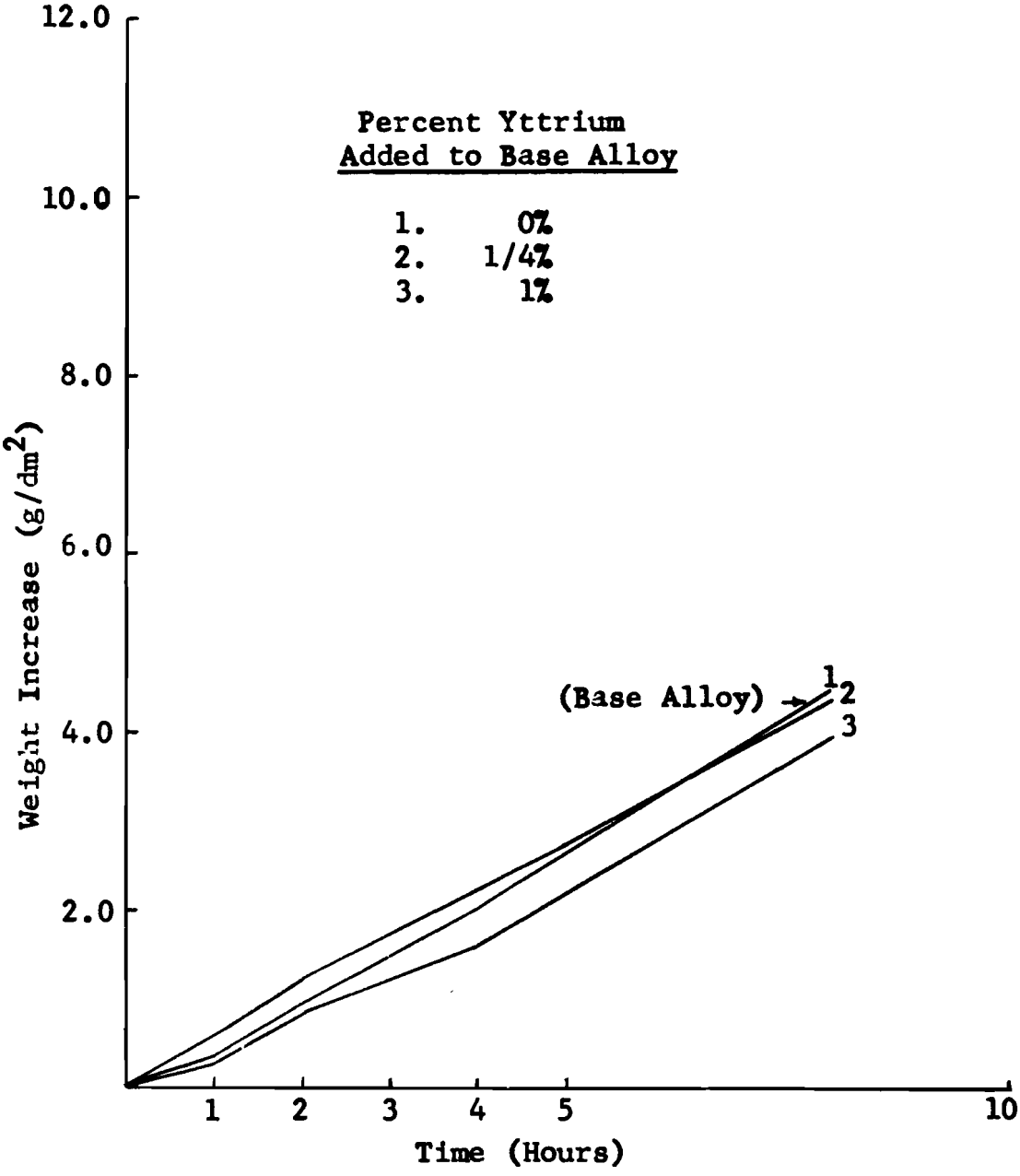

Figure 20. Atmospheric Corrosion of a Niobium Alloy Containing 7% Titanium and 28% Tungsten with Yttrium Additions. Dry Air at 1000°C.

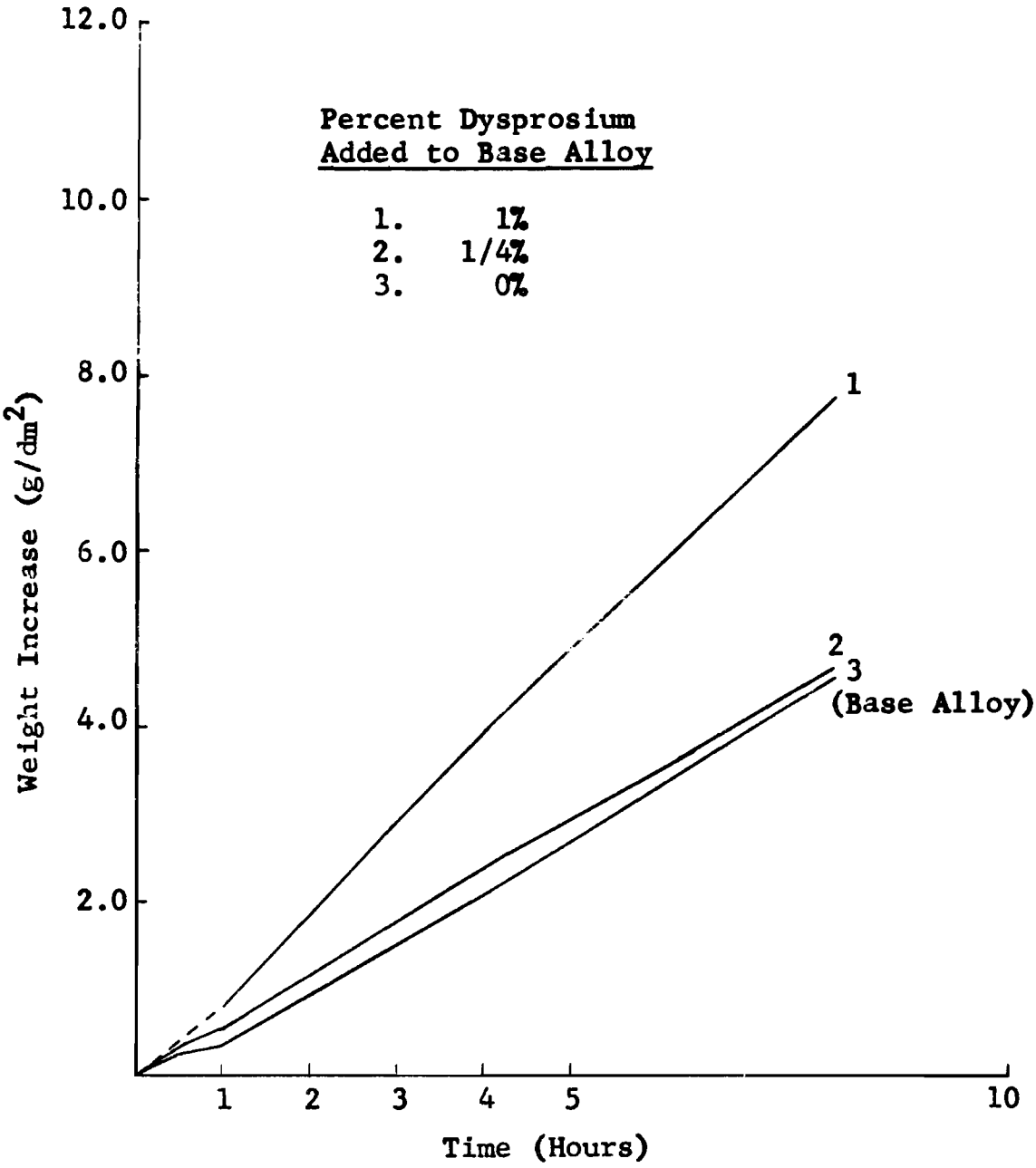

Figure 21. Atmospheric Corrosion of a Niobium Alloy Containing 7% Titanium and 28% Tungsten with Dysprosium Additions. Dry Air at 1000°C.

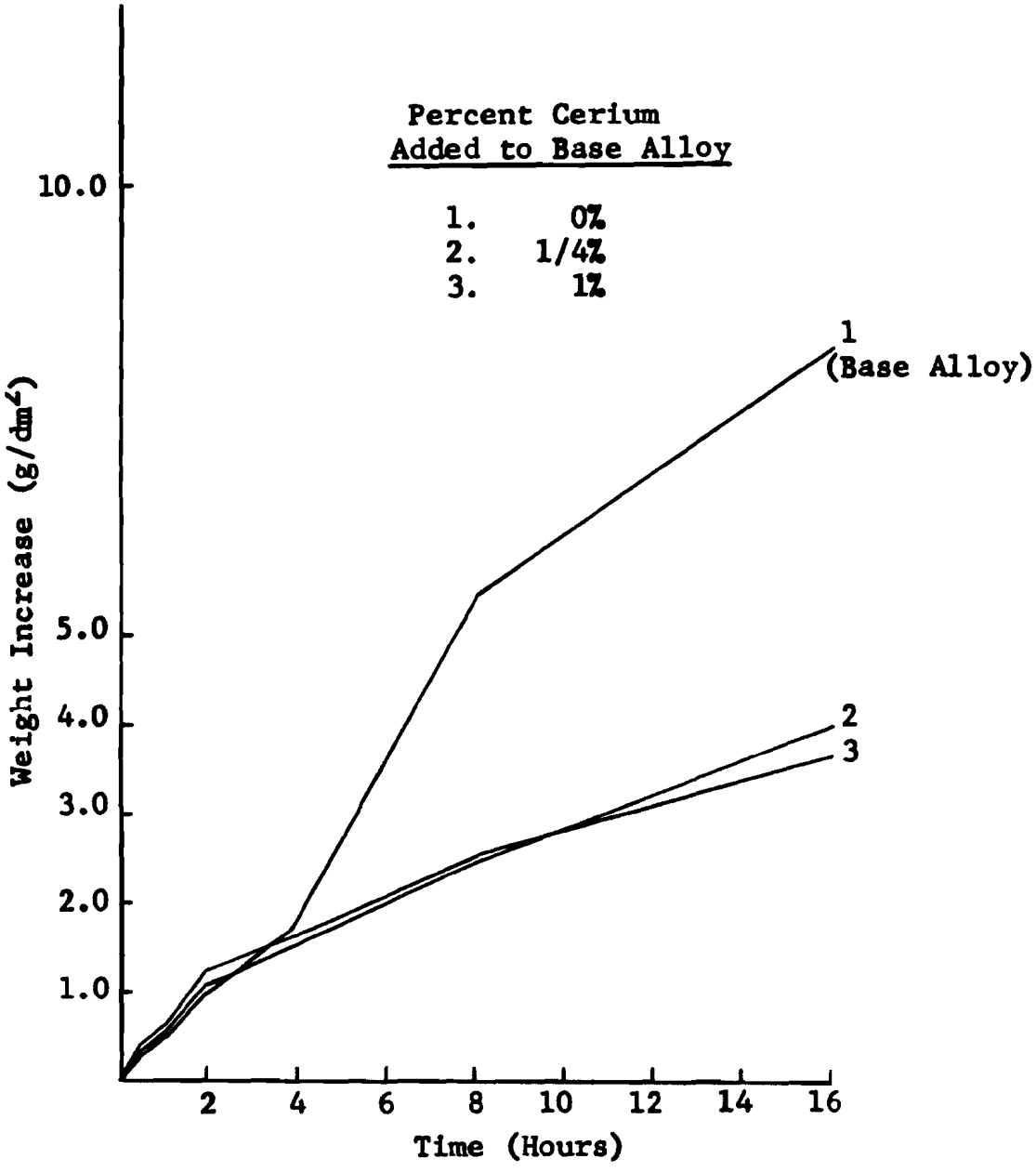

Figure 22. Atmospheric Corrosion of a Niobium Alloy Containing 7% Titanium, 20% Tungsten, and 3% Molybdenum with Cerium Additions. Dry Air at 1000°C.

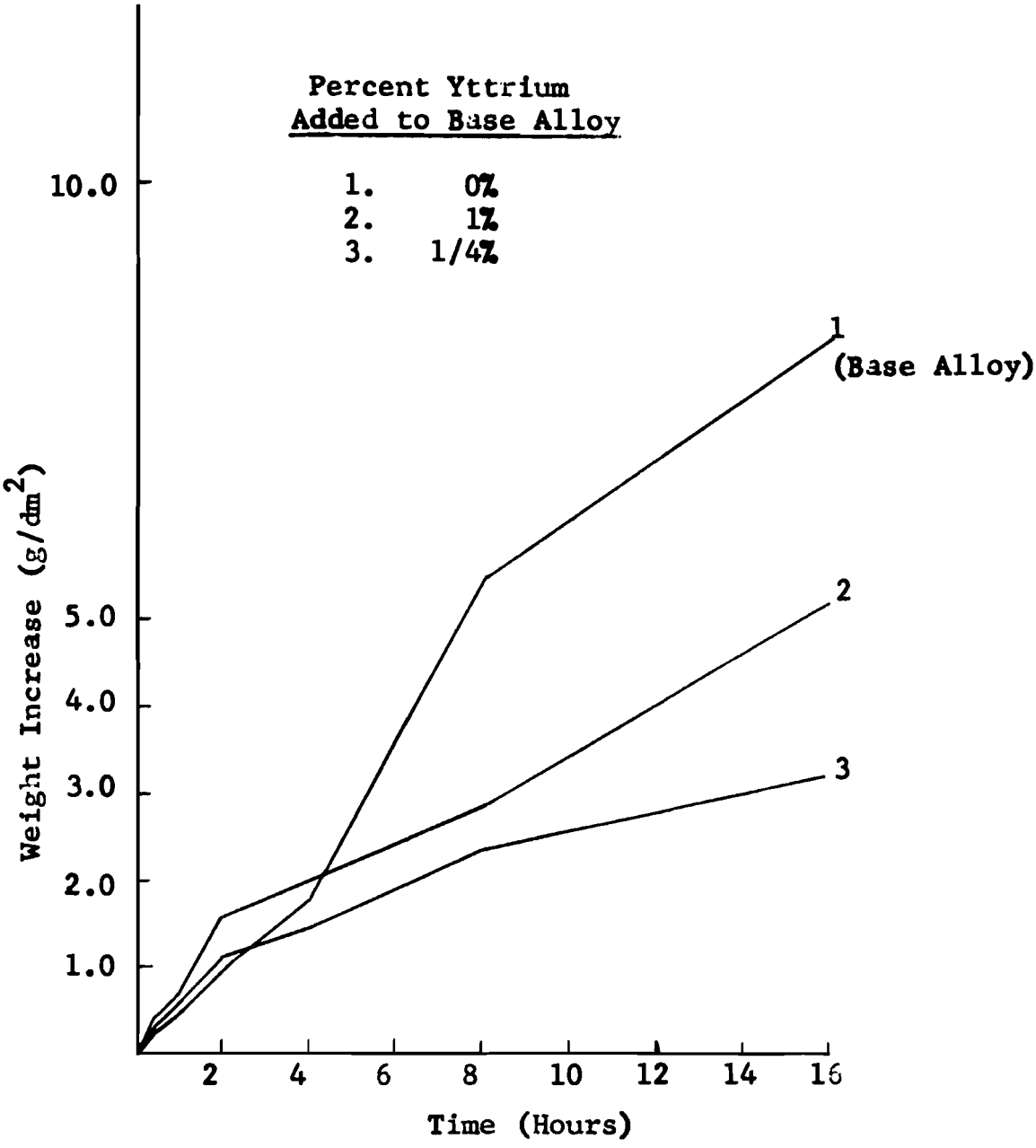

Figure 23. Atmospheric Corrosion of a Niobium Alloy Containing 7% Titanium, 20% Tungsten, and 3% Molybdenum with Yttrium Additions. Dry Air at 1000°C.

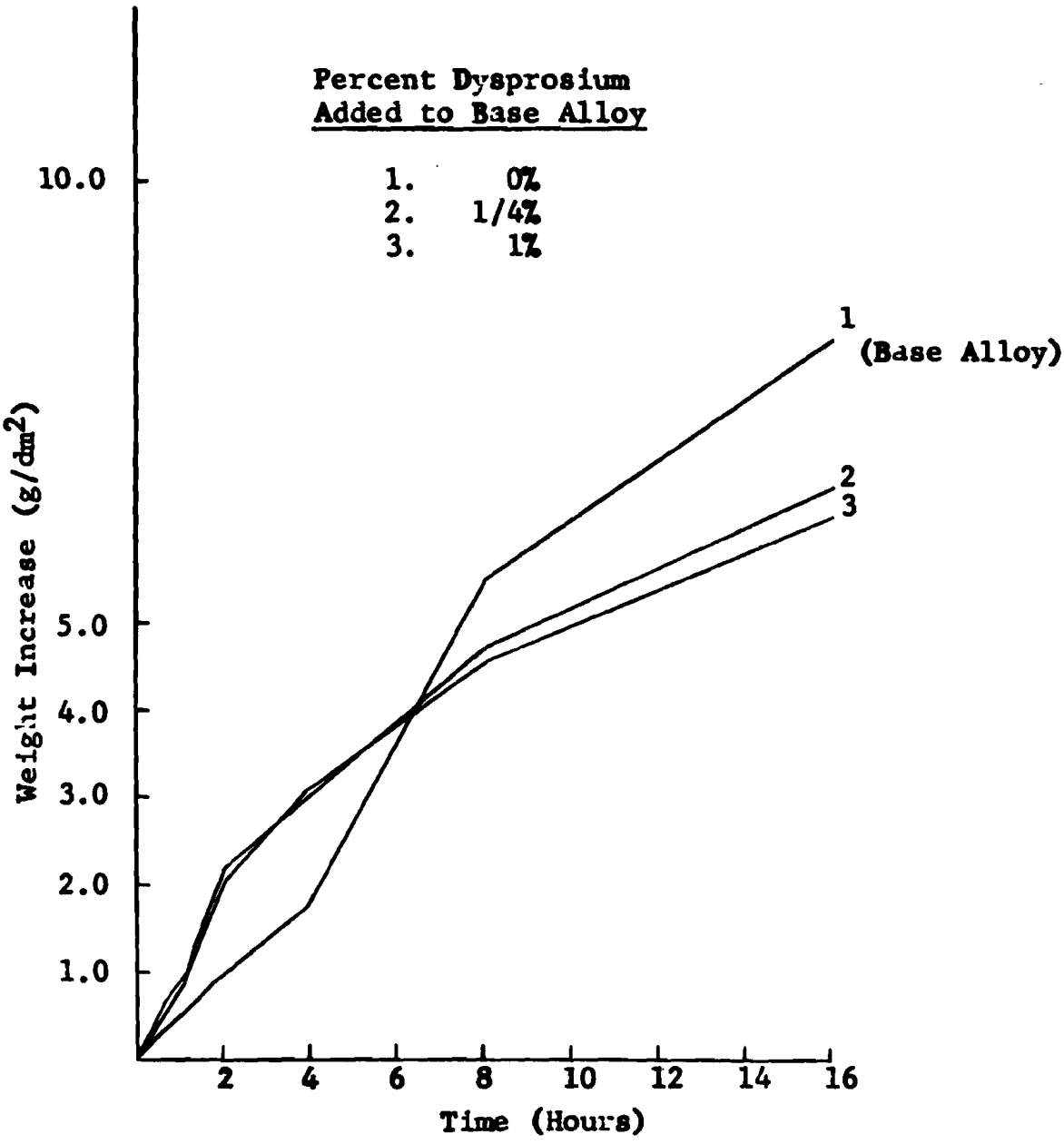

Figure 24. Atmospheric Corrosion of a Niobium Alloy Containing 7% Titanium, 20% Tungsten, and 3% Molybdenum with Dysprosium Additions. Dry Air at 1000°C.

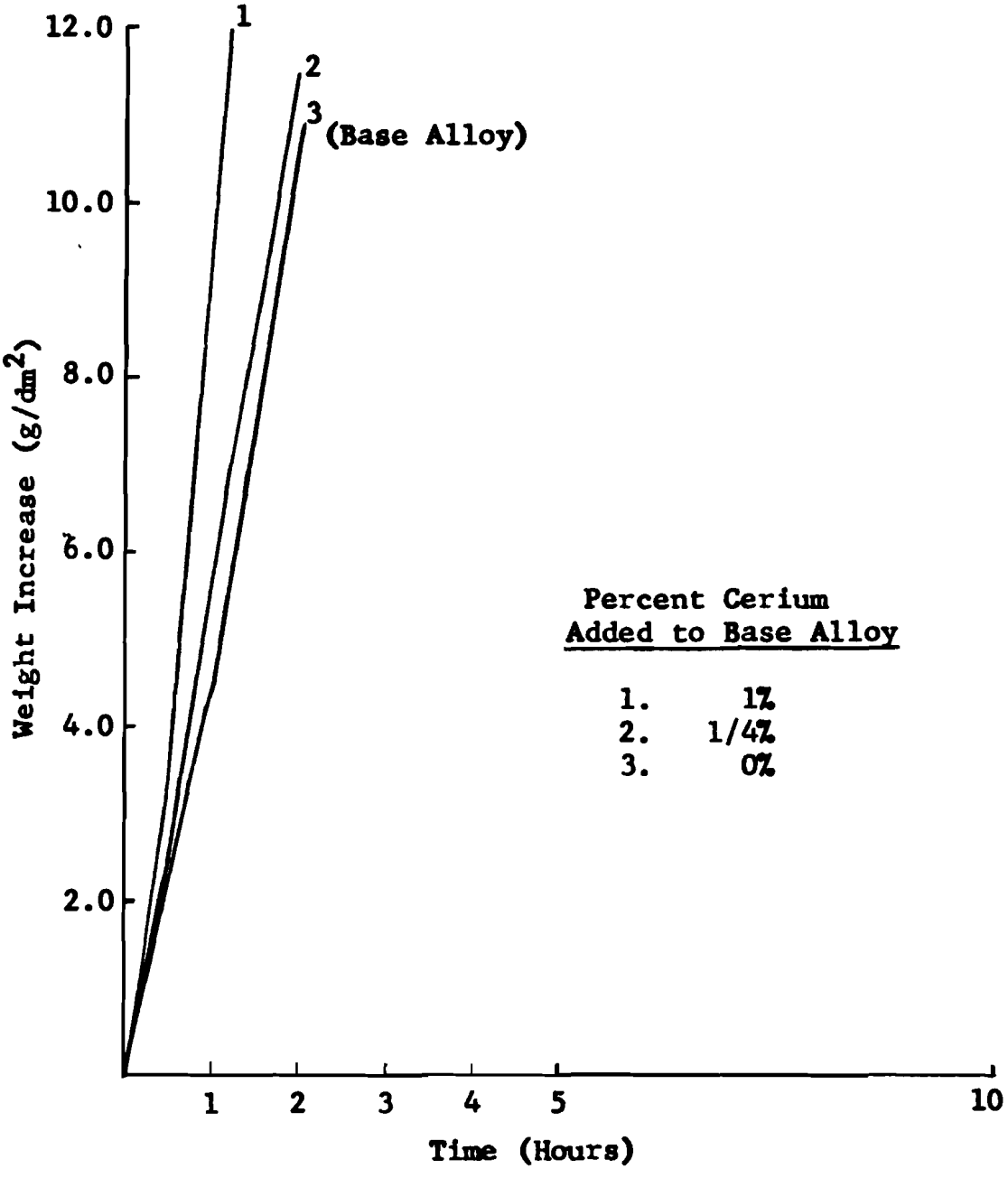

Figure 25. Atmospheric Corrosion of a Niobium Alloy Containing 8% Hafnium and 20% Tungsten with Cerium Additions. Dry Air at 1000°C.

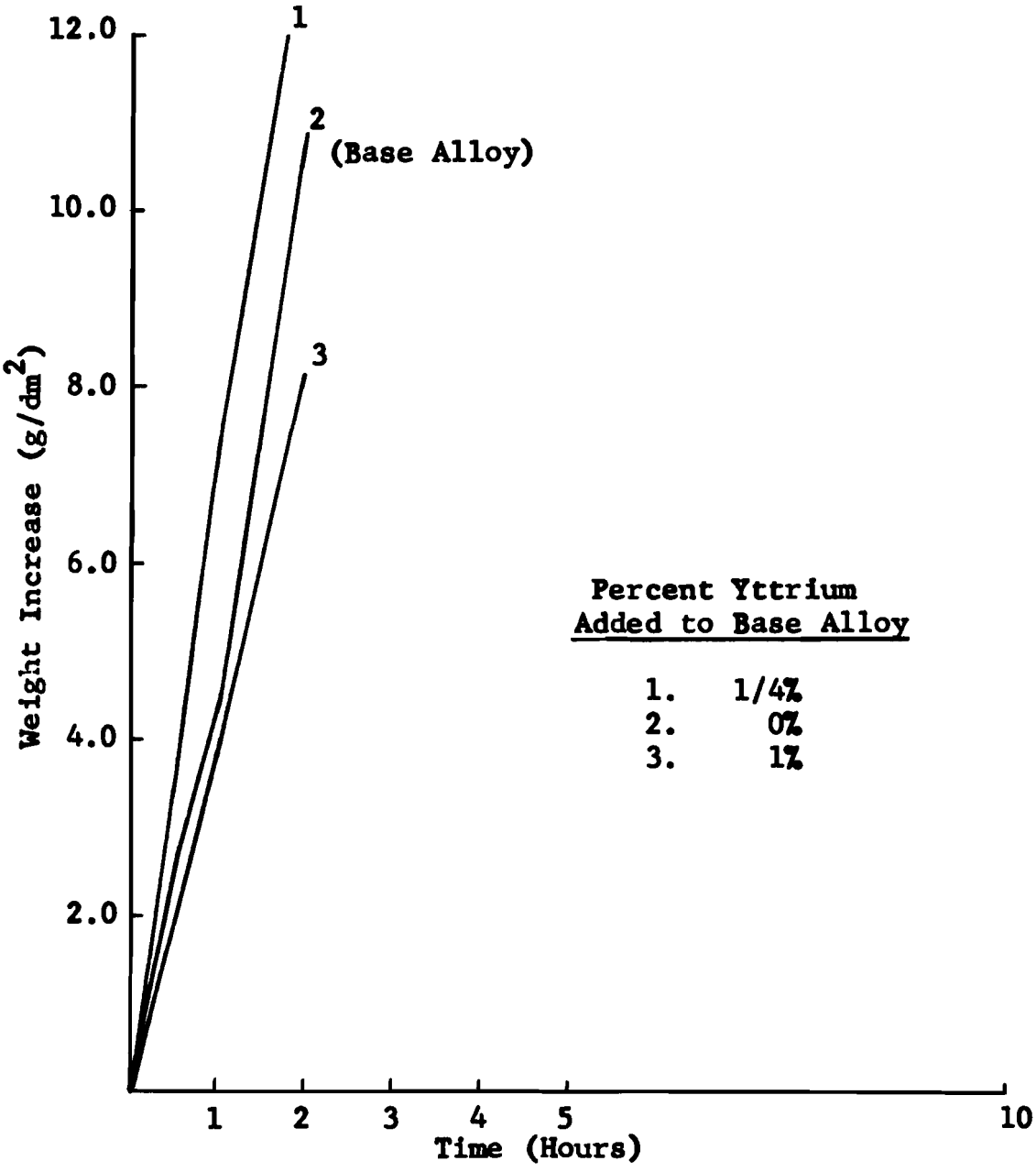

Figure 26. Atmospheric Corrosion of a Niobium Alloy Containing 8% Hafnium and 20% Tungsten with Yttrium Additions. Dry Air at 1000°C.

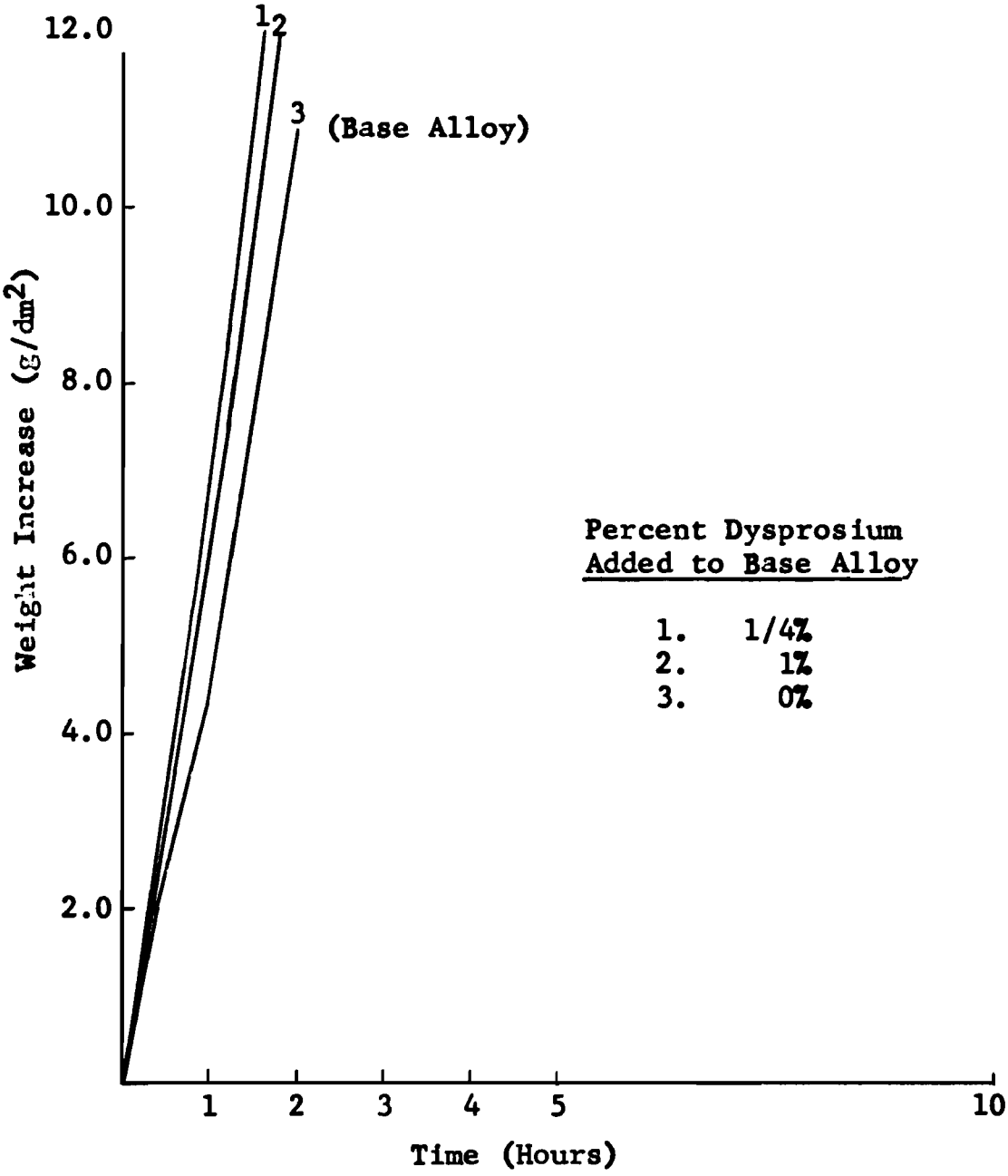

Figure 27. Atmospheric Corrosion of a Niobium Alloy Containing 8% Hafnium and 20% Tungsten with Dysprosium Additions. Dry Air at 1000°C.

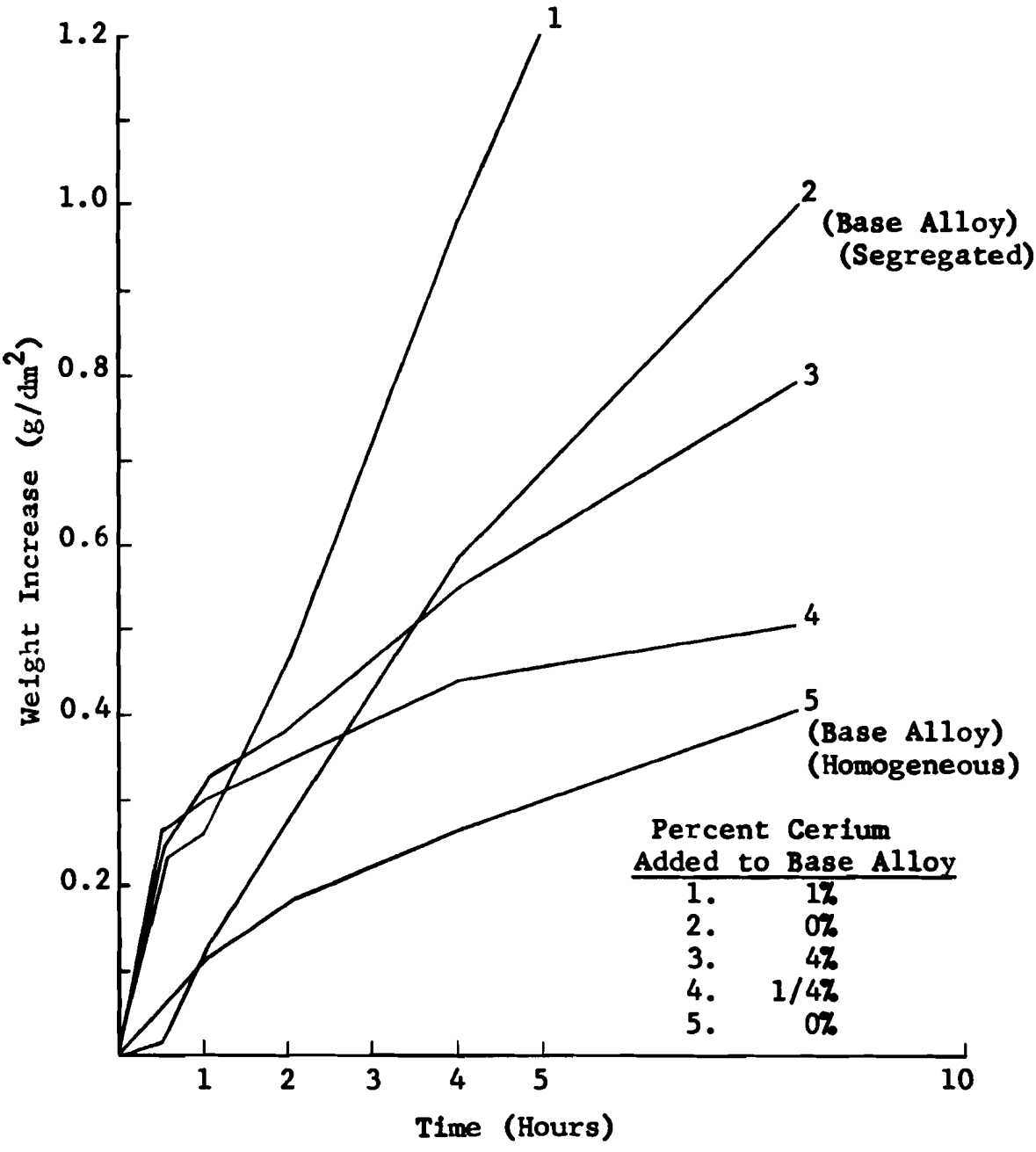

Figure 28. Atmospheric Corrosion of a Niobium Alloy Containing 42% Titanium and 4% Aluminum with Cerium Additions. Dry Air at 1000°C. This is Figure 7 of the Fourth Quarterly Report (3) as revised by the Addition of Corrosion Results for a Homogeneous Base Alloy.

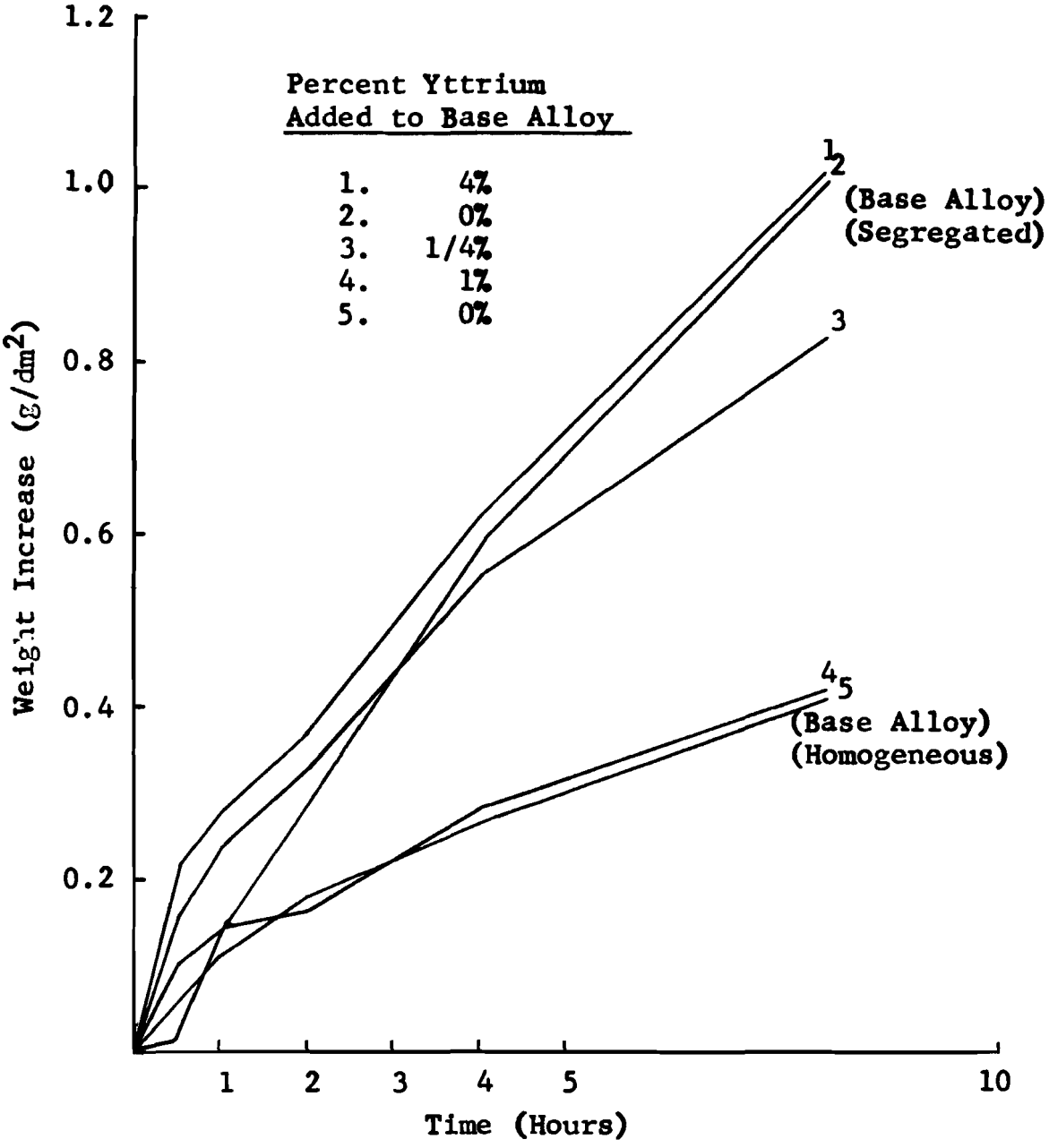

Figure 29. Atmospheric Corrosion of a Niobium Alloy Containing 42% Titanium and 4% Aluminum with Yttrium Additions. Dry Air at 1000°C. This is Figure 8 of the Fourth Quarterly Report (3) as revised by the Addition of Corrosion Results for a Homogeneous Base Alloy.

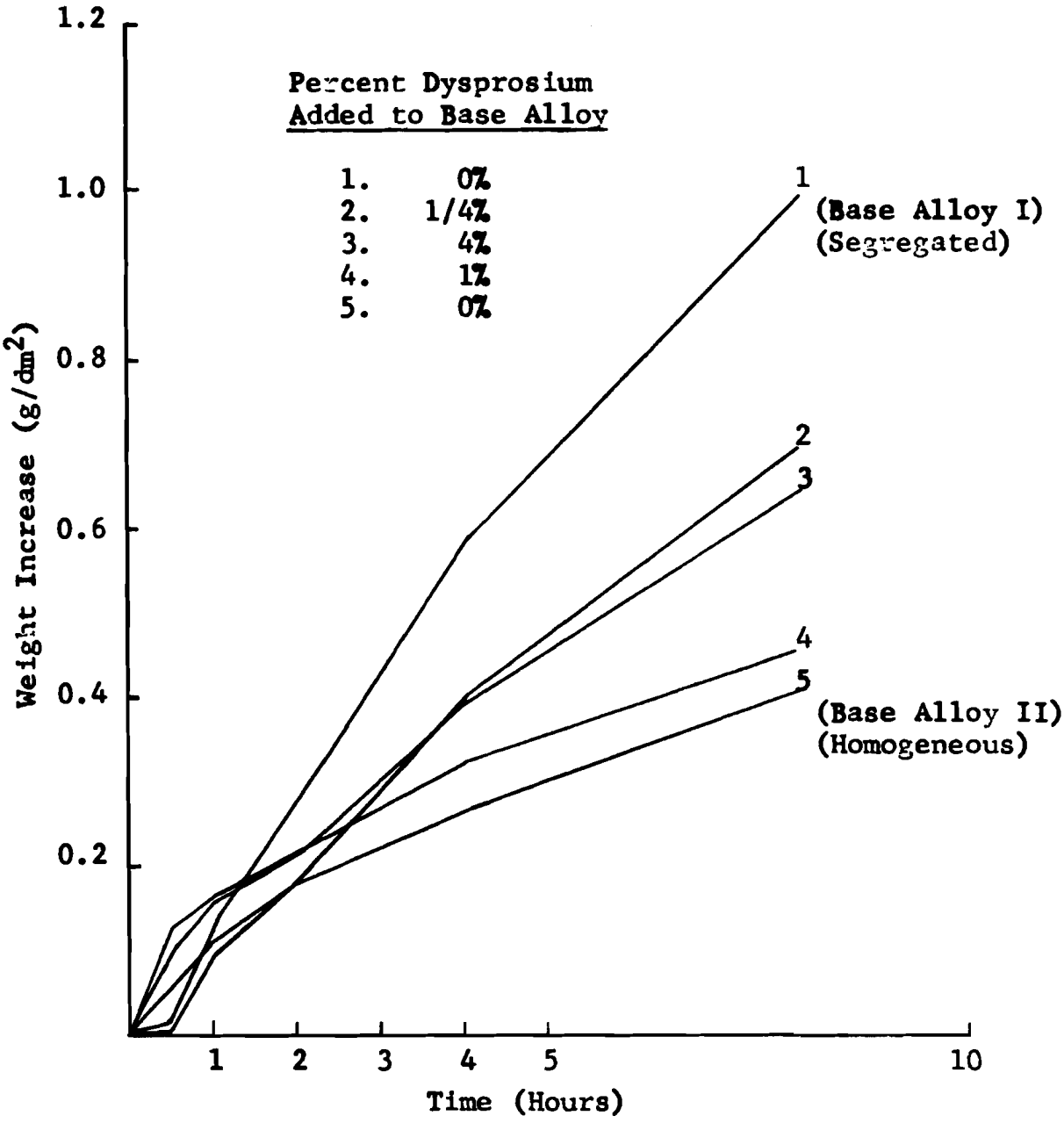

Figure 30. Atmospheric Corrosion of a Niobium Alloy Containing 42% Titanium and 4% Aluminum with Dysprosium Additions. Dry Air at 1000°C. This is Figure 9 of the Fourth Quarterly Report (3) as revised by the Addition of Corrosion Results for a Homogeneous Base Alloy.

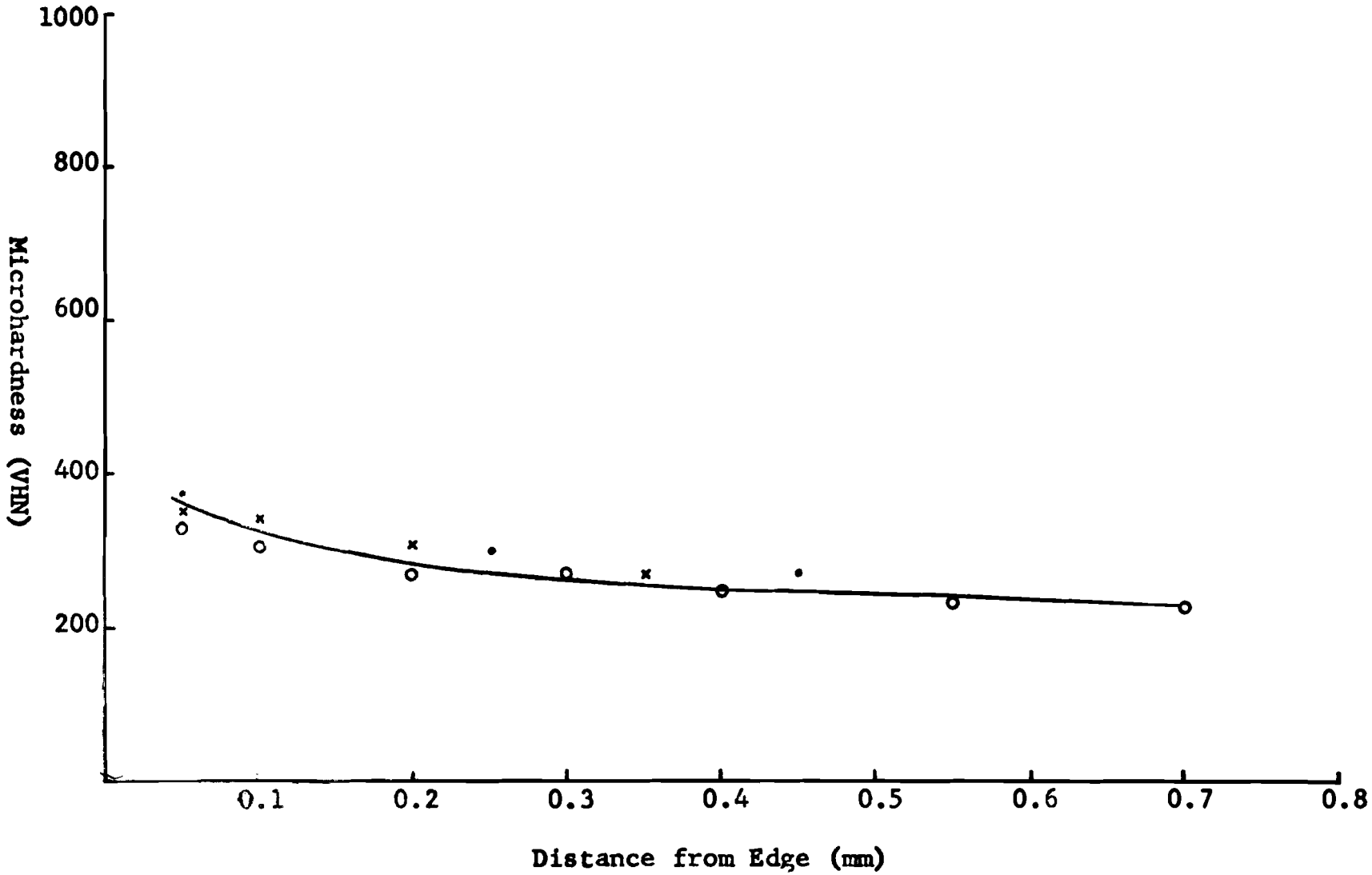

Figure 31. Microhardness of a Niobium Metal Specimen. Three Areas of the Specimen After Atmospheric Corrosion Test.

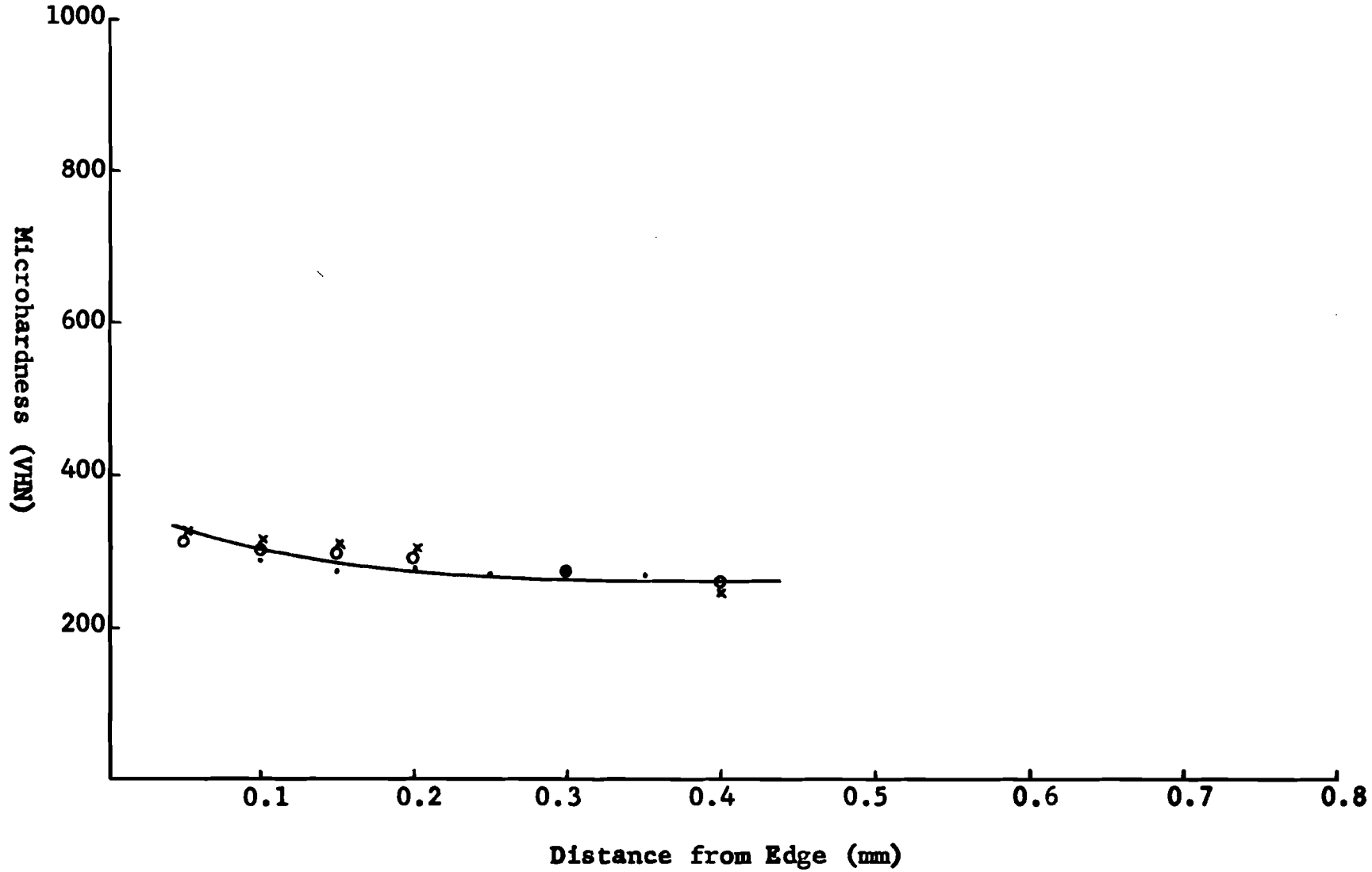

Figure 32. Microhardness of a Niobium Metal Specimen. Three Areas of the Specimen After Atmospheric Corrosion Test.

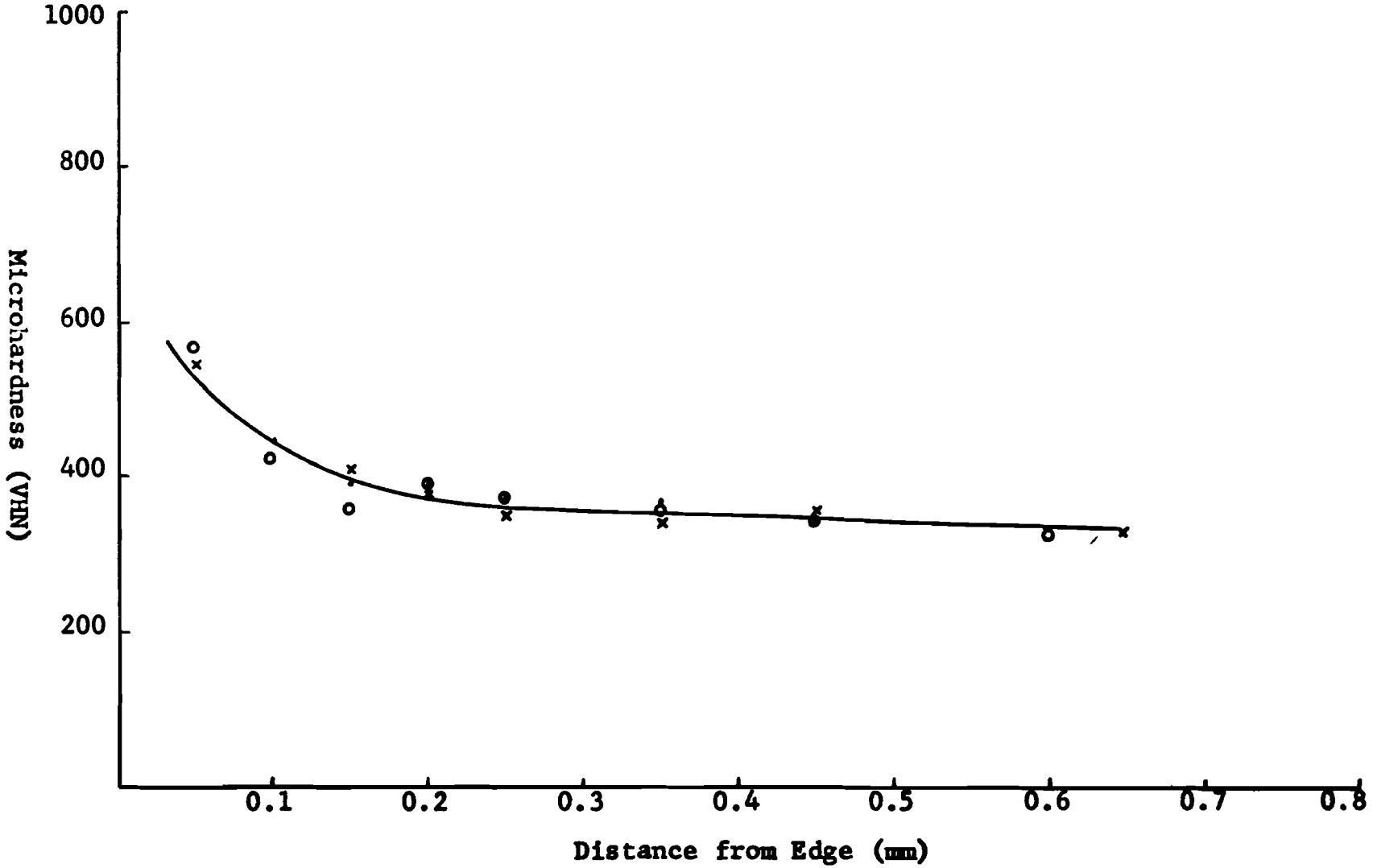

Figure 33. Microhardness of a Niobium Alloy Containing 42.0% Titanium and 4.0% Aluminum. Three Areas of the Specimen After Atmospheric Corrosion Test.

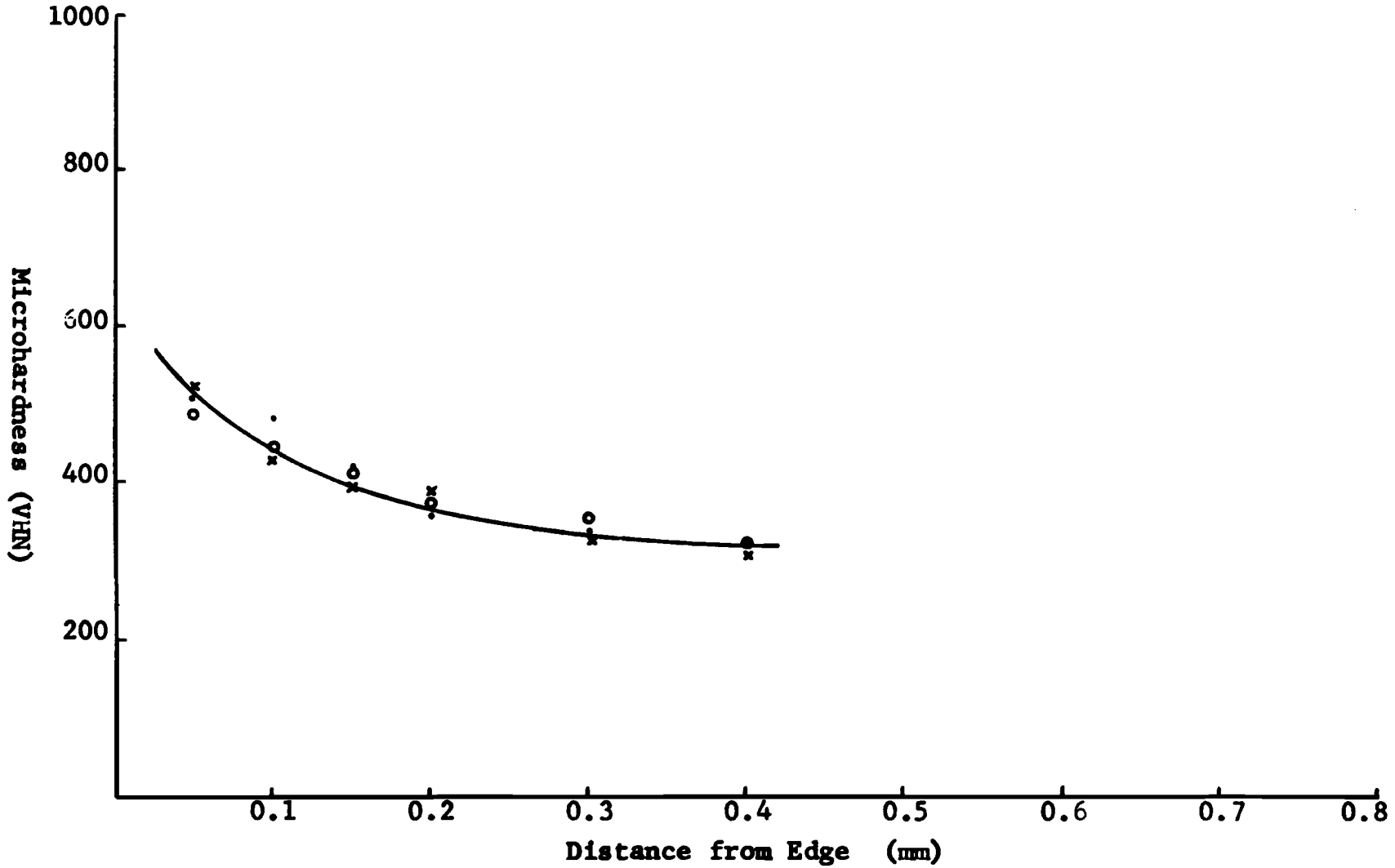

Figure 34. Microhardness of a Niobium Alloy Containing 42.0% Titanium, 4.0% Aluminum, and 1/4% Cerium. Three Areas of the Specimen After Atmospheric Corrosion Test.

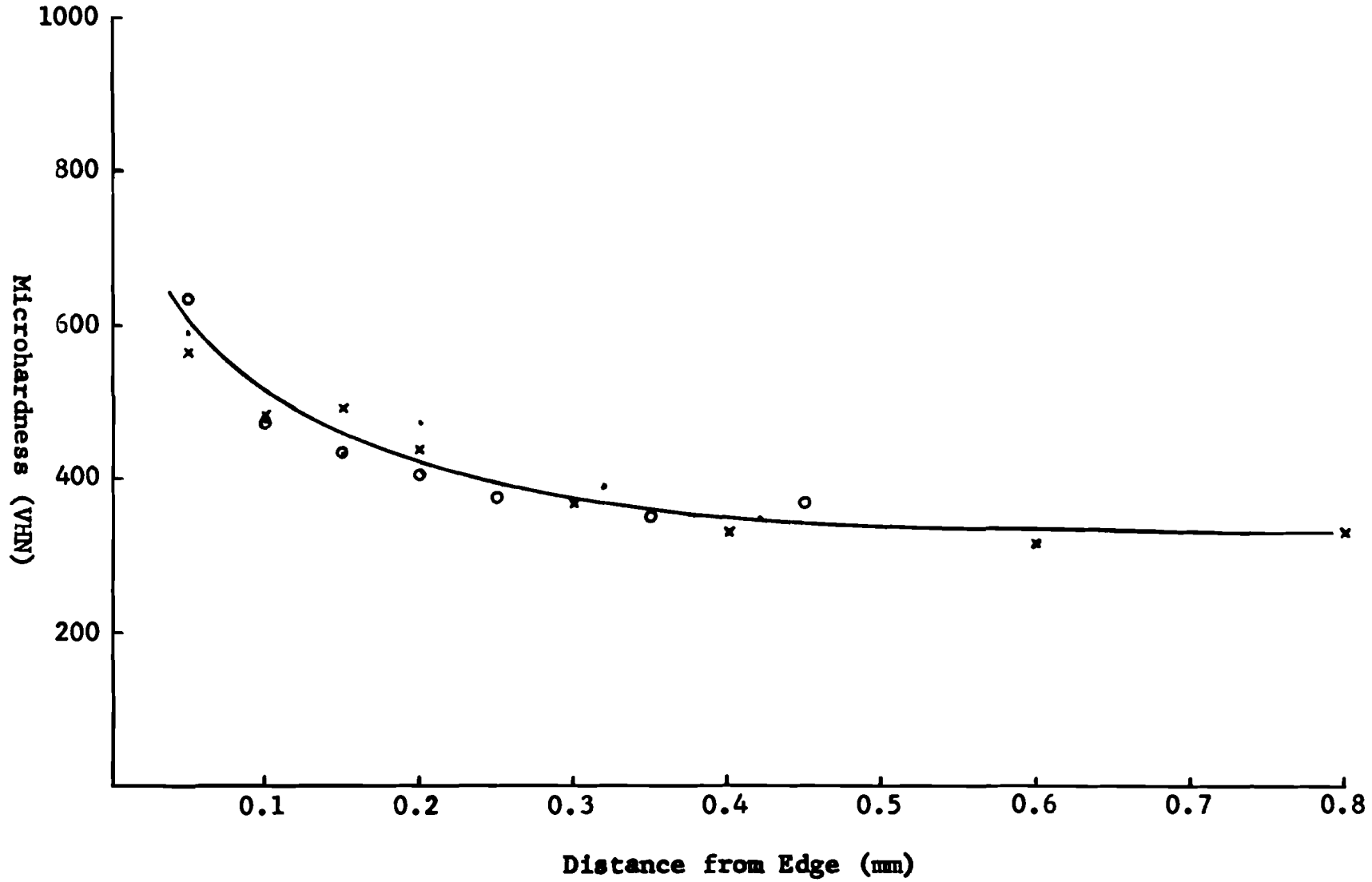

Figure 35. Microhardness of a Niobium Alloy Containing 42.0% Titanium, 4.0% Aluminum, and 1% Cerium. Three Areas of the Specimen After Atmospheric Corrosion Test.

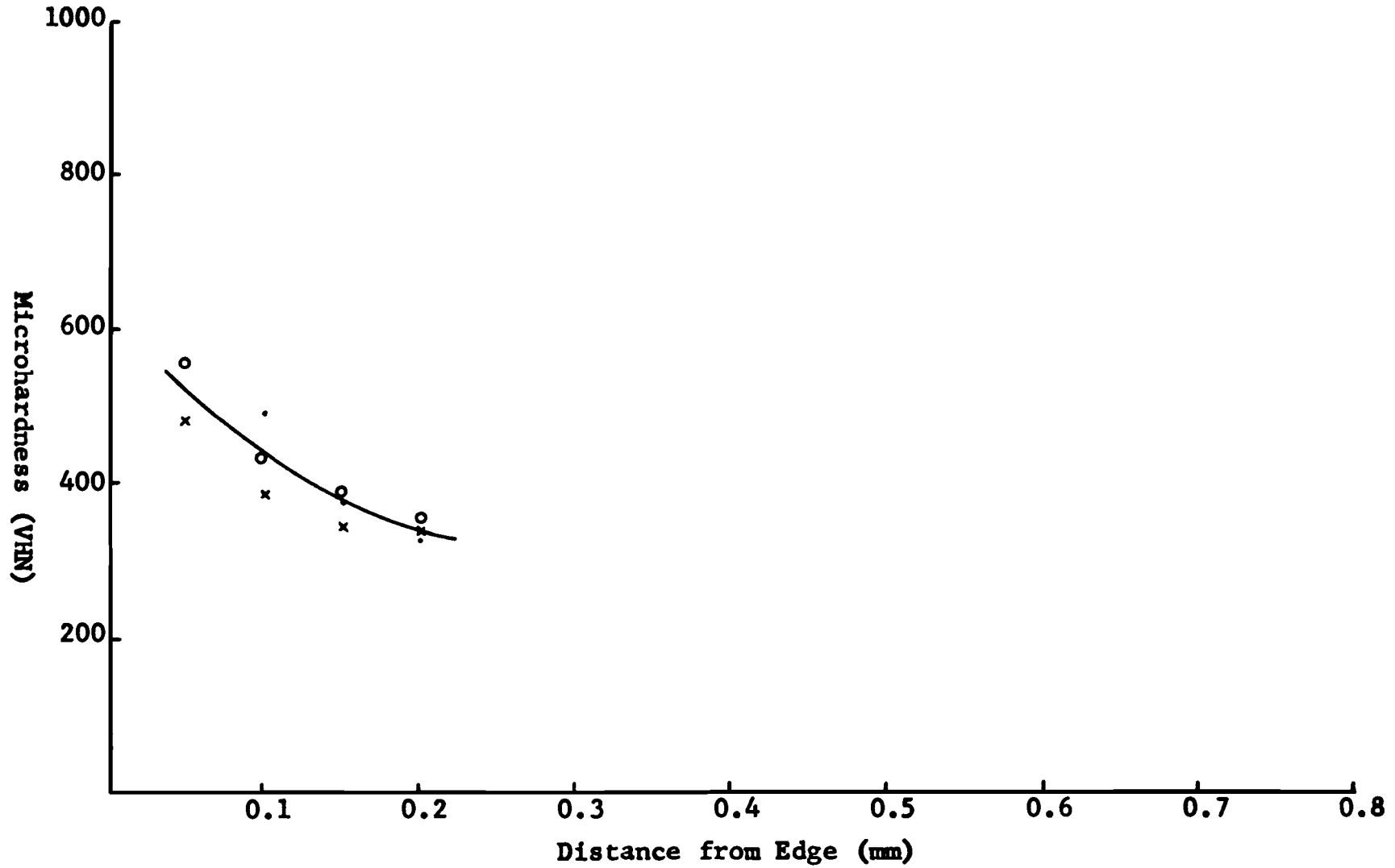

Figure 36. Microhardness of a Niobium Alloy Containing 42.0% Titanium, 4.0% Aluminum, and 4% Cerium. Three Areas of the Specimen After Atmospheric Corrosion Test.

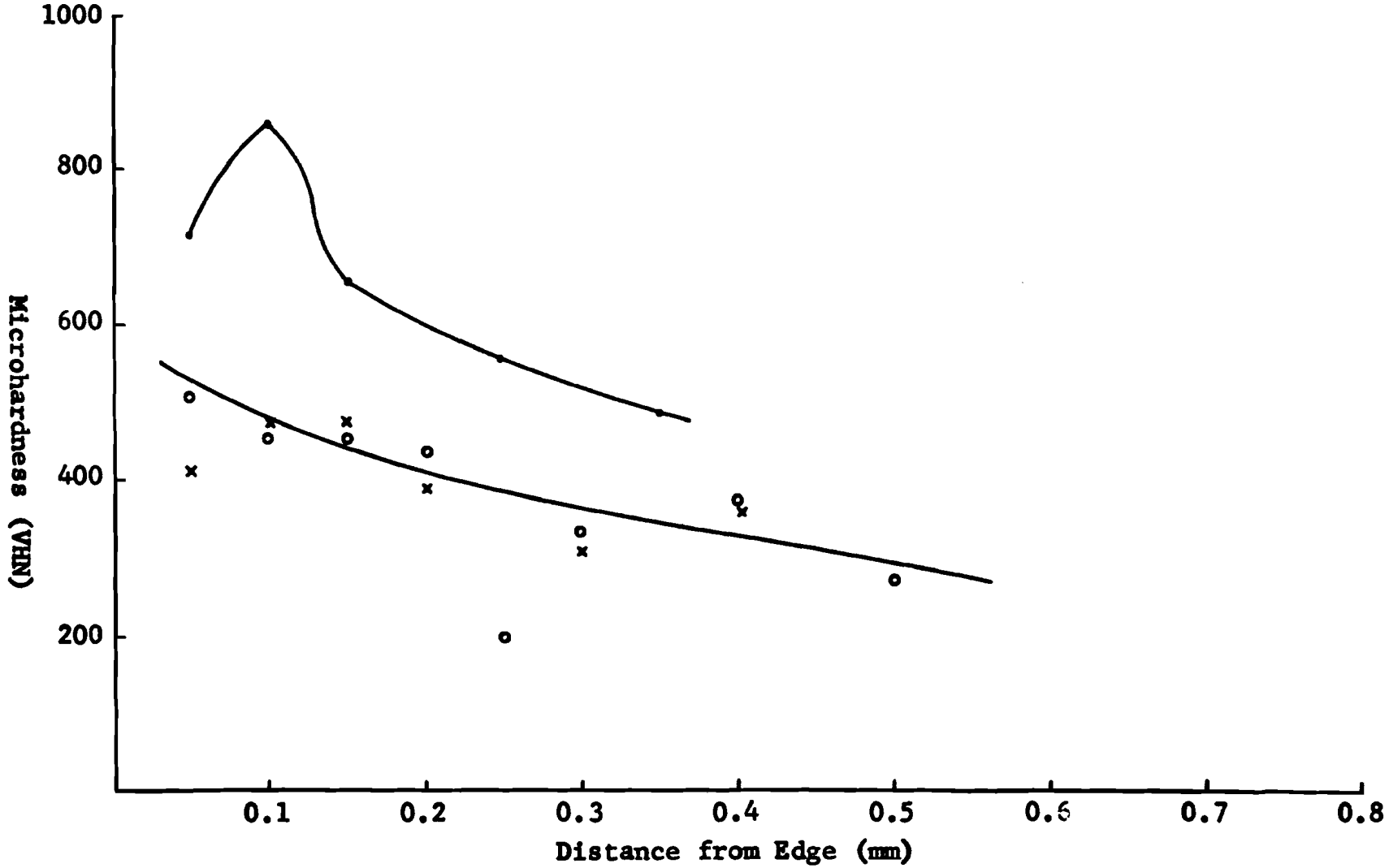

Figure 37. Microhardness of a Niobium Alloy Containing 42.0% Titanium, 4.0% Aluminum, and 1/4% Yttrium. Lower Curve indicates Two Areas of the Specimen with Similar Values; Upper Curve indicates a Third Area which is Harder and shows a different Hardness Pattern, After Atmospheric Corrosion Test.

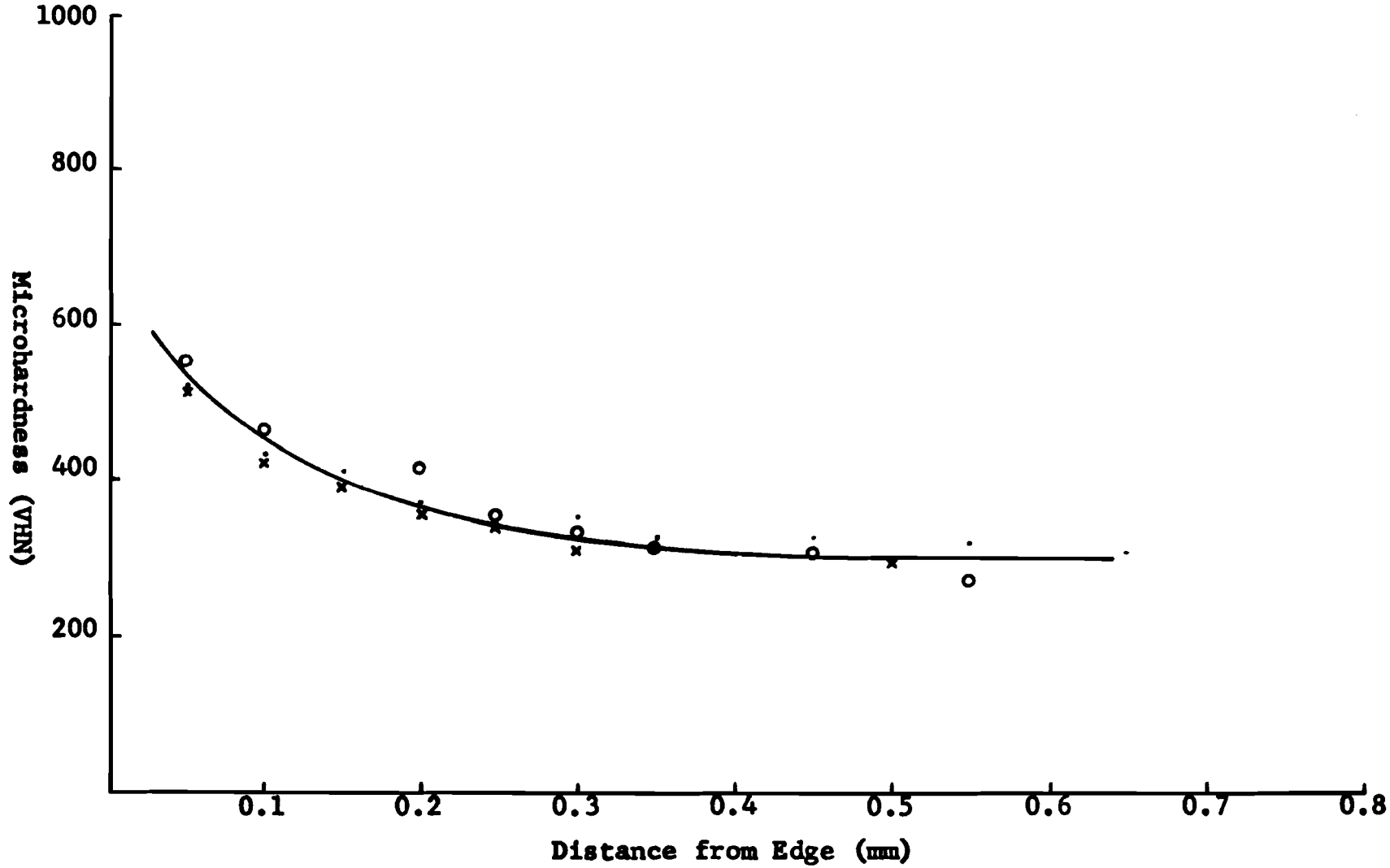

Figure 38. Microhardness of a Niobium Alloy Containing 42.0% Titanium, 4.0% Aluminum and 1% Yttrium. Three Areas of the Specimen After Atmospheric Corrosion Test.

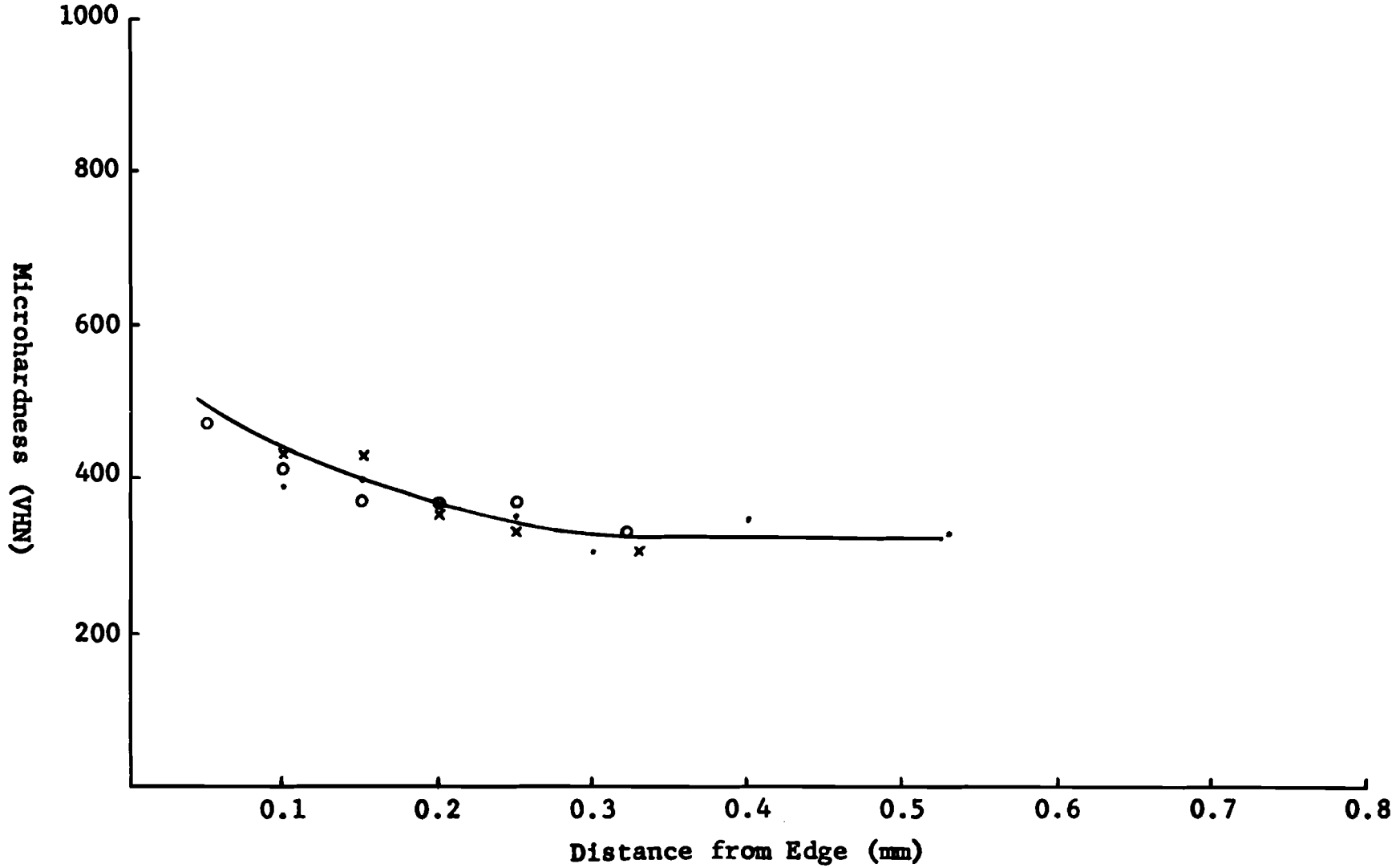

Figure 39. Microhardness of a Niobium Alloy Containing 42.0% Titanium, 4.0% Aluminum and 4% Yttrium. Three Areas of the Specimen After Atmospheric Corrosion Test.

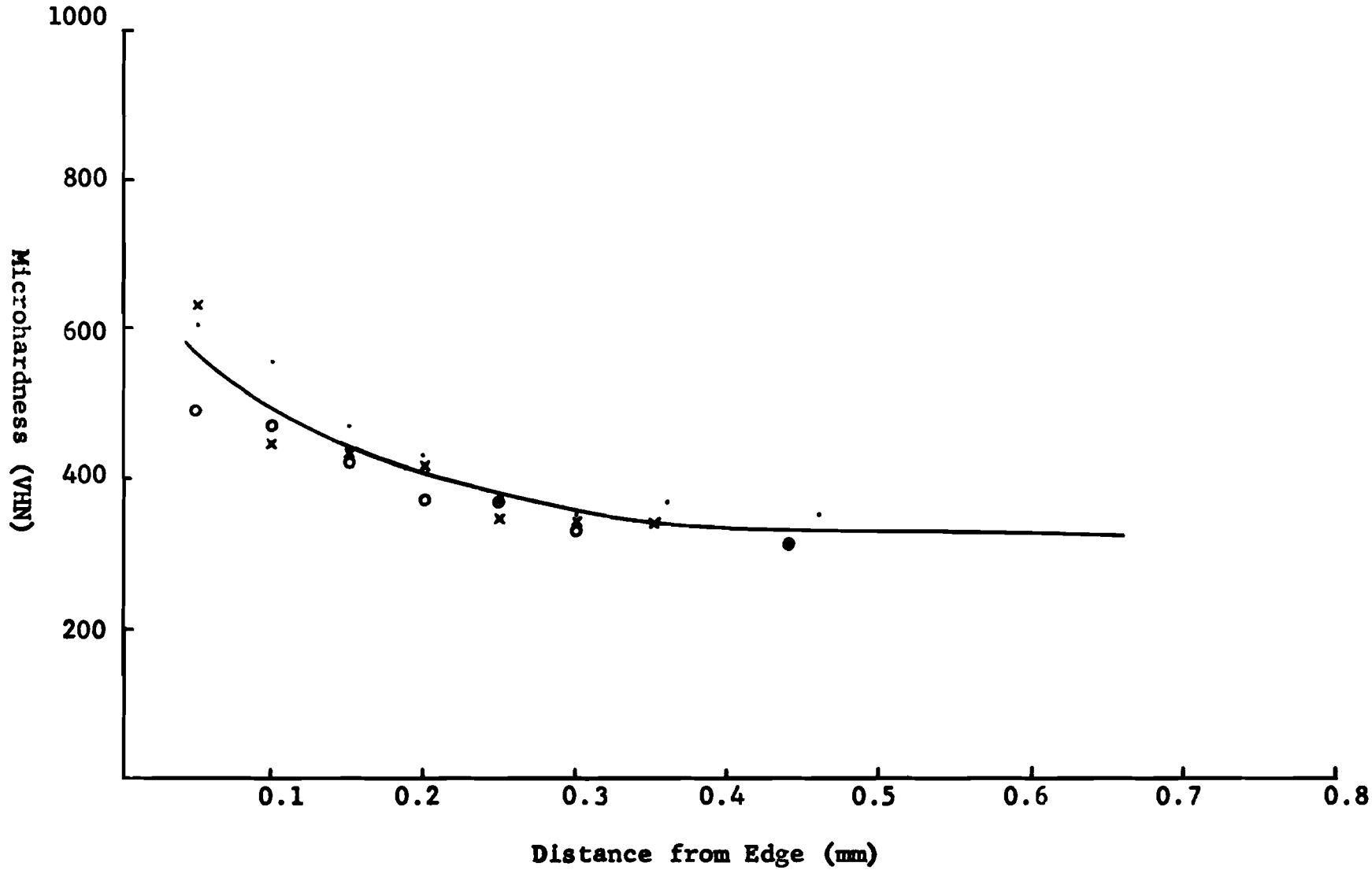

Figure 40. Microhardness of a Niobium Alloy Containing 42.0% Titanium, 4.0% Aluminum and 1/4% Dysprosium. Three areas of the Specimen after Atmospheric Corrosion Test.

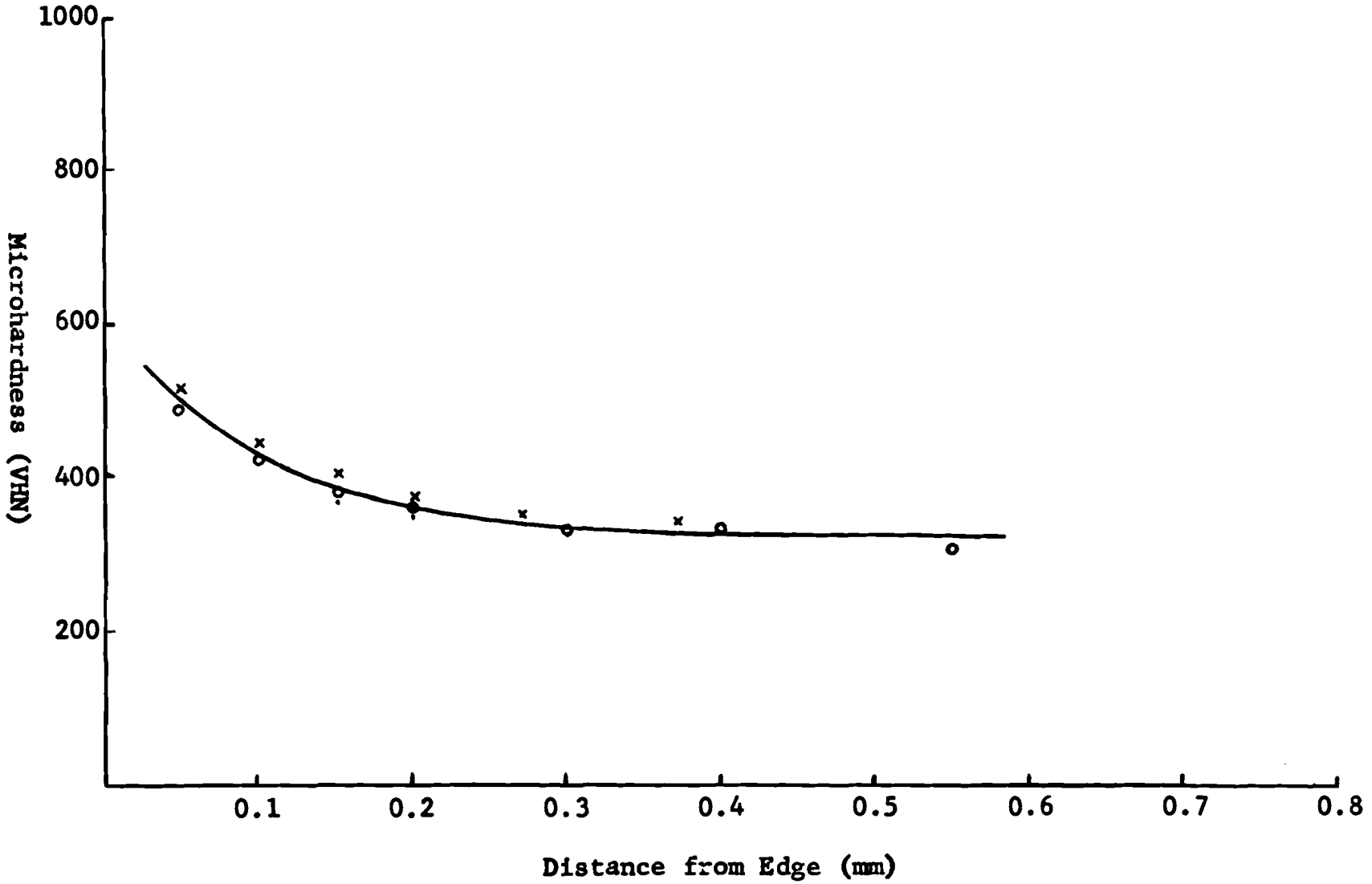

Figure 41. Microhardness of a Niobium Alloy Containing 42% Titanium, 4.0% Aluminum and 1% Dysprosium. Three areas of the Specimen After Atmospheric Corrosion Test.

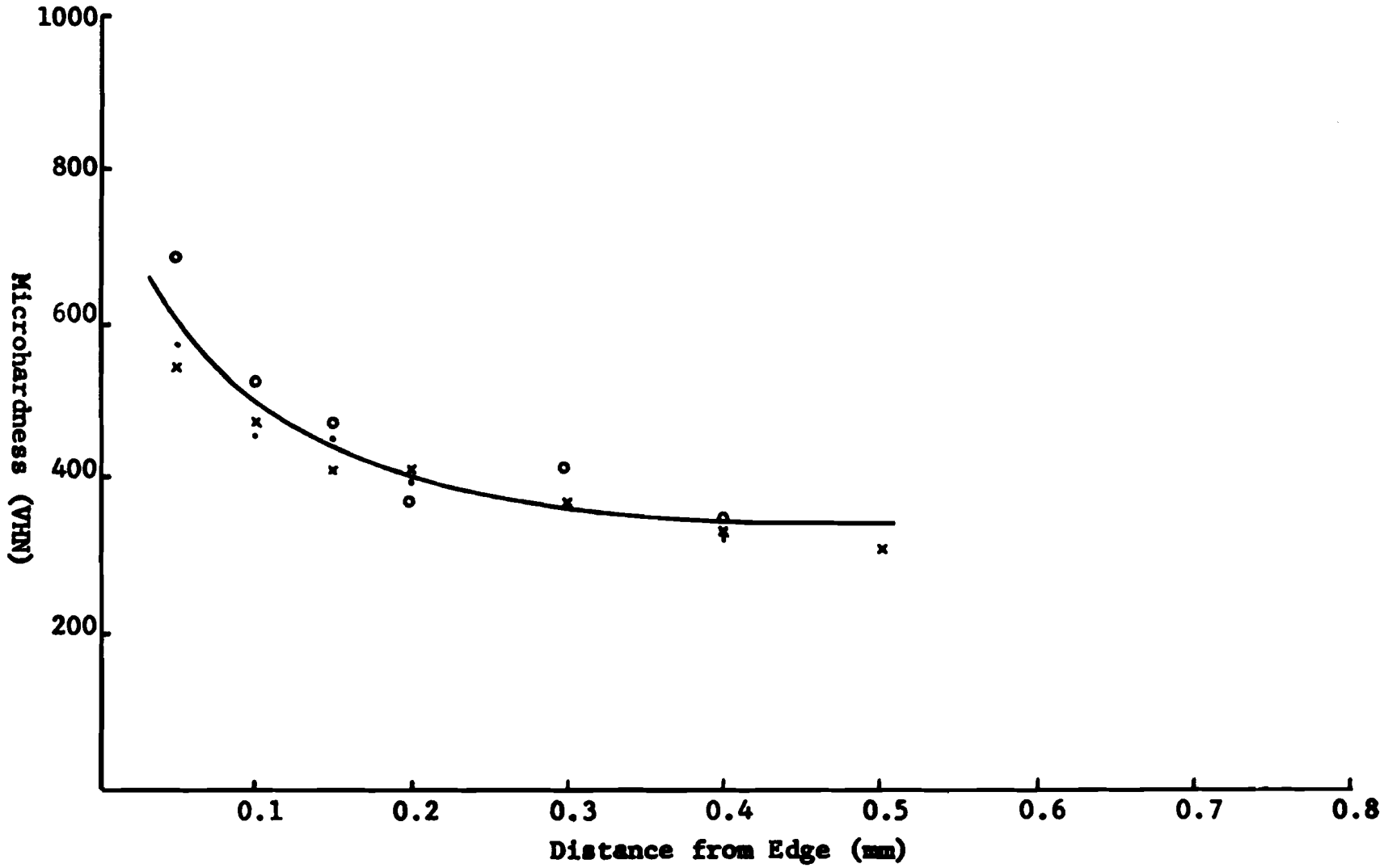

Figure 42. Microhardness of a Niobium Alloy Containing 42% Titanium, 4.0% Aluminum and 4% Dysprosium. Three Areas of the Specimen After Atmospheric Corrosion Test.

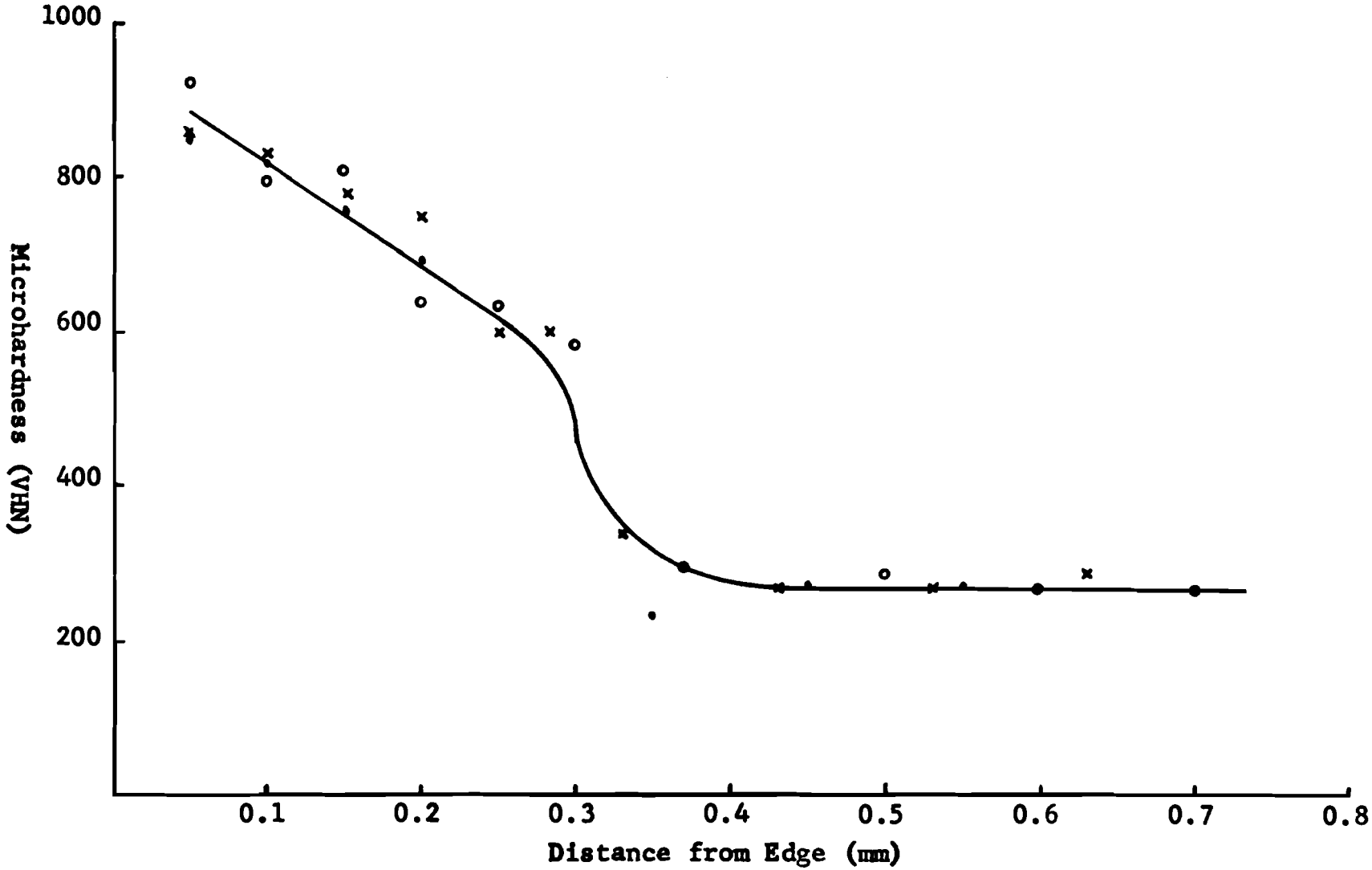

Figure 43. Microhardness of a Niobium Alloy Containing 6.0% Chromium and 8.7% Titanium. Three Areas of the Specimen After Atmospheric Corrosion Test.

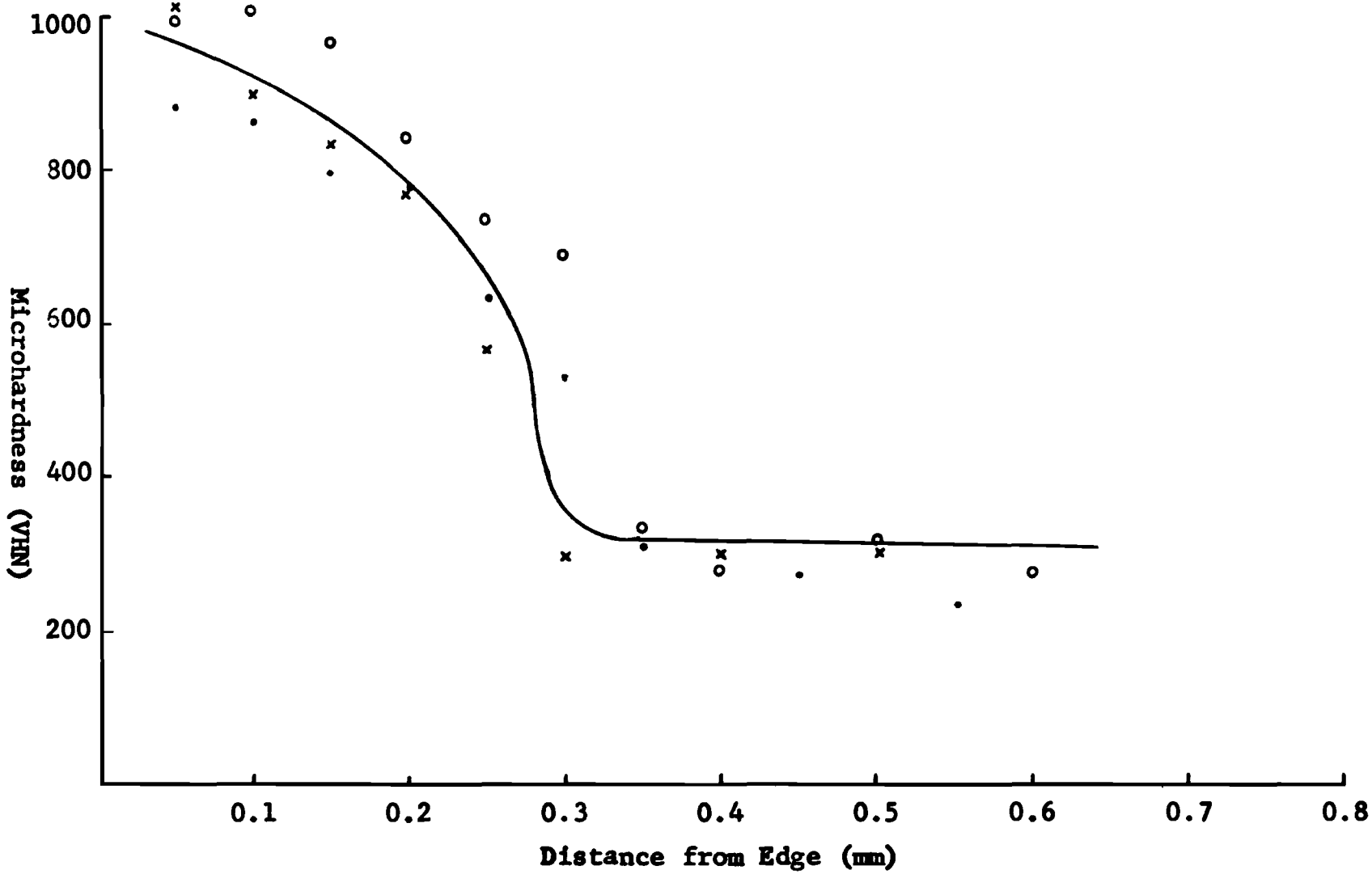

Figure 44. Microhardness of a Niobium Alloy Containing 6.0% Chromium, 8.7% Titanium and 1/4% Cerium. Three Areas of the Specimen After Atmospheric Corrosion Test.

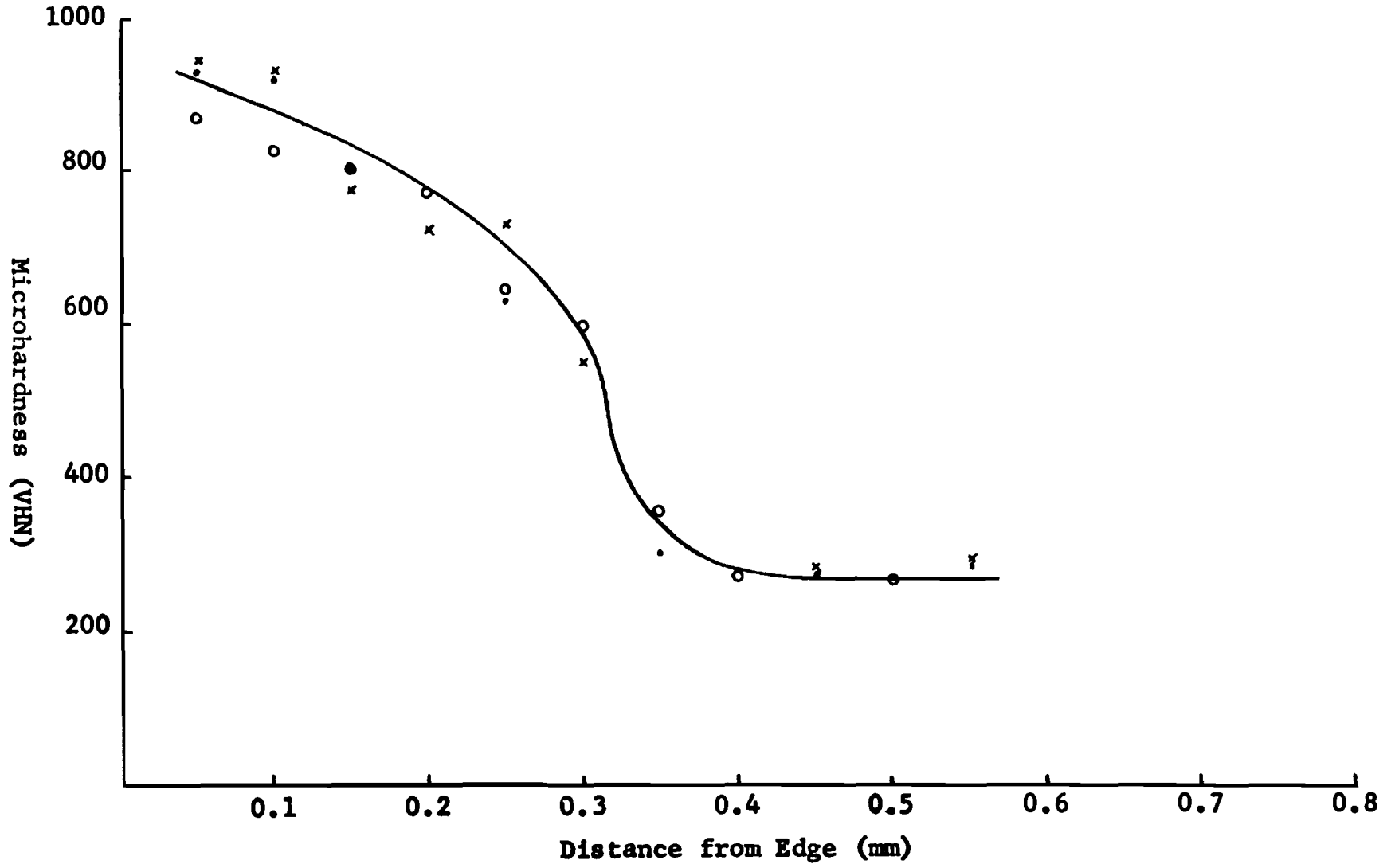

Figure 45. Microhardness of a Niobium Alloy Containing 6.0% Chromium, 8.7% Titanium and 1% Cerium. Three Areas of the Specimen After Atmospheric Corrosion Test.

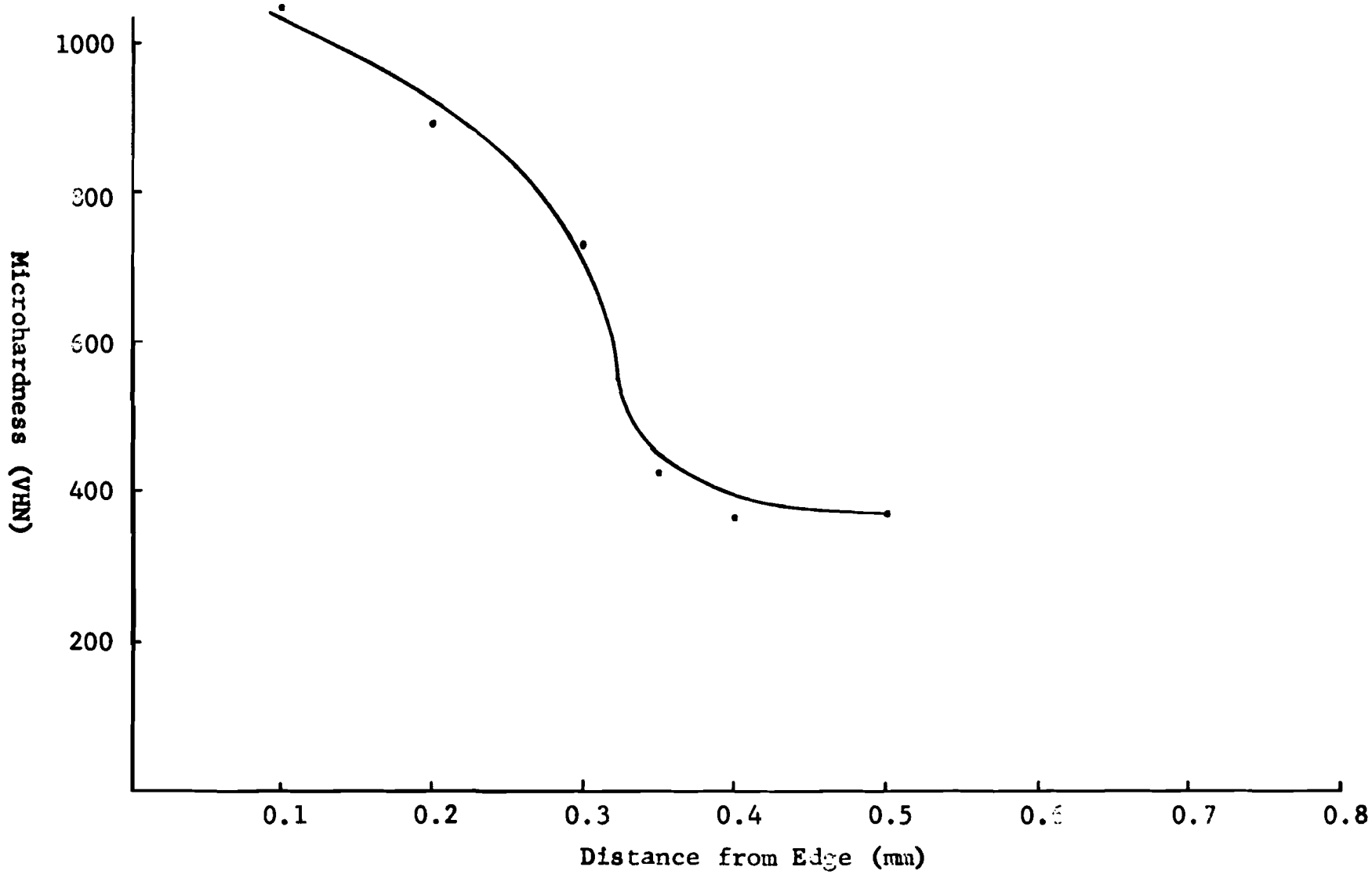

Figure 46. Microhardness of a Niobium Alloy Containing 6.0% Chromium, 8.7% Titanium, and 4% Cerium. After Atmospheric Corrosion Test.

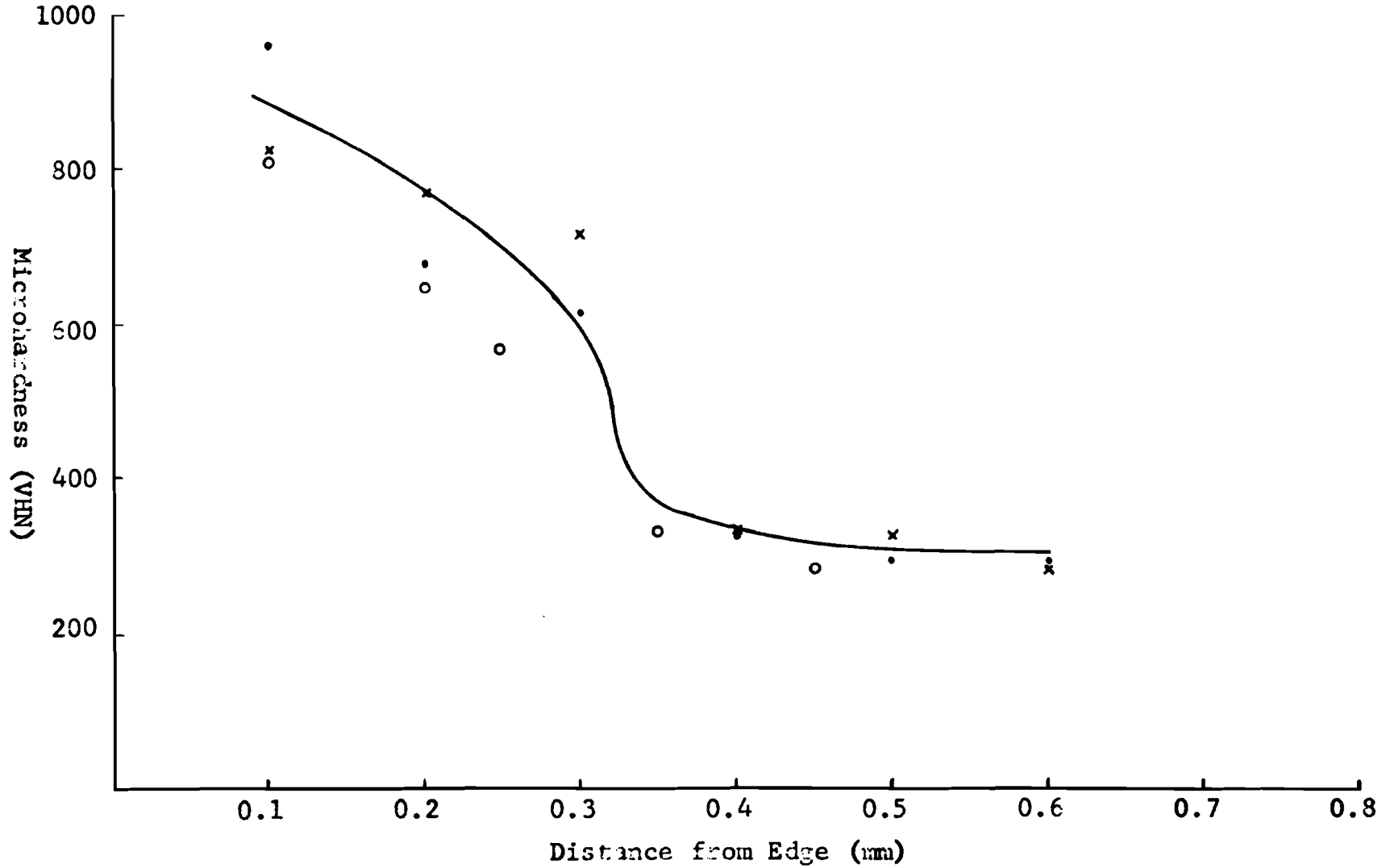

Figure 47. Microhardness of a Niobium Alloy Containing 6.0% Chromium, 8.7% Titanium and 1/4% Yttrium. Three Areas of the Specimen After Atmospheric Corrosion Test.

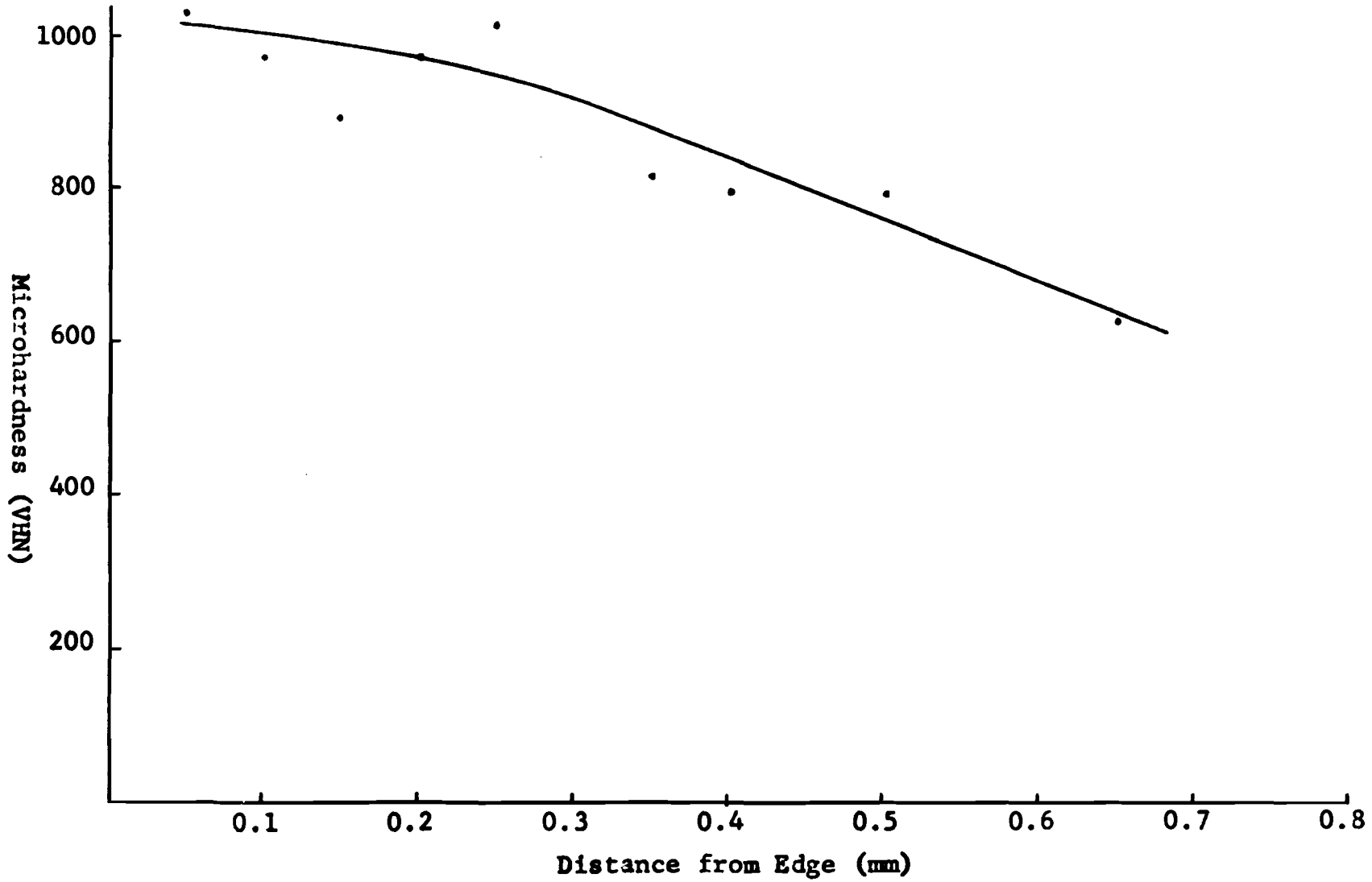

Figure 48. Microhardness of a Niobium Alloy Containing 6.0% Chromium, 8.7% Titanium and 1% Yttrium. After Atmospheric Corrosion Test.

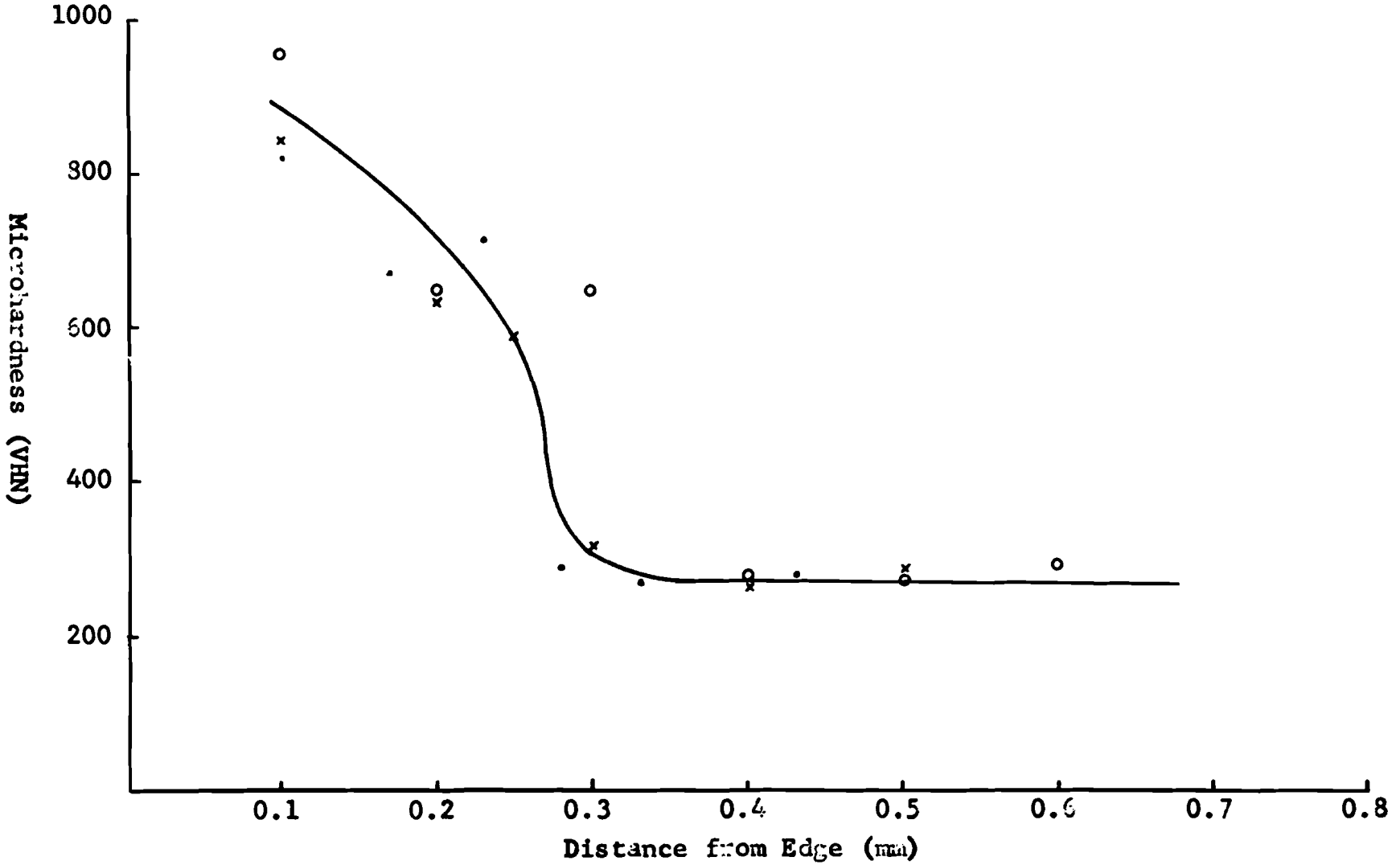

Figure 49. Microhardness of a Niobium Alloy Containing 9.0% Chromium, 8.7% Titanium and 4% Yttrium. Three Areas of the Specimen After Atmospheric Corrosion Test.

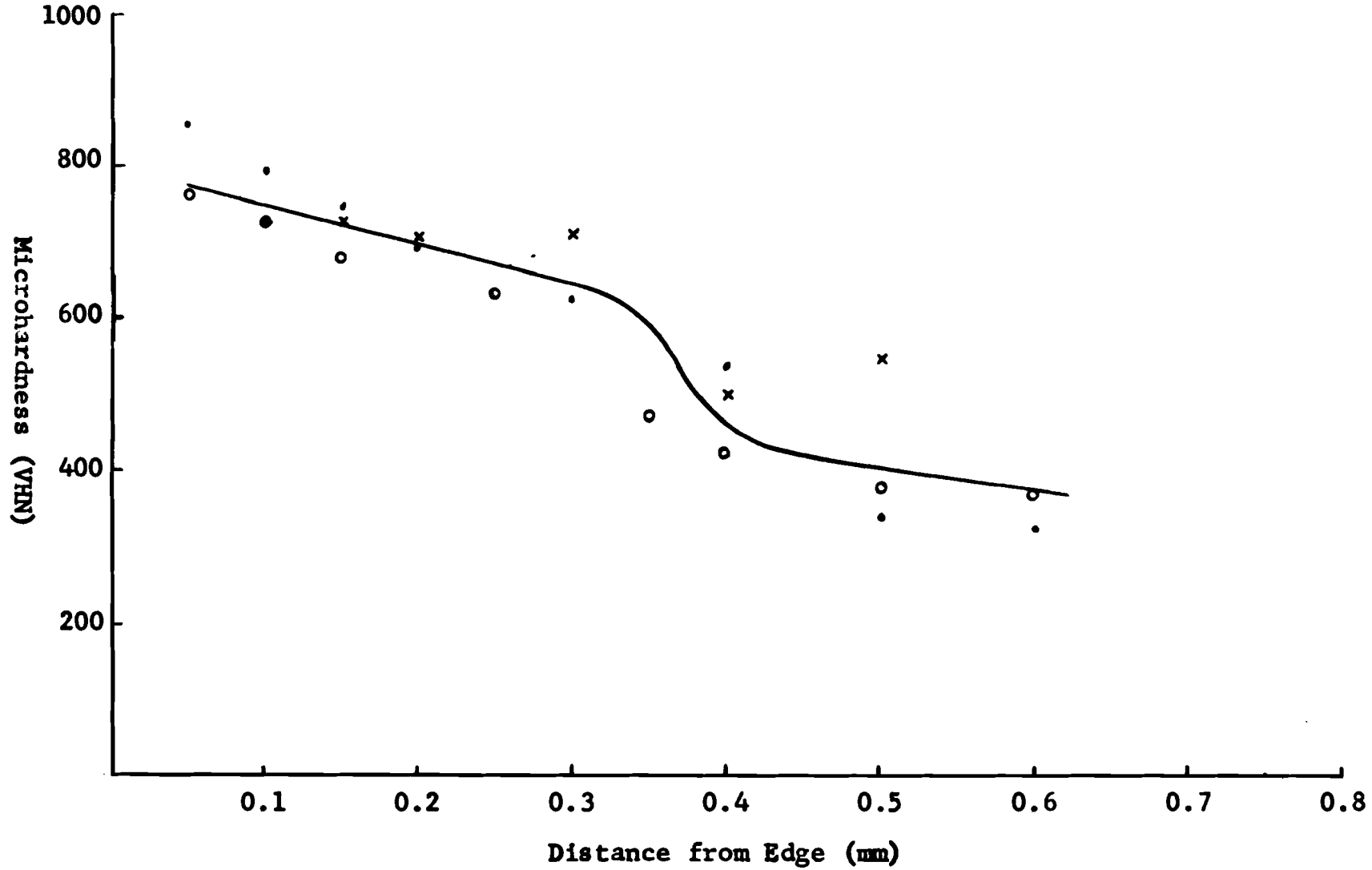

Figure 50. Microhardness of a Niobium Alloy Containing 6.0% Chromium, 8.7% Titanium, and 1/4% Dysprosium. Three Areas of the Specimen After Atmospheric Corrosion Test.

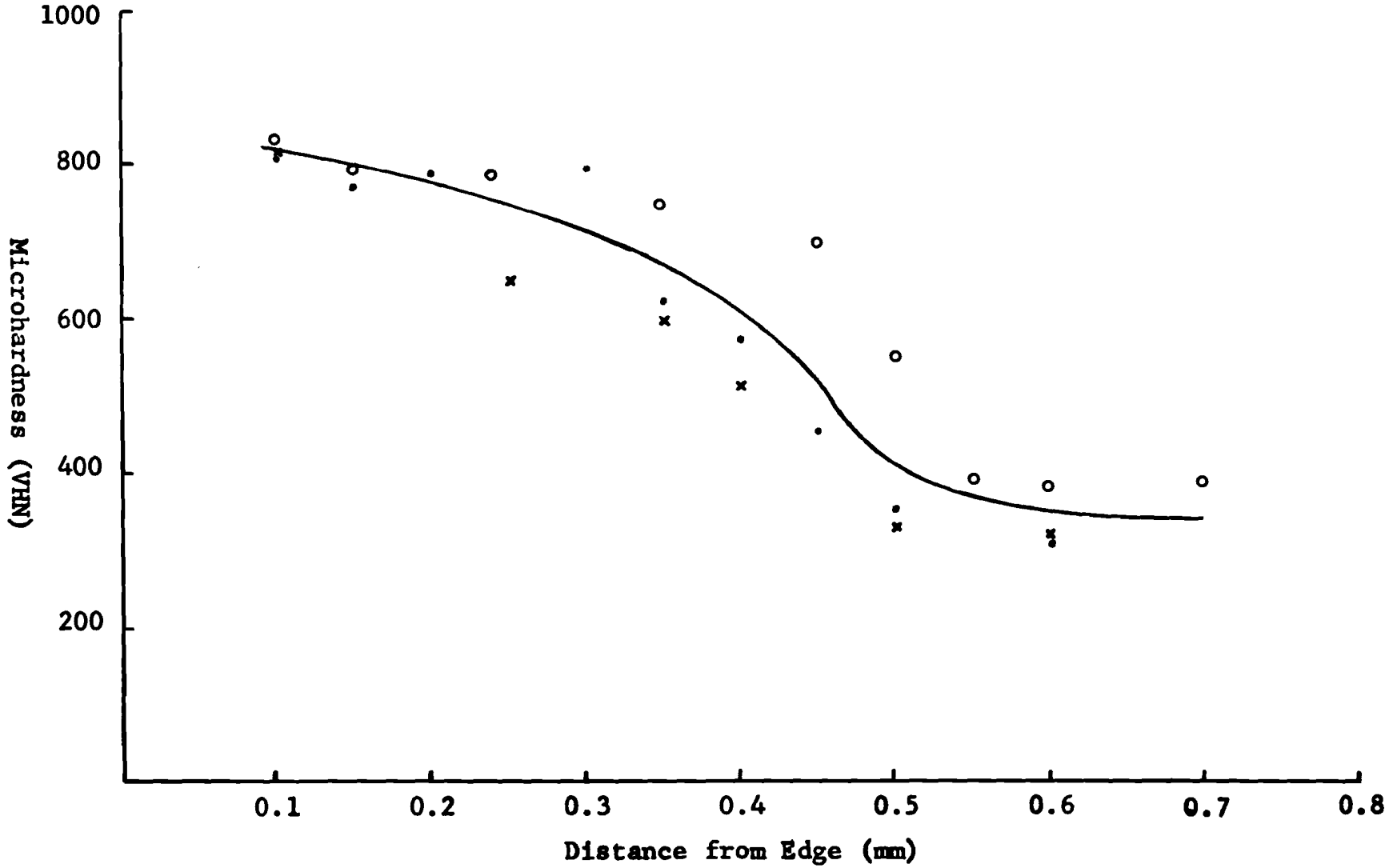

Figure 51. Microhardness of a Niobium Alloy Containing 6.0% Chromium, 8.7% Titanium, and 1% Dysprosium. Three Areas of the Specimen After Atmospheric Corrosion Test.

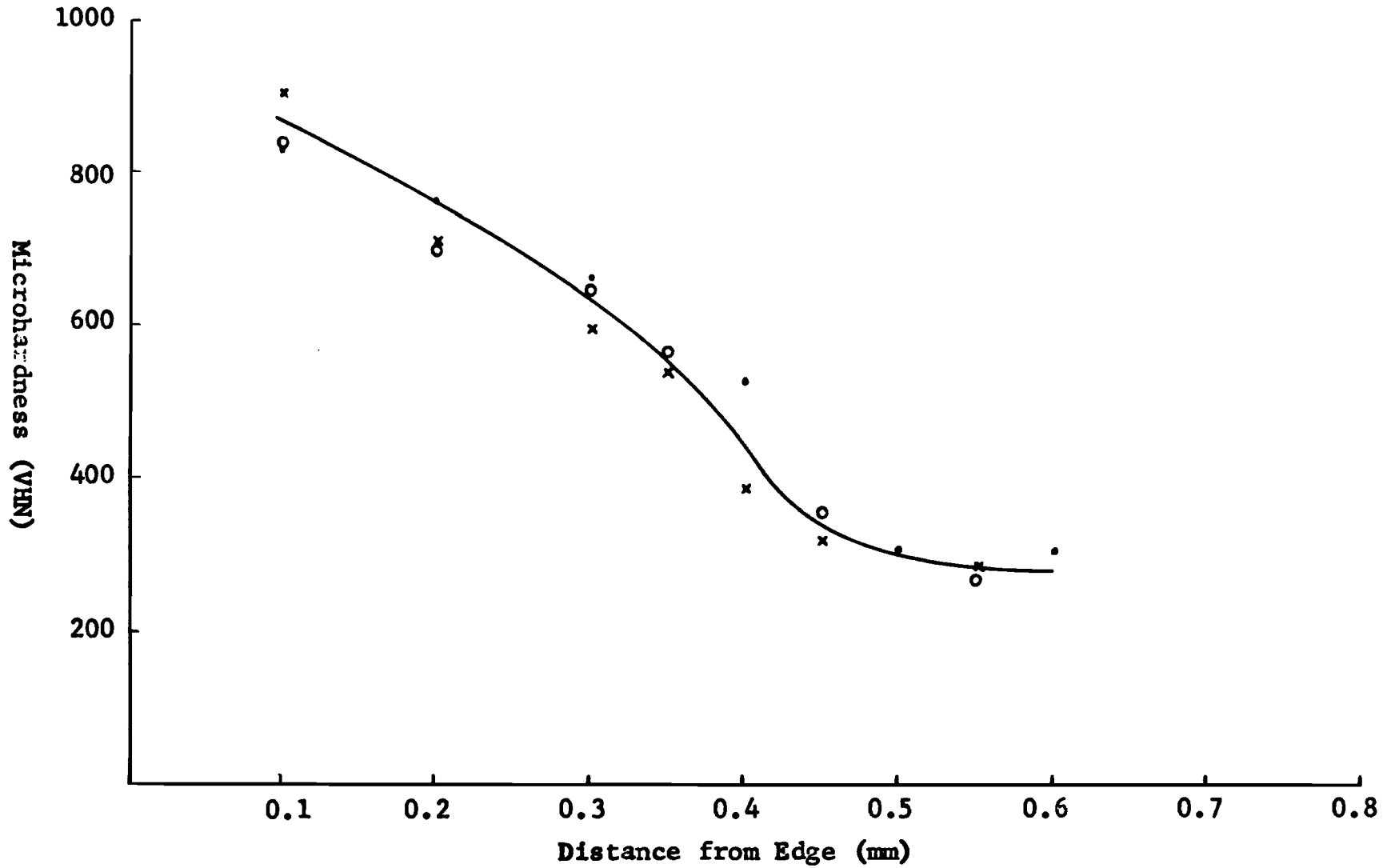

Figure 52. Microhardness of a Niobium Alloy Containing 6.0% Chromium, 8.7% Titanium and 4% Dysprosium. Three Areas of the Specimen After Atmospheric Corrosion Test.

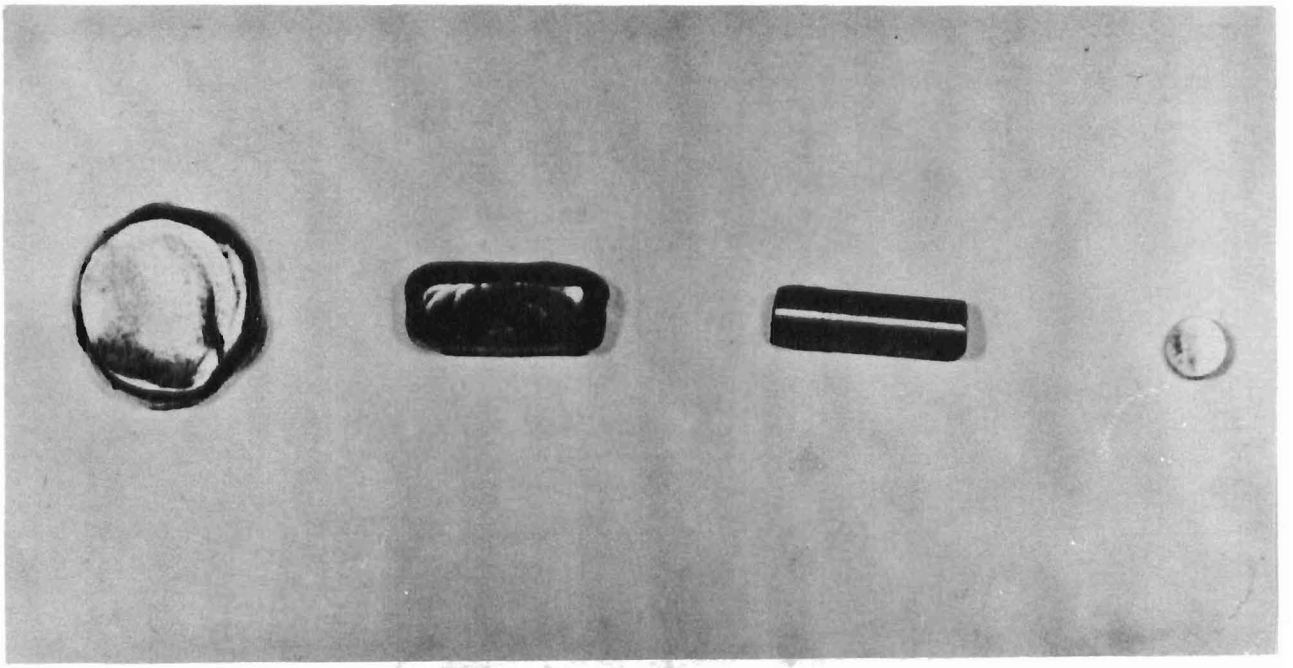

Figure 53. Specimen Preparation for Atmospheric Corrosion Tests. Alloy Button (left) is first prepared by non-consumable arc-melting. It is then arc-melted into a rectangular mold, machined into a cylinder and cut into test specimens. Reduced approximately 30% for reproduction.

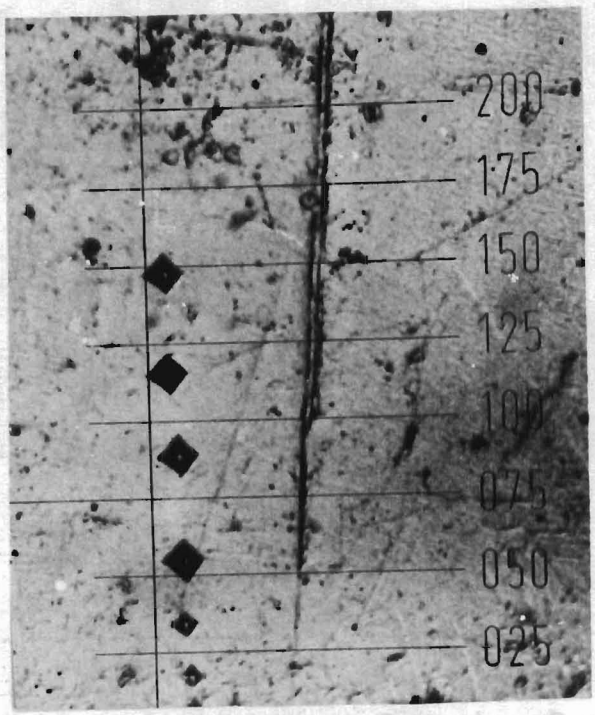

Figure 54. Microhardness Traverse Perpendicular to the Edge of a Niobium Alloy. Scale units are microns. Vickers diamond, 25 gram load. 400X.

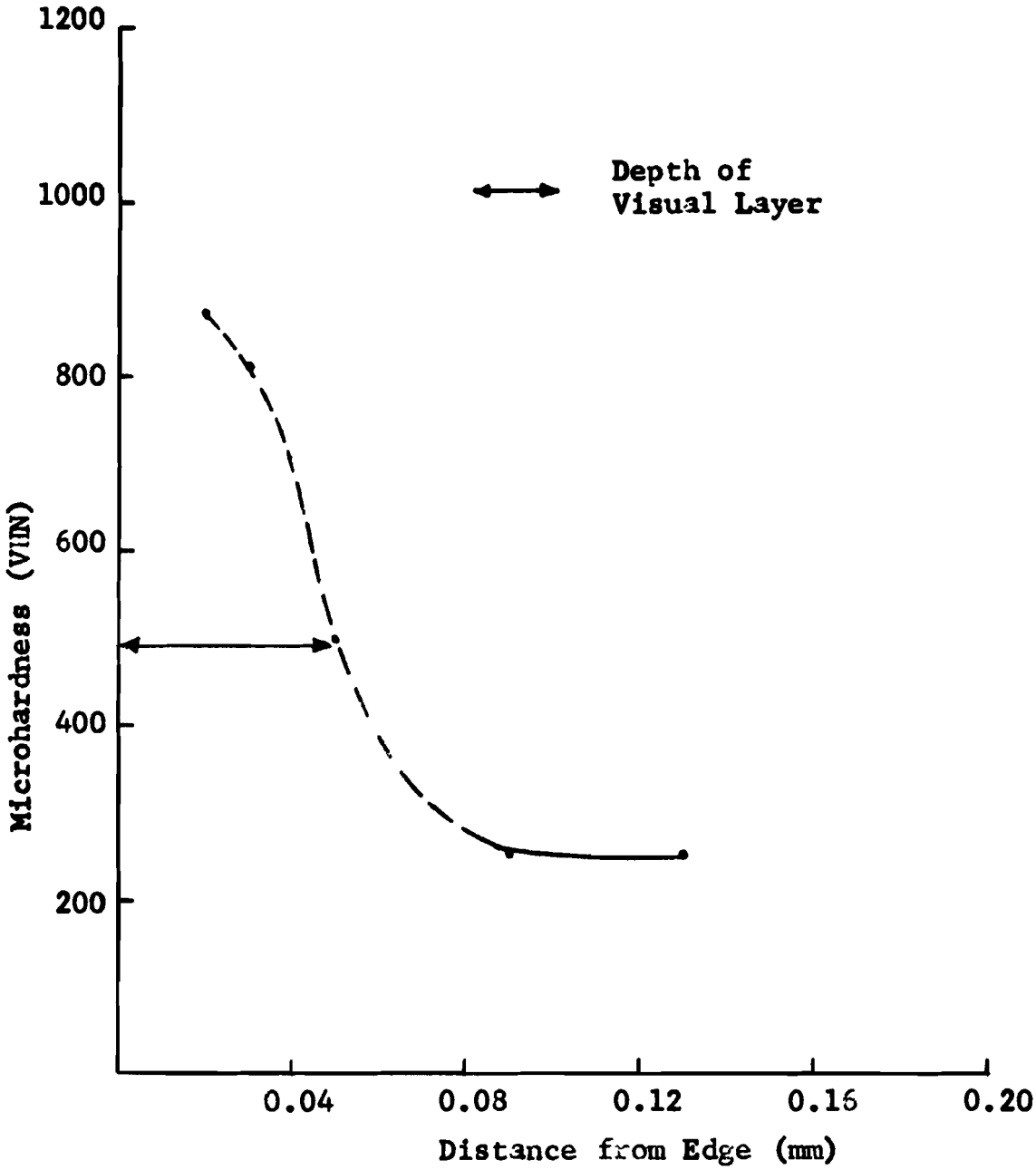

Figure 55. Microhardness of a Niobium Alloy Containing 20% Tungsten, 2% Titanium, and 0.5% Yttrium.

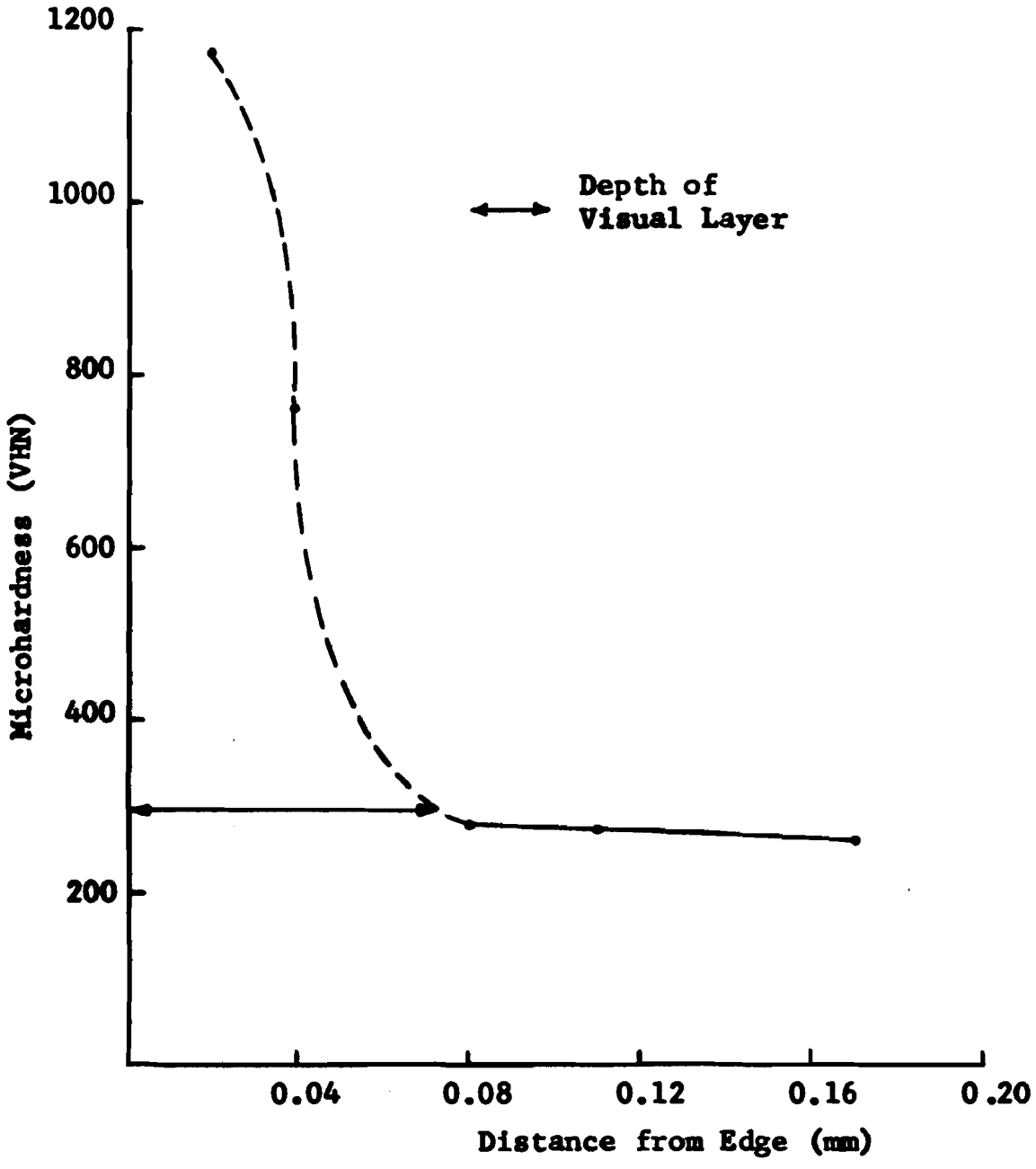

Figure 56. Microhardness of a Niobium Alloy Containing 20% Tungsten, 2% Titanium, and 1% Yttrium.

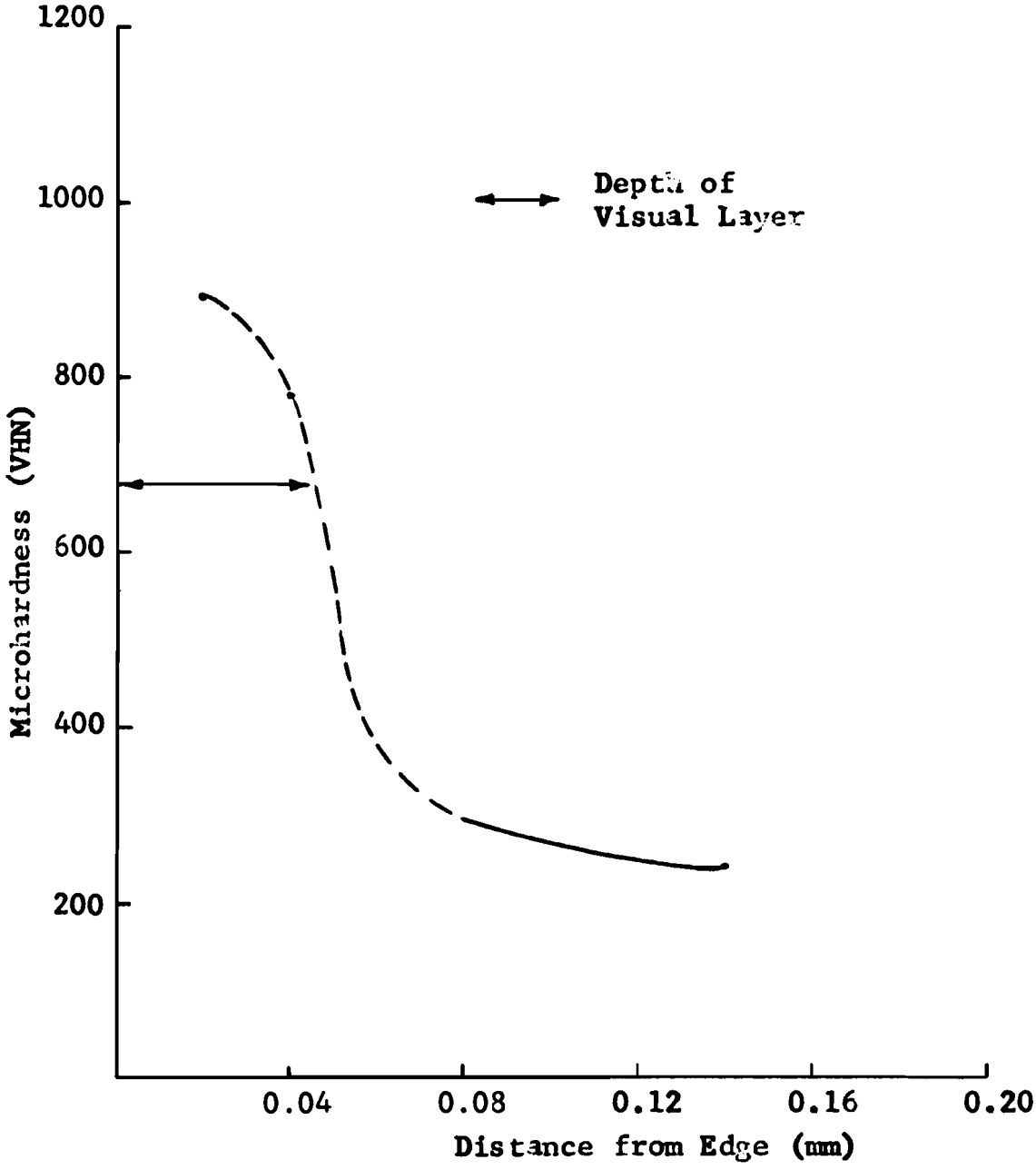

Figure 57. Microhardness of a Niobium Alloy Containing 20% Tungsten, 2% Titanium, and 2% Yttrium.

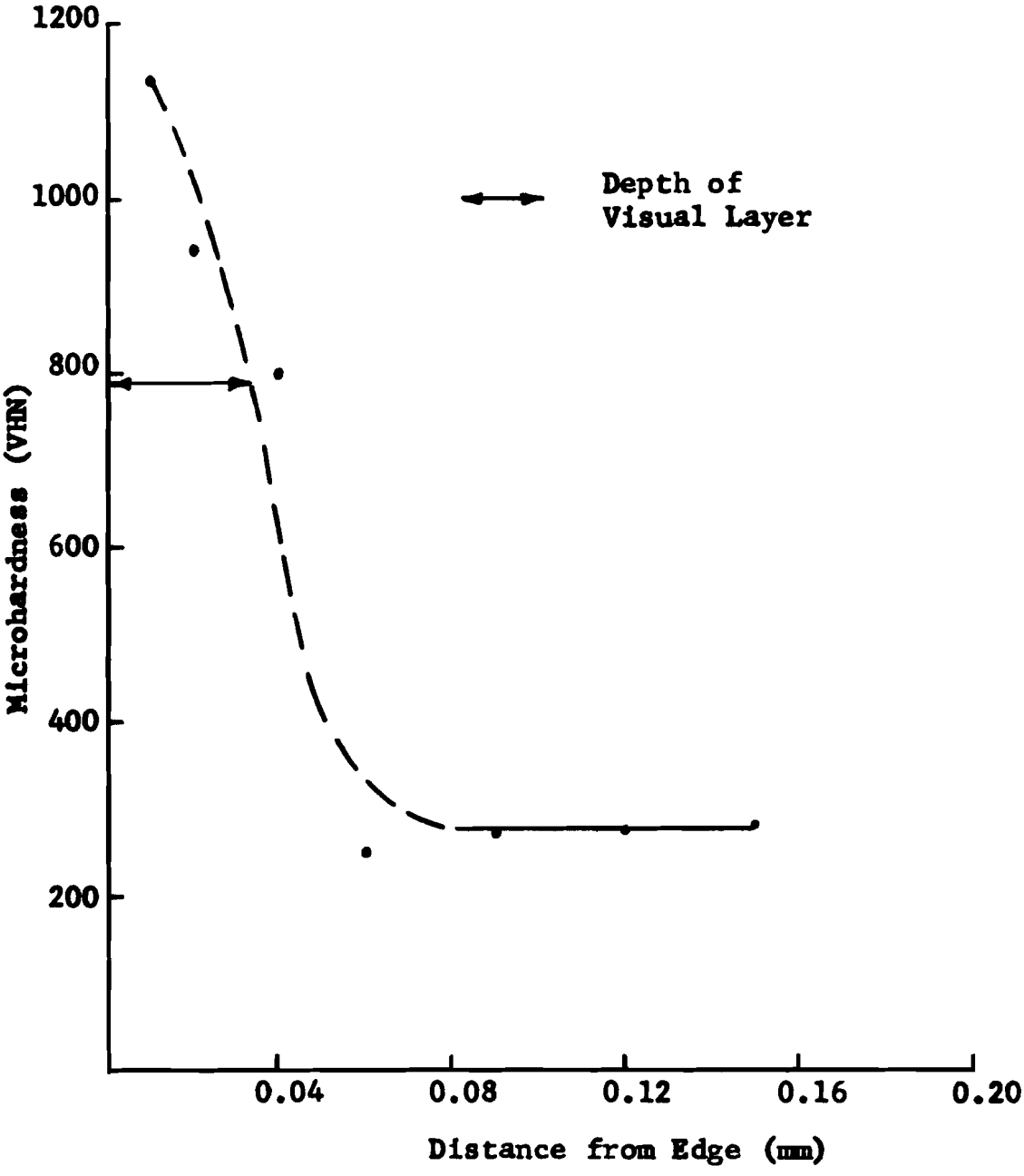

Figure 58. Microhardness of a Niobium Alloy Containing 20% Tungsten, 2% Titanium, and 0.5% Erbium.

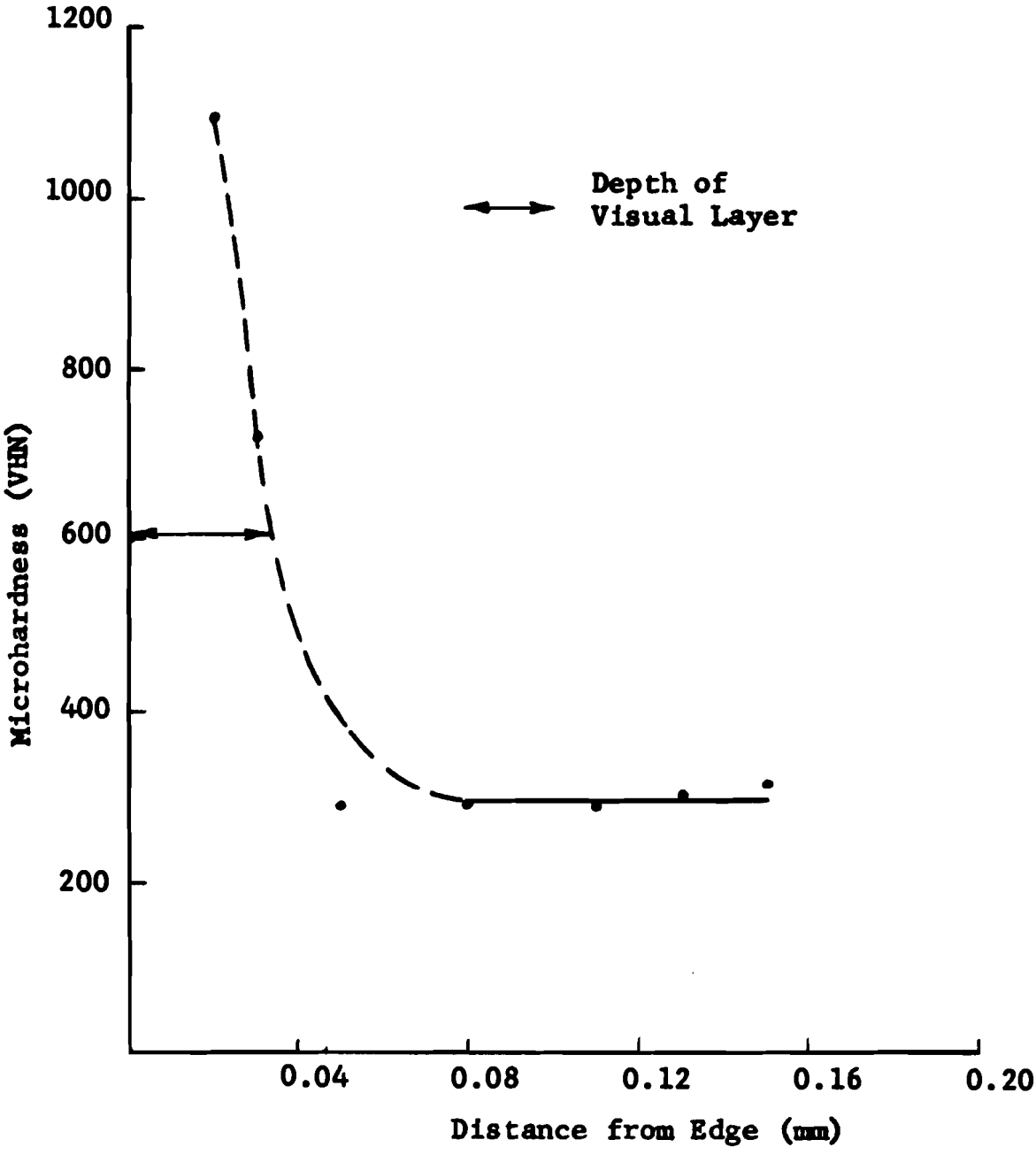

Figure 59. Microhardness of a Niobium Alloy Containing 20% Tungsten, 2% Titanium, and 1% Erbium.

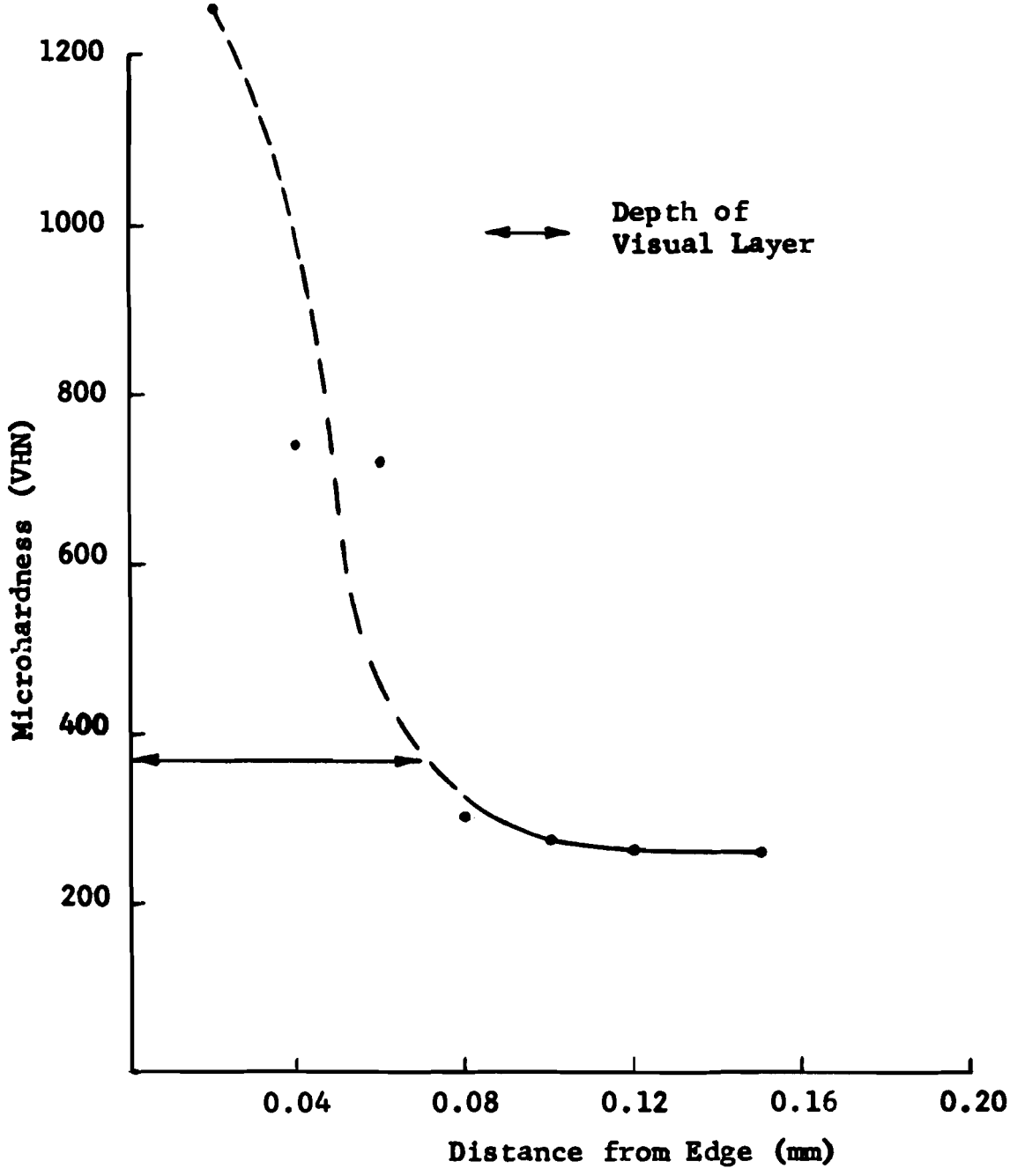

Figure 60. **Microhardness of a Niobium Alloy Containing 20% Tungsten, 2% Titanium, and 2% Erbium.**

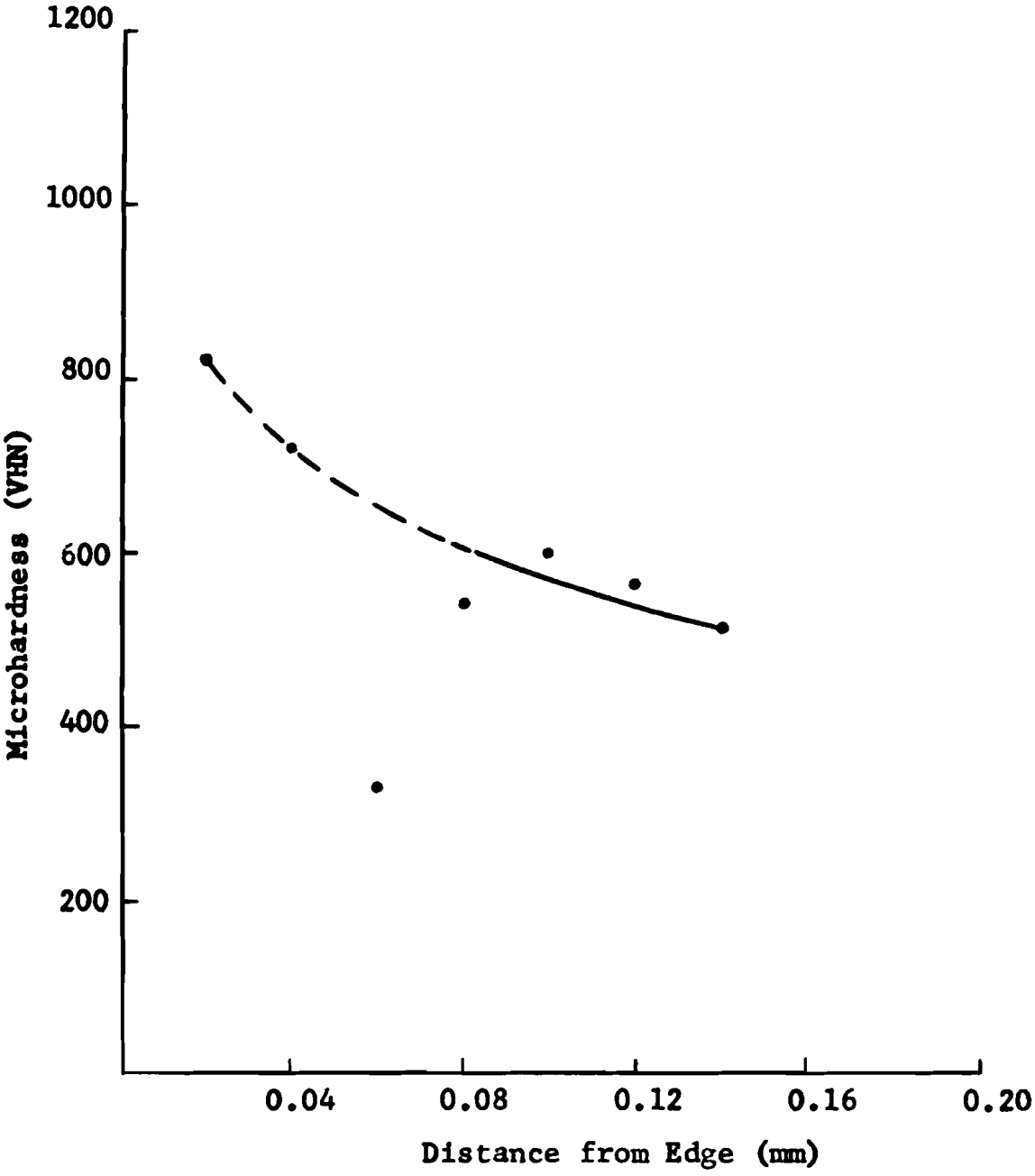

Figure 61. Microhardness of a Niobium Alloy Containing 15% Tungsten, 5% Molybdenum, 2% Platinum, and 0.5% Yttrium.

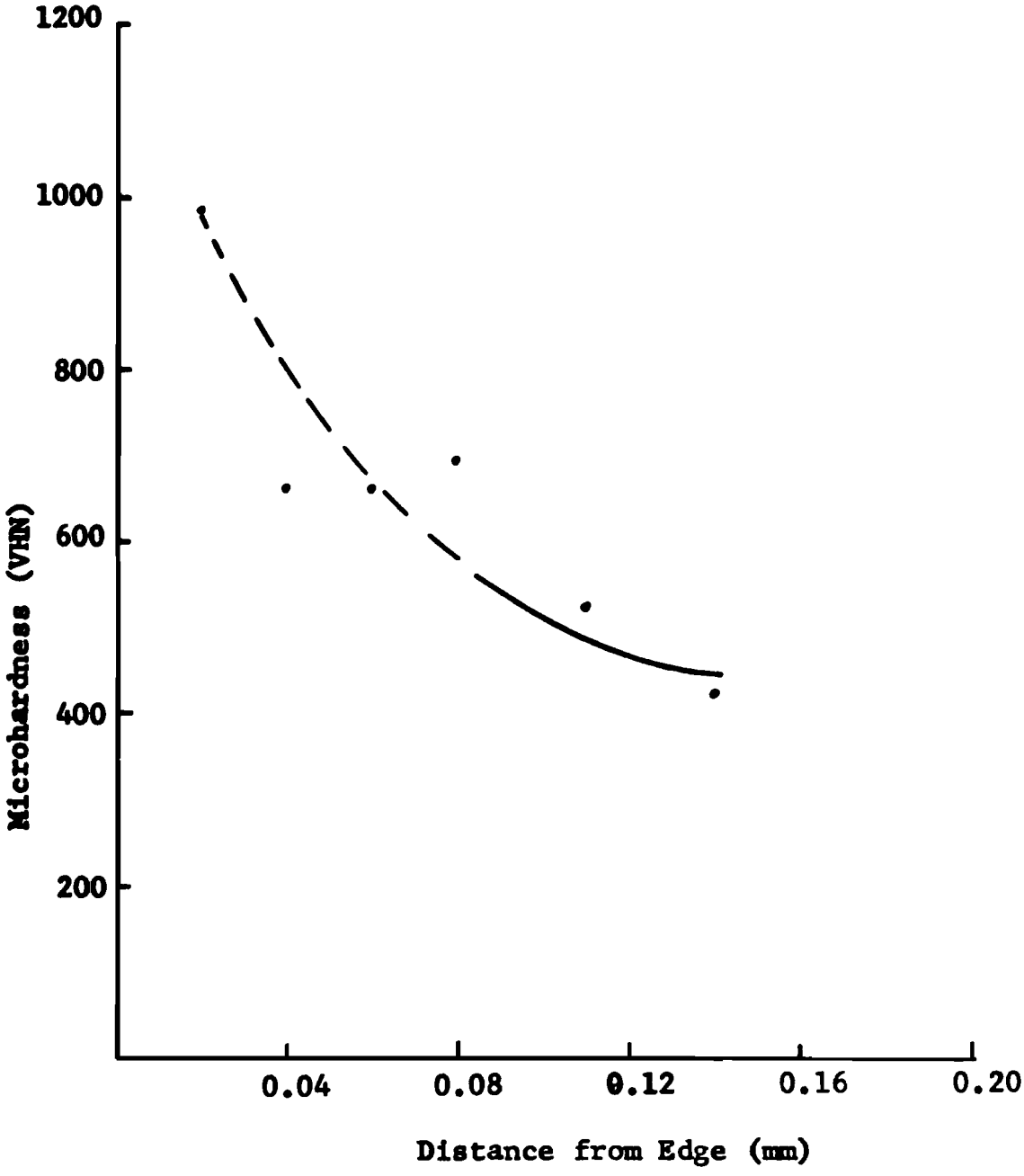

Figure 62. Microhardness of a Niobium Alloy Containing 15% Tungsten, 5% Molybdenum, 2% Platinum, and 1% Yttrium.

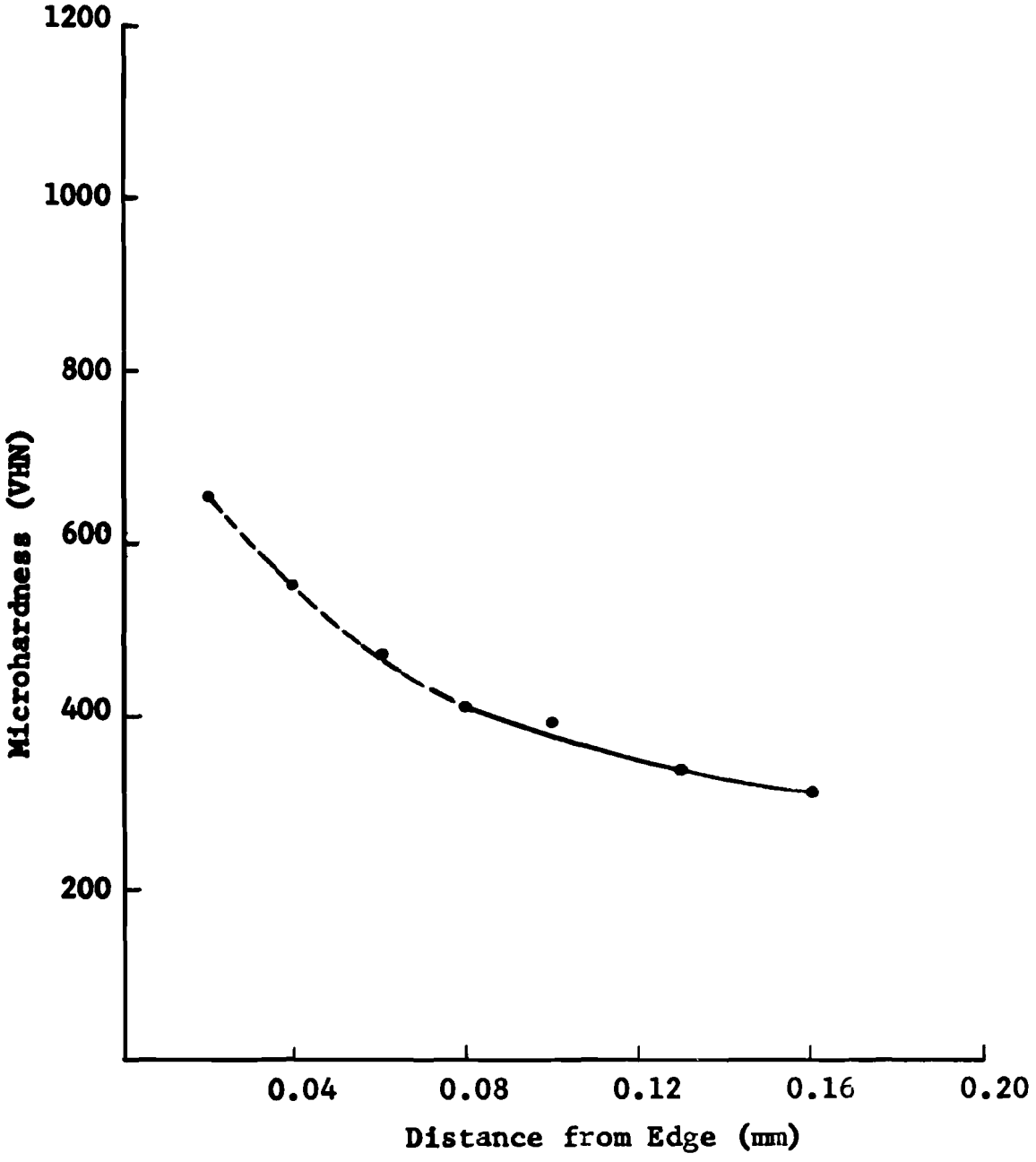

Figure 63. Microhardness of a Niobium Alloy Containing 15% Tungsten, 5% Molybdenum, 2% Platinum, and 2% Yttrium.

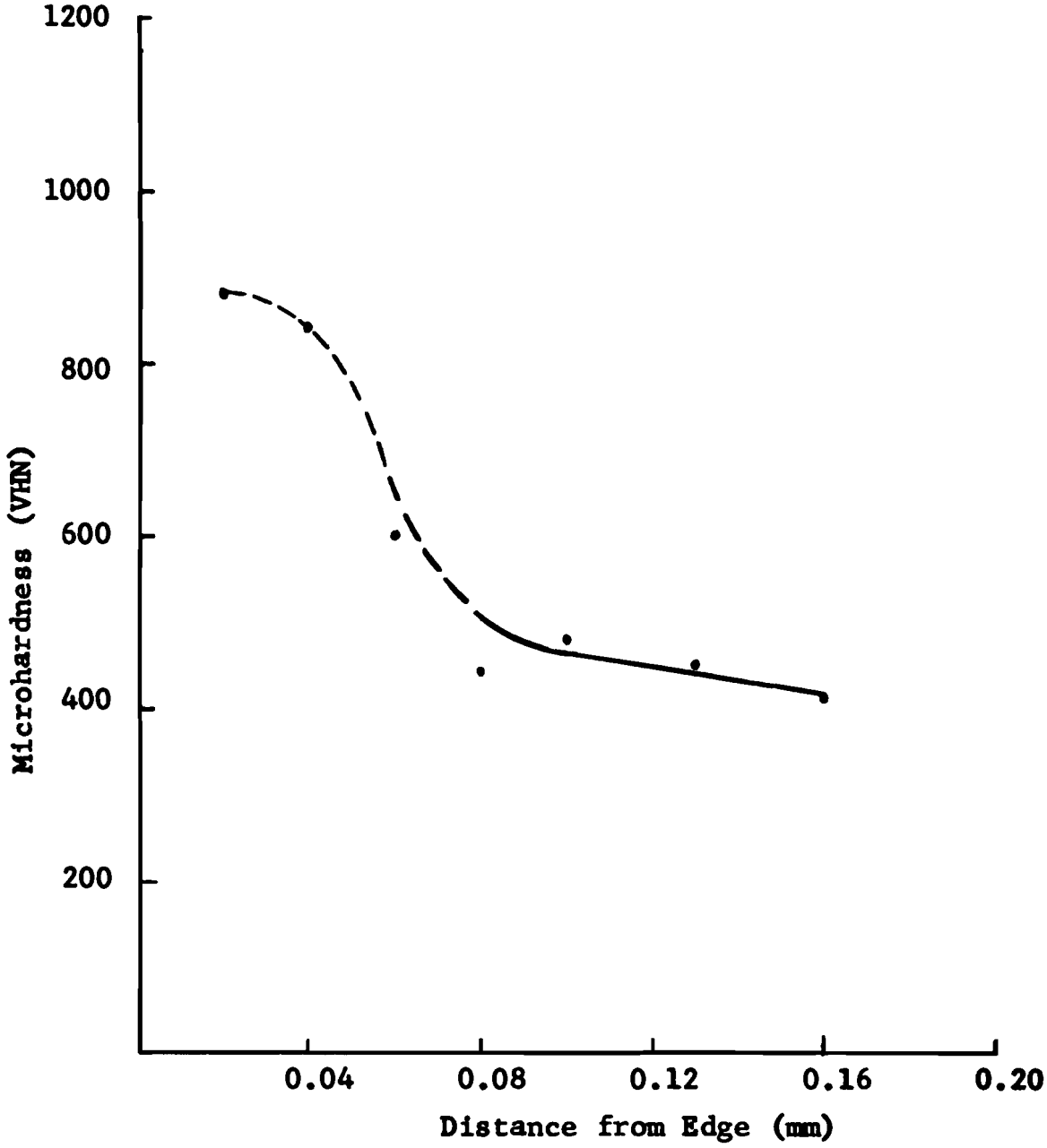

Figure 64. Microhardness of a Niobium Alloy Containing 15% Tungsten, 5% Molybdenum, 2% Platinum, and 0.5% Erbium.

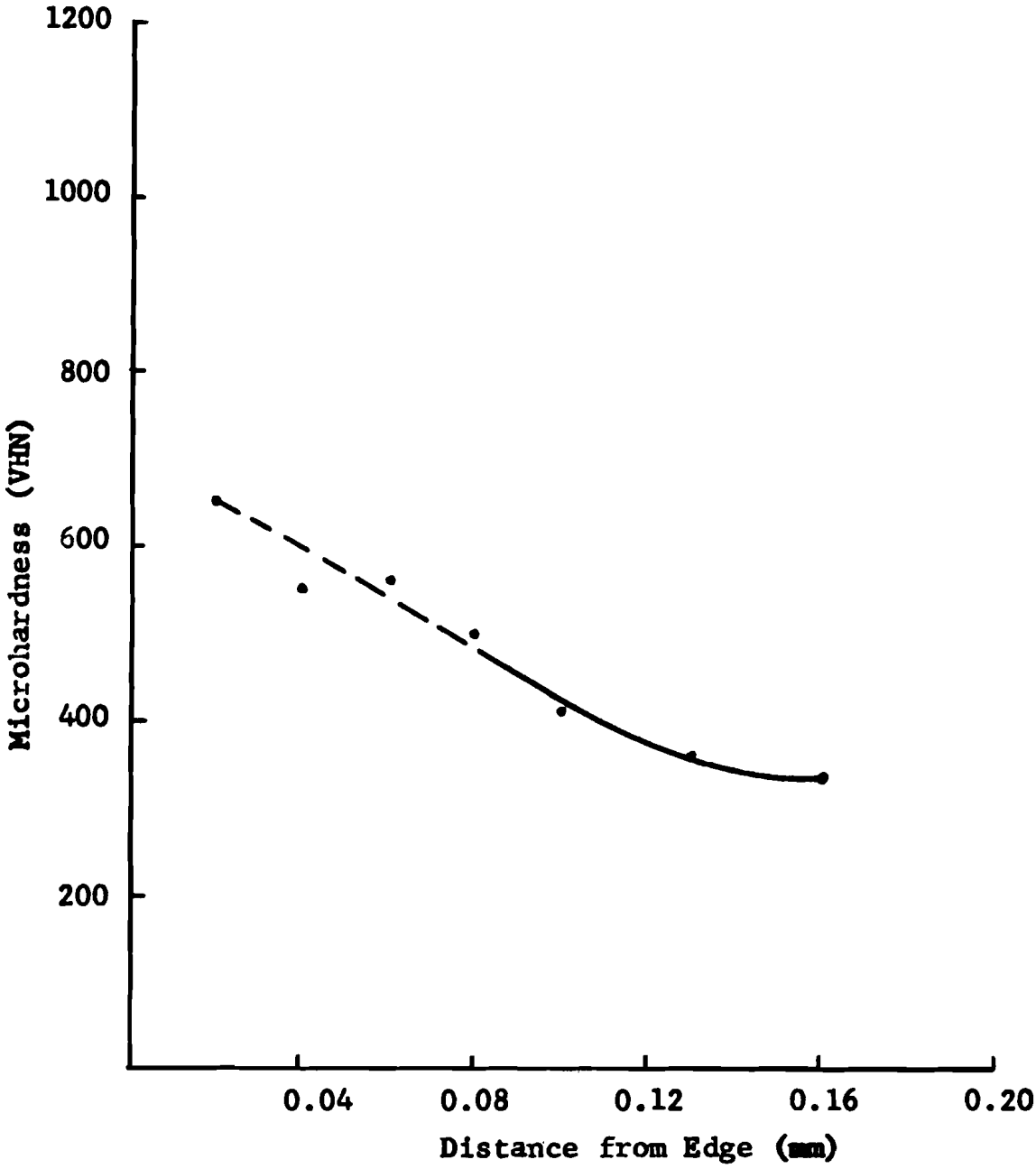

Figure 65. Microhardness of a Niobium Alloy Containing 15% Tungsten, 5% Molybdenum, 2% Platinum, and 1% Erbium.

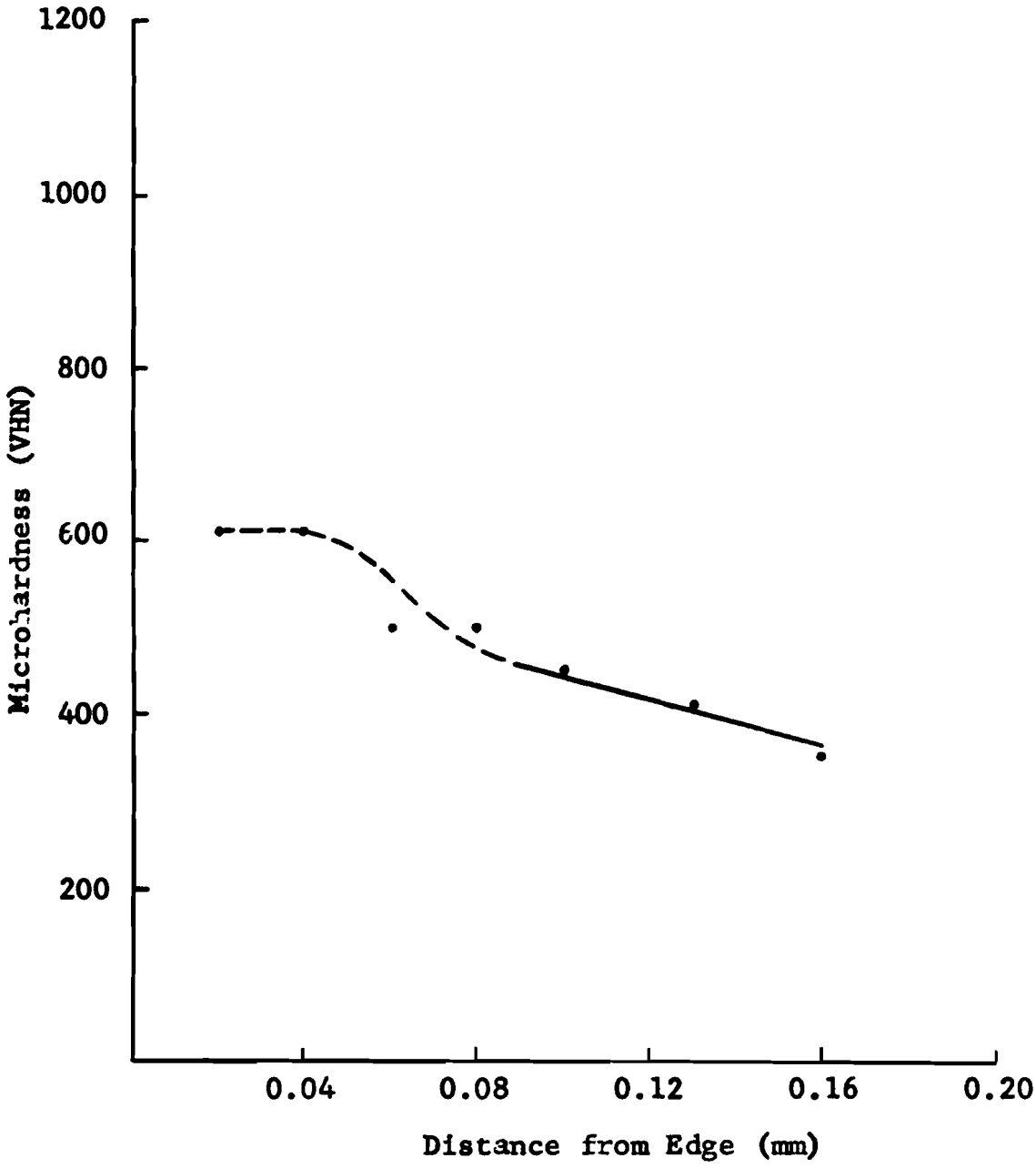

Figure 66. Microhardness of a Niobium Alloy Containing 15% Tungsten, 5% Molybdenum, 2% Platinum, and 2% Erbium.

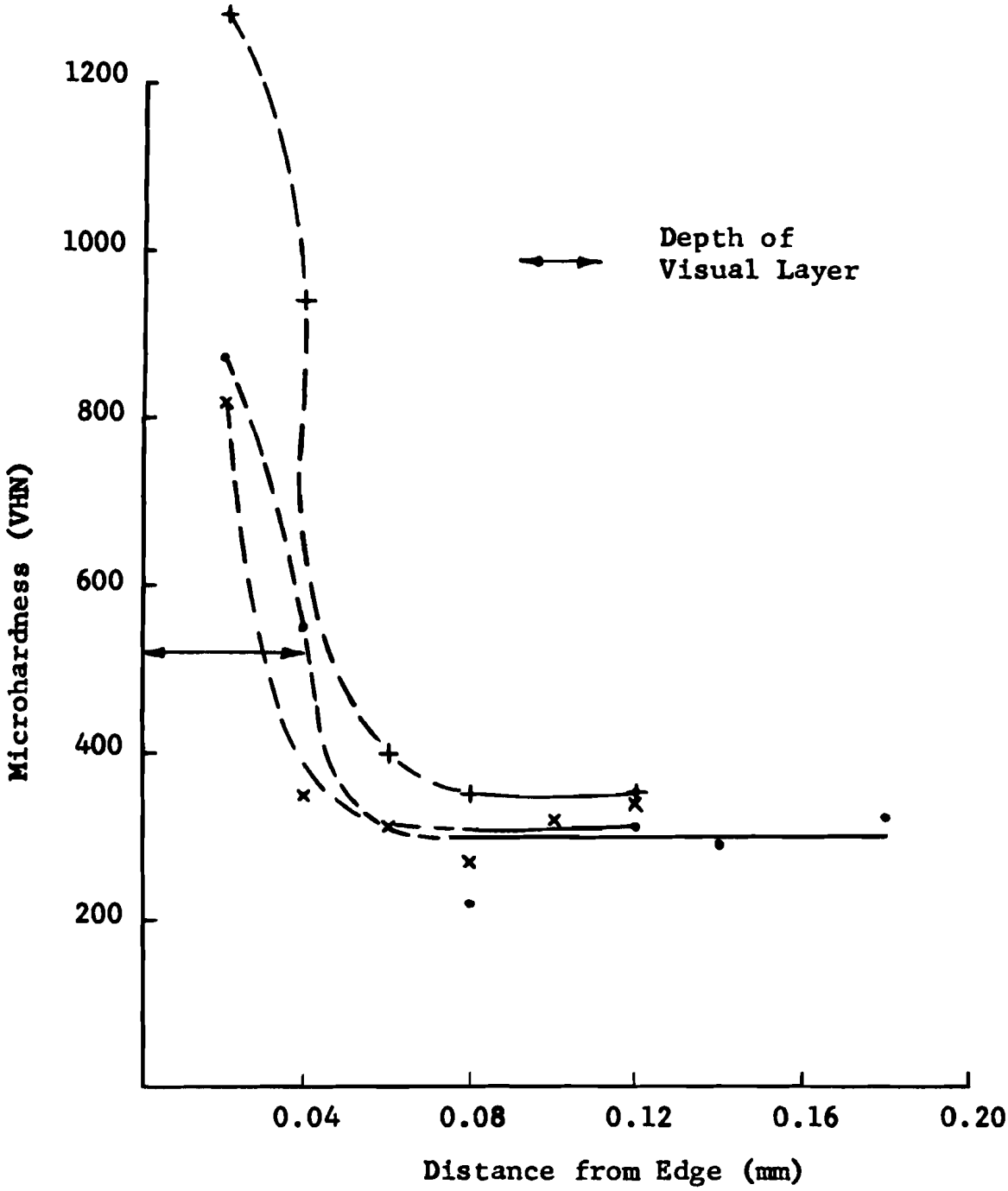

Figure 67. Microhardness of a Niobium Alloy Containing 20% Tungsten and 2% Titanium. Heat No. K865.

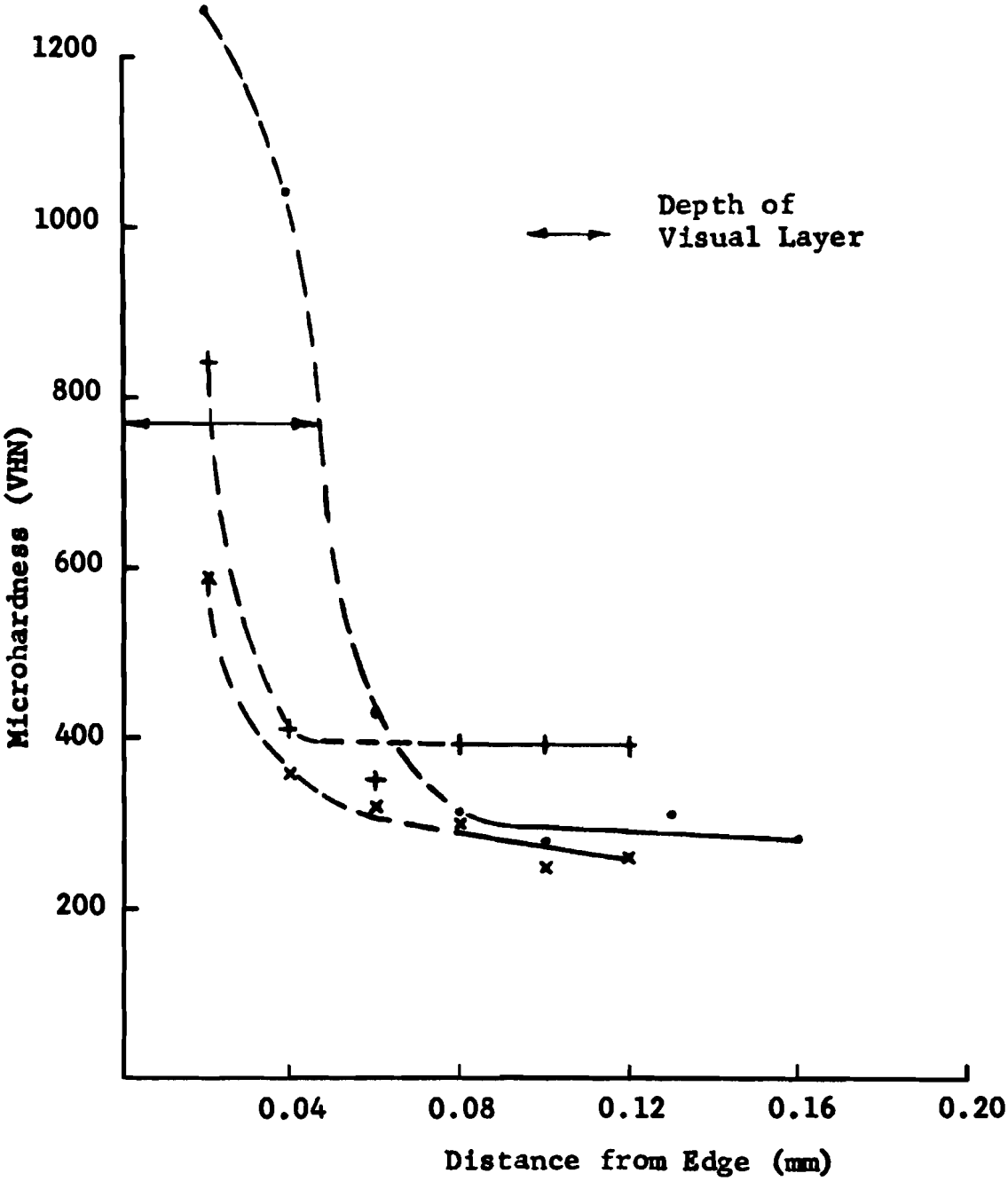

Figure 68. Microhardness of a Niobium Alloy Containing 20% Tungsten and 2% Titanium. Heat No. K864.

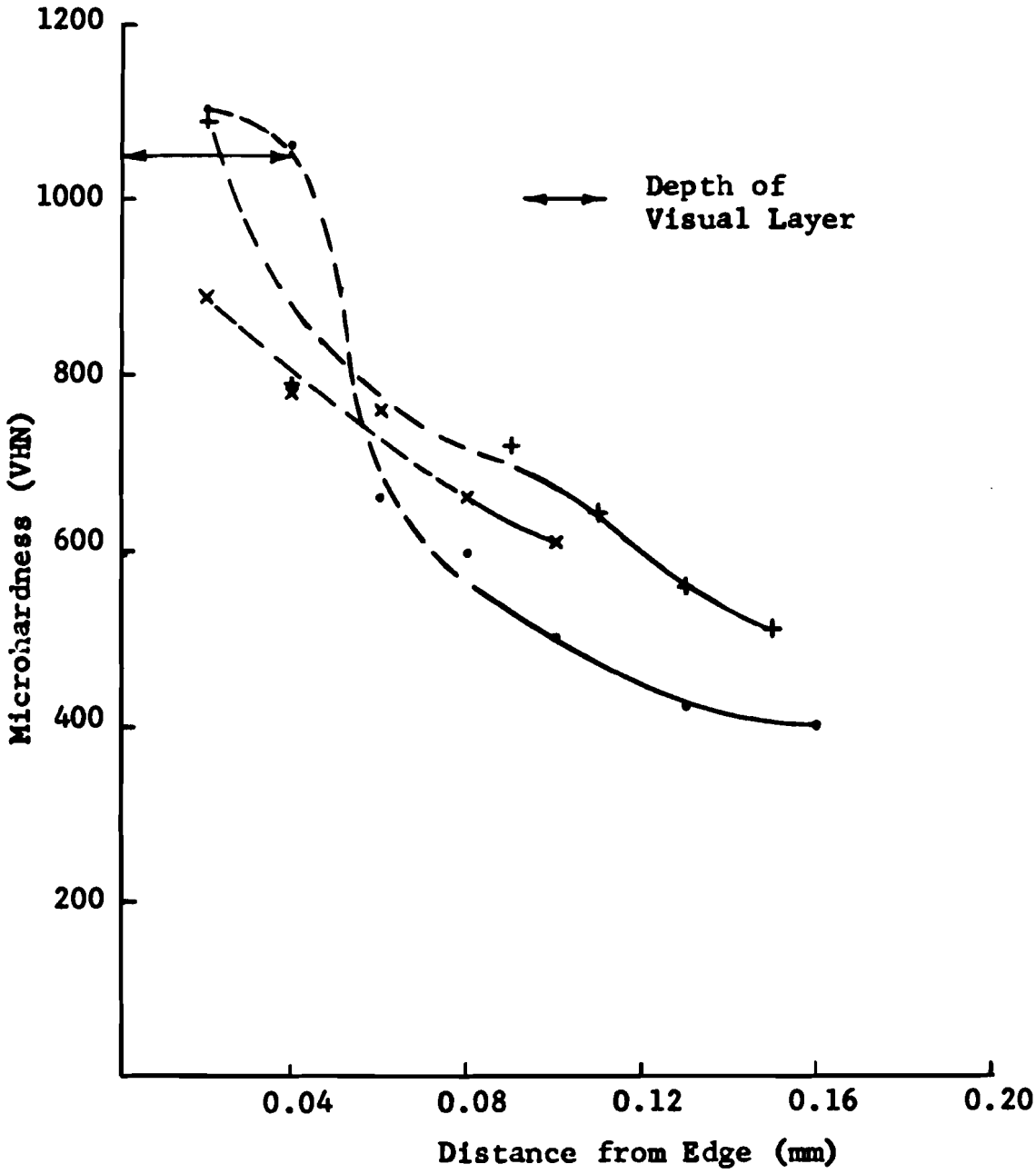

Figure 69. Microhardness of a Niobium Alloy Containing 15% Tungsten, 5% Molybdenum, and 2% Platinum.

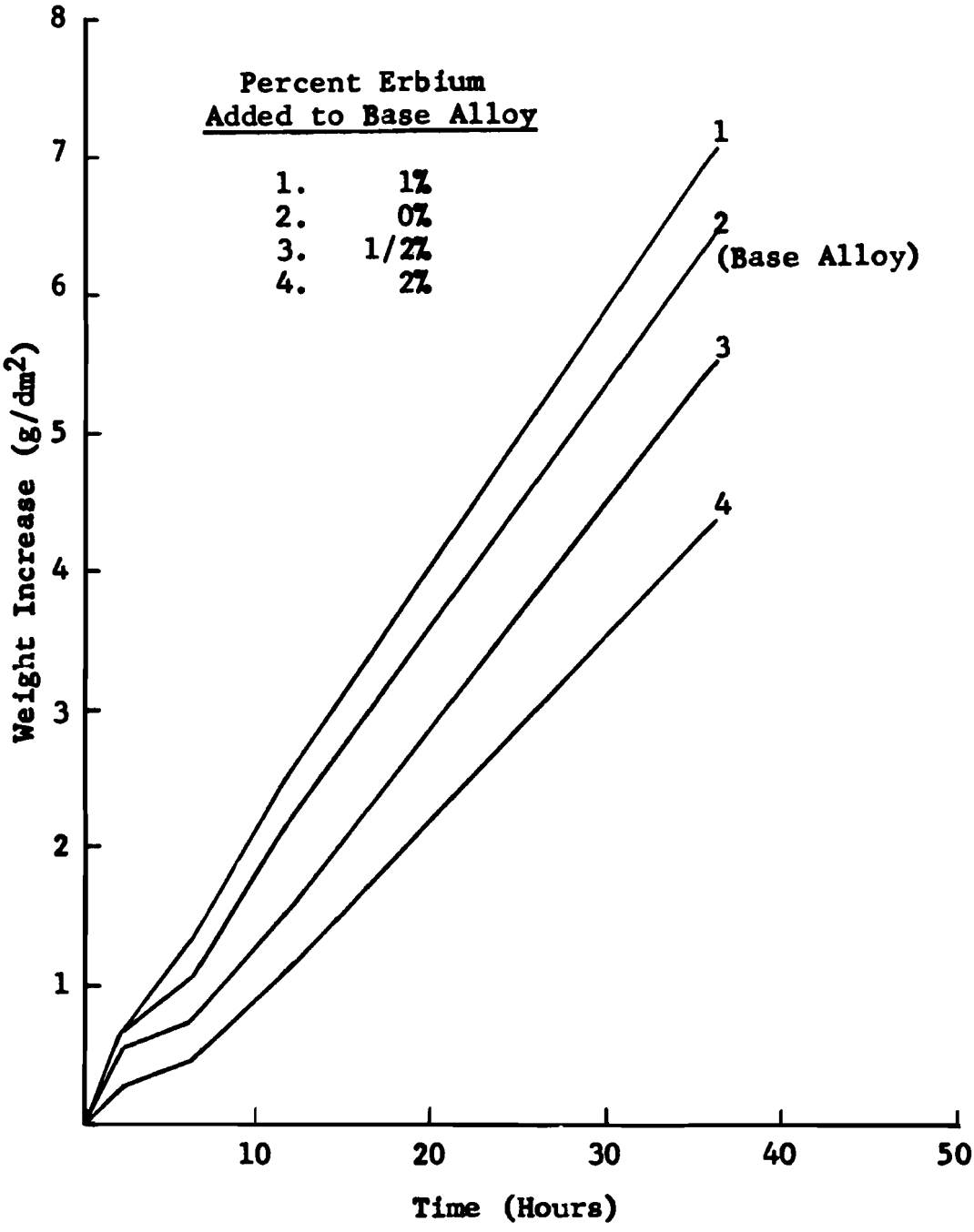

Figure 70. Atmospheric Corrosion of a Niobium Alloy Containing 15% Tungsten, 5% Molybdenum, and 2% Platinum with Erbium Additions. Dry Air at 600°C.

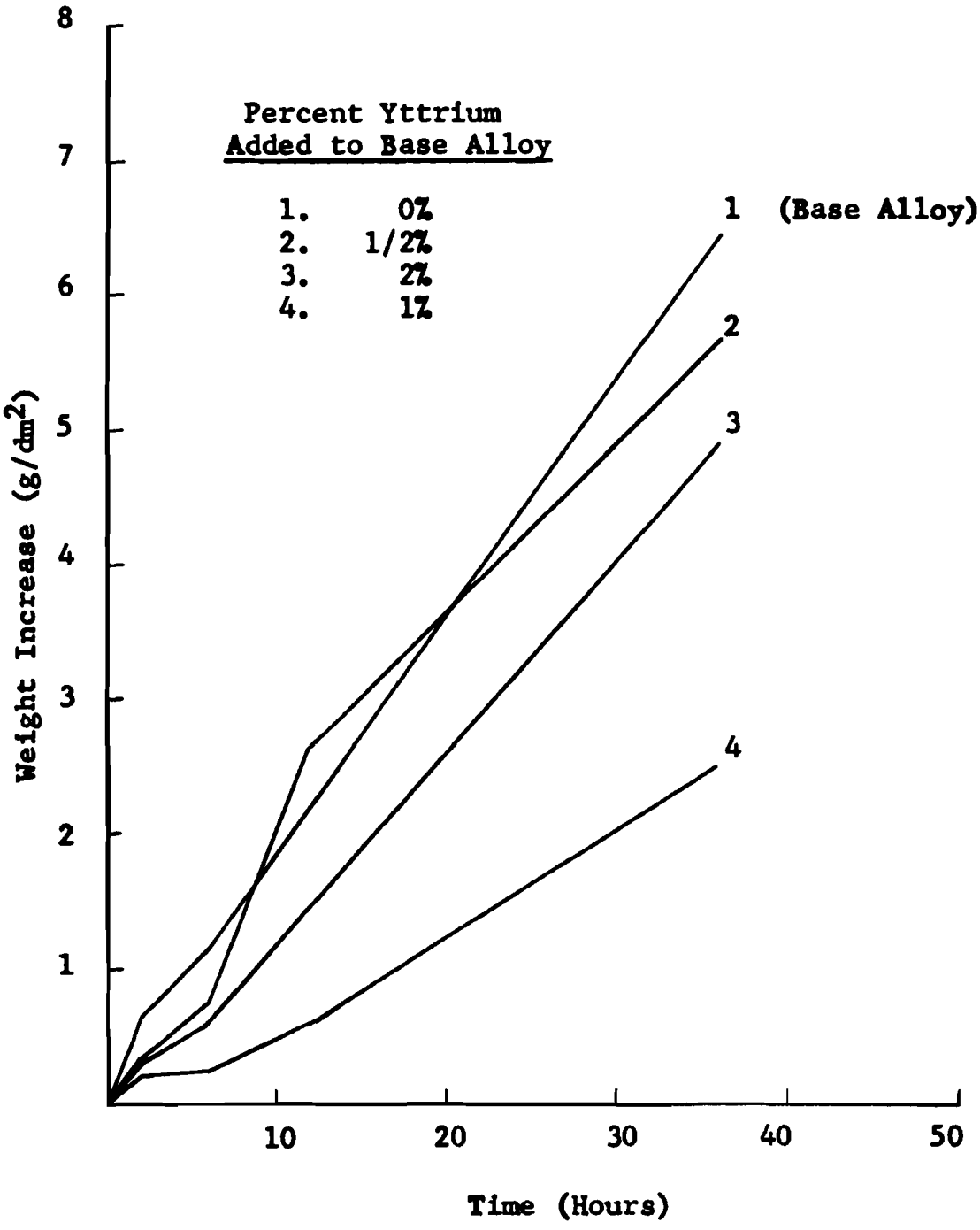

Figure 71. Atmospheric Corrosion of a Niobium Alloy Containing 15% Tungsten, 5% Molybdenum, and 2% Platinum with Yttrium Additions. Dry Air at 600°C.

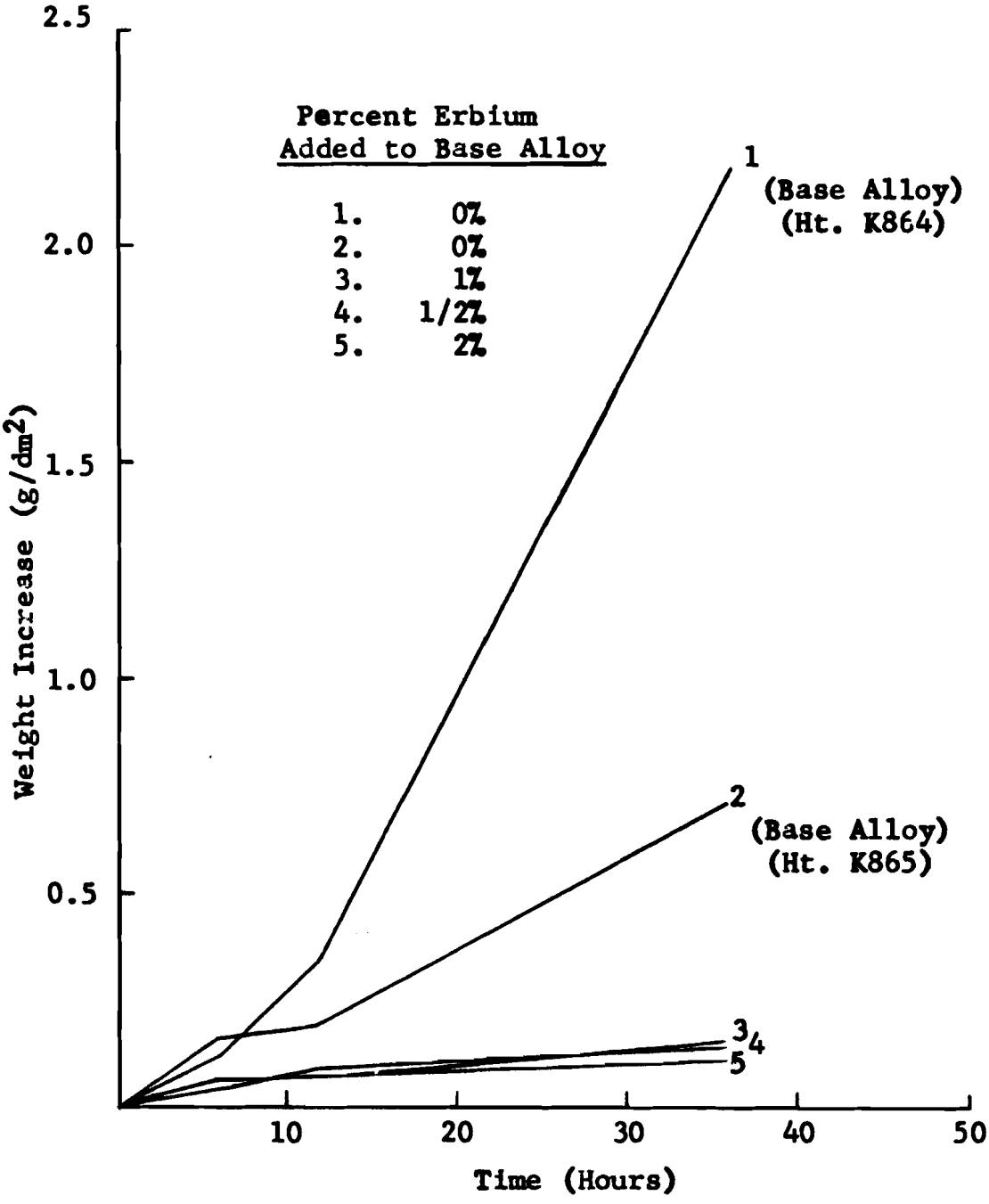

Figure 72. Atmospheric Corrosion of a Niobium Alloy Containing 20% Tungsten and 2% Titanium with Erbium Additions. Dry Air at 600°C.

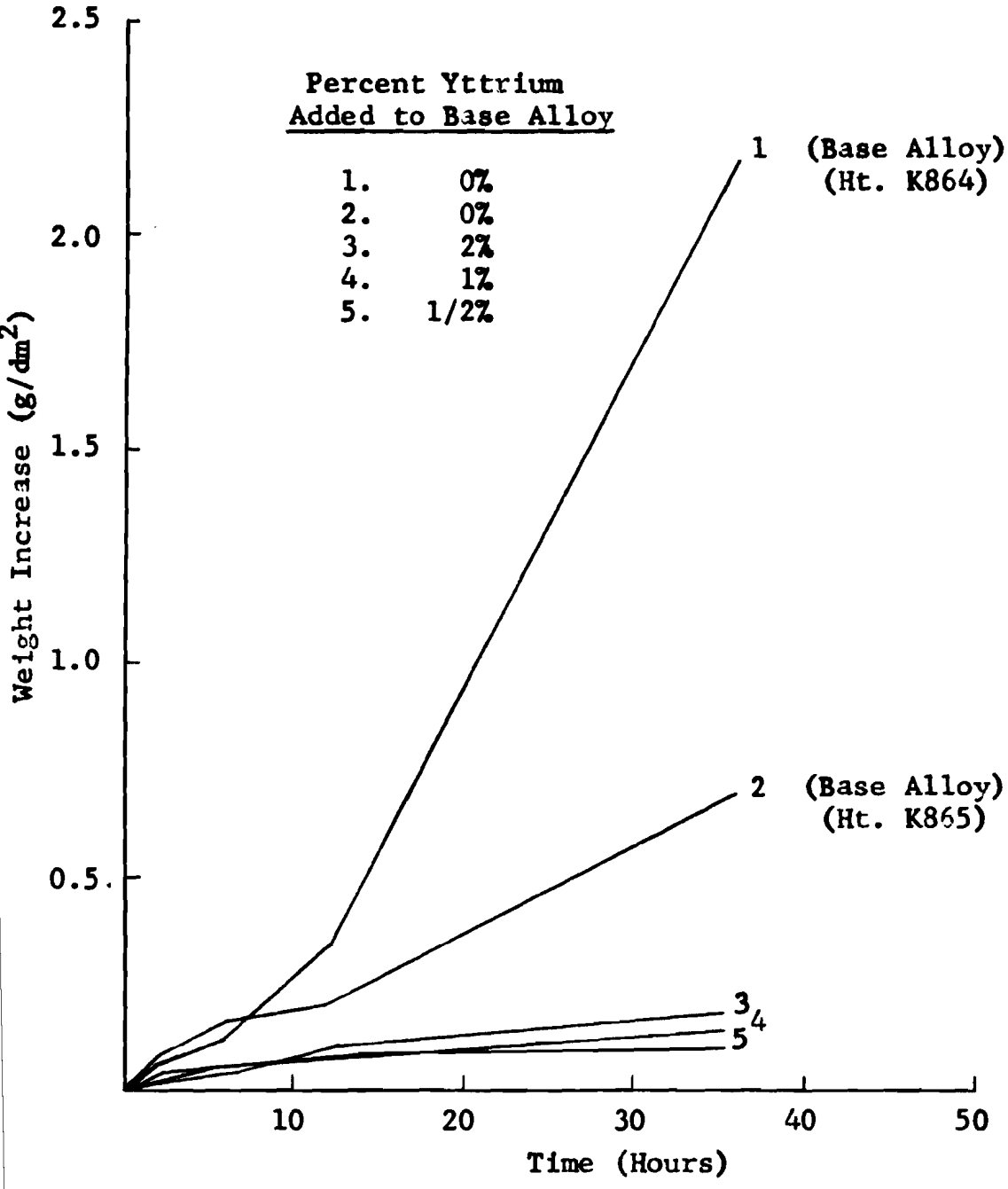

Figure 73. Atmospheric Corrosion of a Niobium Alloy Containing 20% Tungsten and 2% Titanium with Yttrium Additions. Dry Air at 600°C.

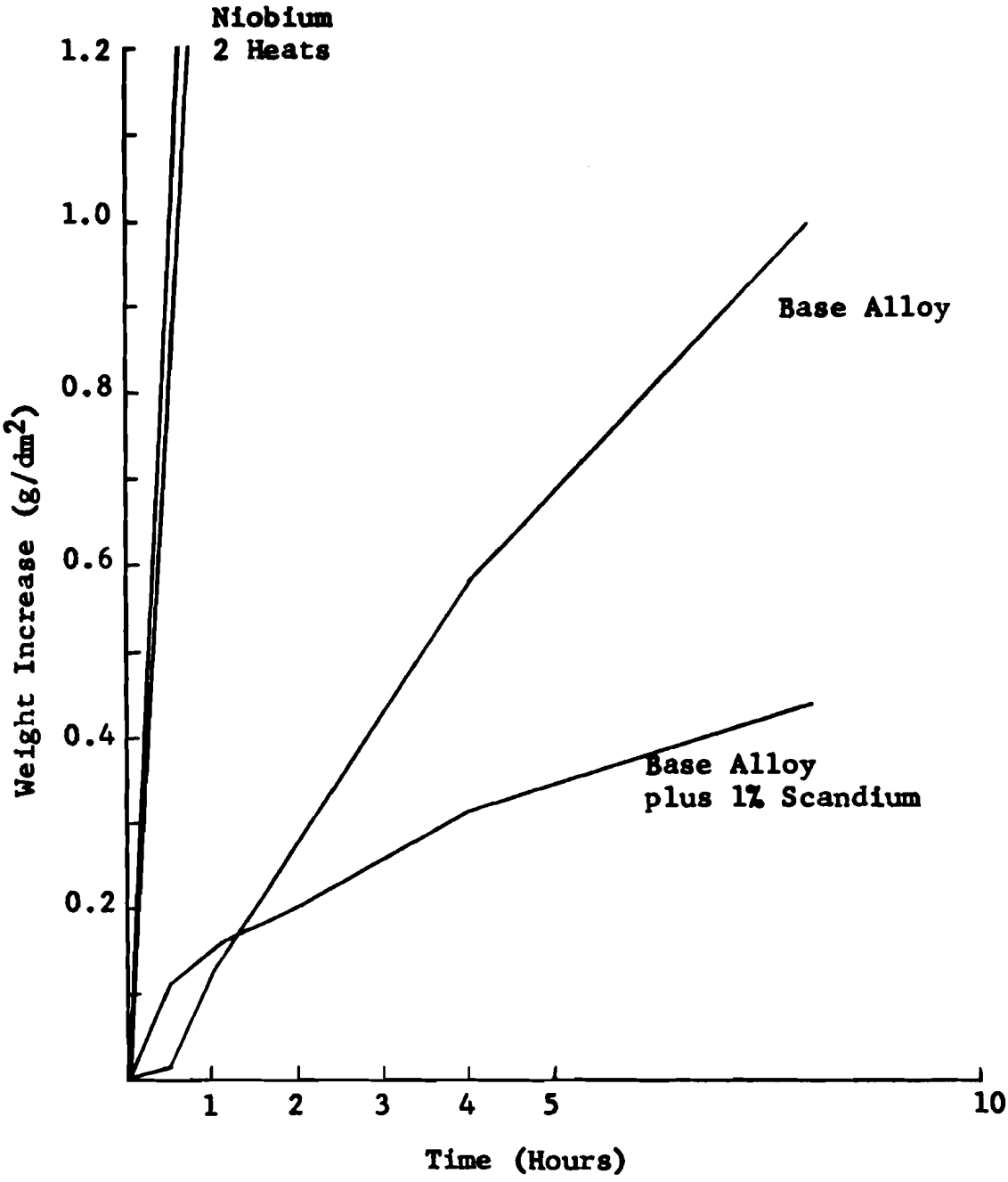

Figure 74. Atmospheric Corrosion of a Niobium Alloy Containing 42% Titanium and 4% Aluminum with Scandium Addition. Dry Air at 1000°C.

X-RAY DIFFRACTION PATTERNS OF CORROSION PRODUCTS

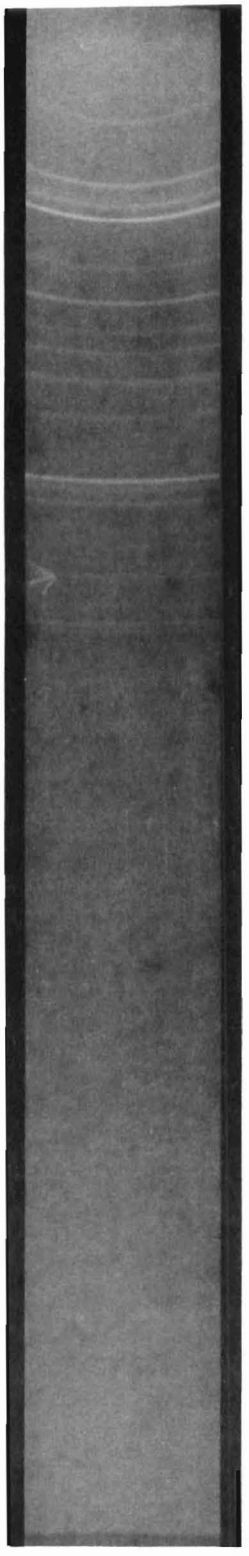

FIGURE 75
1-Alpha

FIGURE 76
1-Beta

FIGURE 77
1-Gamma

X-RAY DIFFRACTION PATTERNS OF CORROSION PRODUCTS

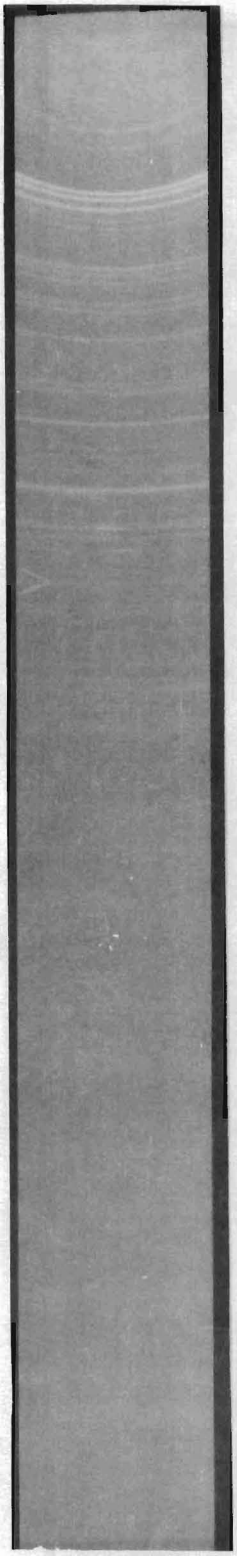

FIGURE 78
1-Delta

FIGURE 79
2-Alpha

FIGURE 80
2-Beta

X-RAY DIFFRACTION PATTERNS OF CORROSION PRODUCTS

FIGURE 81
3

FIGURE 82
4-Alpha

FIGURE 83
4-Beta